PATENT
Docket No.: **746210-100**

IN THE UNITED STATES PATENT AND TRADEMARK OFFICE

Applicant	:	Spadafora et al.	Examiner: Shobha Kantamneni
Serial No.	:	10/500,270	
Cnfrm. No.	:	9338	Art Unit: 1617
Filed	:	December 23, 2002	
For	:	NON-NUCLEOSIDIC INHIBITORS OF REVERSE TRANSCRIPTASE AS ANTAGONISTS OF CELL PROLIFERATION AND INDUCERS OF CELL DIFFERENTIATION	

DECLARATION OF FRANÇOIS ICHAS, PH.D. UNDER 37 CFR § 1.132

Mail Stop Amendment
Commissioner for Patents
P.O. Box 1450
Alexandria, VA 22313-1450

I, FRANÇOIS ICHAS, Ph.D., hereby declare:

1. I received a Certificate of Clinical and Therapeutical Synthesis from the Doctoral School of University Victor Segalen-Bordeaux 2 in Bordeaux, France in 1996, a Ph.D. in Biomedical Sciences from the University Victor Segalen-Bordeaux 2 in 1996, and a Post-doctoral degree from the University Victor Segalen-Bordeaux 2, in 2001.

2. I am currently Department Director for INSERM U916 VINCO (Validation and Identification of New Targets in Oncology) at the University Victor Segalen-Bordeaux 2 in Bordeaux, France. I have held this position since 2007. From 2003 to 2007, I was the Research Director of the INSERM E.347 team in molecular pharmacology and oncology, and conducted translation research at the CLCC Bergonié (Regional Anti-Cancer Center) in oncology .

3. The primary focus of my research is oncology and the development of new cancer therapies. I have authored over 35 peer-reviewed research articles in the field(s) of mitochondrial functions, cellular pathways implicated in programmed cell death, and manipulation of those pathways in cancer cells. A copy of my Curriculum Vitae, listing my publications, awards, and other professional achievements is attached as Exhibit 1.

4. I have reviewed the above referenced patent application, the pending claims in that application, as well as the teachings of Grimaudo *et al.*, "Selective Induction of Apoptosis in Multidrug Resistant HL60R Cells by the Thiazolobenzoimidazole Derivative 1-(2,6-difluorophenyl)-1H,3H-thiazolo[3,4-a]benzimidazole (TBZ)," *Eur. J. Cancer* 34:1756-1763 (1998) ("Grimaudo") and Ghori *et al.*, "Telomerase Inhibition as a Potential New Therapy for Colorectal Cancer," *Colorectal Disease* 2(2):106-112 (2000) ("Ghori"). I understand that the United States Patent and Trademark Office ("PTO") has taken the position that the claims of the above referenced patent application would have been obvious in view of the teachings of Grimaudo and the teachings of Ghori. I disagree with that conclusion, and I am presenting this declaration to explain why the claimed subject matter would not have been obvious to one of skill in the art in view of either Grimaudo or Ghori.

5. Grimaudo investigated the cytotoxicity of 1-(2,6-difluorophenyl)-1*H*,3*H*-thiazolo[3,4-a]benzimidazole ("TBZ"), a non-nucleoside reverse transcriptase inhibitor ("NNRTI"), on human acute myeloid leukemic HL60 parental and drug resistant (HL60R) cell lines. Grimaudo showed that TBZ exhibits cytotoxic activity in the both HL60 and HL60R cells lines at a concentration of 50 μM (IC_{50}), a concentration that is 50-fold higher than the concentration of TBZ required to inhibit viral reverse transcriptase (RT) activity in several human primary cells and cell lines (*see* Grimaudo at p. 1760, col. 1, second full para. and col. 2, fourth full para.). Since the cytotoxic effects of TBZ were observed at such a higher concentration than required to inhibit viral RT, it is highly unlikely that TBZ's cytotoxic activity in these cells is related to its viral RT inhibitory properties.

6. That TBZ's mechanism of cytotoxicity is unrelated to its RT inhibitory activity is further supported by Grimaudo's observation that TBZ caused a selective induction of apoptosis in the HL60 drug resistant cell line compared to the parental cell line (*see* Grimaudo at

Figure 2 and Figure 5, and corresponding text at p. 1760, col. 1, second and third full paras.). While Grimaudo does not delineate TBZ's mechanism of cytotoxicity in the HL60 cell lines, based on TBZ's selective induction of apoptosis in the HL60R line, Grimaudo speculates a mode of action that involves bypassing drug resistance-related mechanisms such as the multidrug transporter (*see id.* at p. 1762, col. 1, first para.) or a differential interaction with topoisomerase II (*see* id. at 1761, col. 1 and 2).

7. The authors of Grimaudo, in consideration of the unique results obtained with TBZ, suggest that future studies should explore the mechanism of its anti-tumor and pro-apoptotic action. Grimaudo further suggests using TBZ derivatives that are metabolized more slowly than TBZ, and therefore retain their activity. I find no suggestion in Grimaudo that other NNRTIs would have the same anti-tumor effect in the HL60 cells or other cancer cells. Indeed, given the expectation that TBZ's effects were independent of its RT-inhibitory activity, Grimaudo's focus exclusively on TBZ derivatives rather than on other NNRTI's is entirely reasonable. Therefore, based on the data and conclusions of Grimaudo, one of skill in the art would have no reasonable expectation that NNRTIs, that are structurally unrelated to TBZ, such as nevirapine, efavirenz, delavirdine, and compounds in the class of 5,11-dihydro-6h-dipyrido[3,2-b:2',3'-e][1,4]diazepines, would exert similar cytotoxic effects in parental or drug-resistant cancer cell lines, simply based on their shared ability to inhibit viral RT. None of the data presented by Grimaudo substantiates such a conclusion.

8. In a subsequent publication by Grimaudo et al., "Apoptotic Effects of Thiazolobenzimidazole Derivatives on Sensitive and Multidrug Resistant Leukaemic Cells," *Eur. J. Cancer* 37(1):122–30 (2001) (Grimaudo 2001) (attached hereto as Exhibit 2), the results from the continued investigation of the cytotoxic activity of TBZ derivatives on the same cell lines (as used in Grimaudo) are presented. Grimaudo 2001 reports that these compounds exert their anti-tumor effects by activating the programmed cell death pathway (Grimaudo 2001 at p. 129, col. 1, last para). Grimaudo 2001 concludes that this activity is, at least in part, caspase mediated, as shown by the ability of caspase inhibitors to reduce the percentage of apoptosis induced by one of the TBZ derivatives (*id.* at para. 2). These findings, which were published well in advance of the filing date of the above referenced patent application, further support that one of skill in the art would have no reasonable expectation, based on the teachings of Grimaudo,

that NNRTIs that are structurally unrelated to TBZ, such as nevirapine, efavirenz, delavirdine, and compounds in the class of 5,11-dihydro-6h-dipyrido[3,2-b:2',3'-e][1,4]diazepines, would exhibit anti-tumor effects similar to that of TBZ.

9. Moreover, one of skill in the art would not generalize the findings of Grimaudo, based on data obtained in one acute myeloid leukemic cell line, to solid tumors, such as carcinomas, tumours of the nervous system, and fibro- and osteo-sarcomas because of there fondamental differences in terms of molecular mechanisms involved in the tumorigenic developement of these two major categories of cancers. Furthermore, an illustration is the fact that strategies used for the therapeutic treatments of these two types of cancers are not similar.

10. For the reasons discussed in paragraphs 5–9 above, I disagree with the PTO's position that one of skill in the art would have found it obvious, based on the teachings of Grimaudo, to counteract the loss of cellular differentiation and to treat cell proliferation in tumor pathologies by administering to a subject a compound in the class of 5,11-dihydro-6h-dipyrido[3,2-b:2',3'-e][1,4]diazepines, nevirapine, efavirenz, delavirdine, or corresponding salts thereof as taught by and claimed in the above referenced patent application.

11. Ghori investigated telomerase inhibition using three nucleoside retroviral reverse transcriptase inhibitors ("NRTI") (*i.e.*, not NNRTIs) as a therapeutic strategy for the treatment of colorectal cancer. Despite Ghori's demonstration that the three tested NRTIs, *i.e.*, azidothymidine (AZT), dideoxythymidine (ddT), and dideoxyguanidine (ddG), inhibited telomerase activity and slowed proliferation in the tumor cell line HT29, there are a number of reasons why one of skill in the art would not have expected other NRTIs or NNRTIs to be useful for inhibiting telomerase activity and treating cell proliferation in tumor pathologies.

12. Firstly, other studies investigating the potential use of NRTIs to inhibit telomerase and treat cancer have reported inconsistent results (reviewed by White et al., "Telomerase Inhibitors," *Trends in Biotech.* 19(3):114–120 (2001) ("White") (attached hereto as Exhibit 3) at p. 118, col. 1, last para.). For example, Strahl and Blackburn, "Effects of Reverse Transcriptase Inhibitors on Telomere Length and Telomerase Activity in Two Immortalized Human Cells Lines," *Mol. Cell. Biol.* 16(10):53–65 (1996) ("Strahl") (attached hereto as Exhibit 4) examined telomerase inhibition, telomere shortening, and cell growth rates in cell lines

derived from B-cell lymphoma and human T-cell leukemia using the nucleoside analogs AZT, arabinofuranyl-guanosine (Ara-G), ddG, deoxyinosine (ddI), deoxyadenosine (ddA), didehydrothymidin (d4T), and the non-nucleoside RT inhibitor phosphonoformic acid (foscarnet) (Strahl at abstract). Strahl reports that while ddG caused reproducible and progressive telomere shortening and telomerase inhibition, no effect on the cell population doubling rates or morphology were observed (*id.*). AZT caused progressive telomere shortening in some but not all T- and B-cell cultures, and prolonged passaging in Ara-G, ddI, ddA, d4t, or foscarnet did not cause reproducible telomere shortening or decreased cell growth rates of viability (*id.*). Similar to the results of Strahl, Murakami et al., "Inhibition of Telomerase Activity and Cell Proliferation by a Reverse Transcriptase Inhibitor in Gynaecological Cancer Cell Lines," *Eur. J. Cancer* 35(6):1027-34 (1999) ("Murakami") (attached hereto as Exhibit 5) reported the inhibition of telomerase activity and/or telomere length by AZT-5' triphosphate and ddI in the HEC-1 human endometrial adenocarcinoma cell line, but not the MCAS human ovarian cancer cell line (Murakami at abstract). In summarizing these divergent results, White concludes:

> [I]t is unlikely that these analogs are functioning through a selective inhibition of telomerase because their reduced proliferation is occurring in the setting of sufficiently long telomeres. A plausible explanation might be that the RTIs have a toxic effect on the cells, perhaps by inhibiting mitochondrial DNA replication leading to the observed reduction in telomerase activity, which is dose-dependent.

White at p. 118, col. 2, first para.. In view of White, Strahl, and Murakami, one of skill in the art would not have had a reasonable expectation that NRTIs other than those disclosed in Ghori, and certainly not NNRTIs would be useful for inhibiting telomerase activity and slowing proliferation of tumor cells.

13. Secondly, while there is at least *a priori* some rationale for testing NRTI mediated inhibition of telomerase based on their common mechanism of action, this rationale does not apply to NNRTIs which are structurally distinct and have a distinct mechanism of action. These differences are discussed more fully below.

14. NRTIs are known to inhibit RT activity by the common mechanism of DNA chain termination. Indeed, any RT will incorporate the NRTI analogues into newly

synthesized DNA, and once incorporated, DNA synthesis is halted (*see* White at p. 118, col. 1, second full para.; Ren et al., "Structure of HIV-2 Reverse Transciptase at 2.35-A Resolution and the Mechanism of Resistance to Non-Nucleoside Inhibitors," *PNAS* 99(22):14410–15 (2002) ("Ren") (attached hereto as Exhibit 6) at p. 14410, col. 1, first para.). Since all nucleoside analogues should bind to the catalytic domain of any RT, it might thus be expected *a priori* that a NRTI should have inhibitory activity on almost any RT. In fact, NRTIs, such as zidovudine and lamivudine, in their 5'-triphosphate forms, exert a broad spectrum of antiviral RT activity, including, for example, inhibition of both HIV-2 and HIV-1 RTs (*id.*).

15. In contrast to nucleoside analogs, NNRTIs act by a completely different mode of action that involves direct binding in a reversible and non-competitive manner to a hydrophobic pocket close to the polymerase catalytic site, in the p66 subunit of RT (*see* Joly and Yeni, "Non-Nucleoside Reverse Transcriptase Inhibitors," *AIDS Rev* 1:37–44 (1999) ("Joly") (attached hereto as Exhibit 7) at para. spanning pp. 37–38). Because the NNRTIs nevirapine, delavirdine, and efavirenze mediate inhibition of HIV-RT by interacting with this specific binding site on the RT enzyme, any slight variation brought about by a single point mutation can have a significant impact on inhibition (*id.*). Accordingly, other retroviral RT enzymes and some mammalian RT enzyme systems that lack this site are unaffected by these NNRTIs (*id.*; *see also* Ren at p. 14410, col. 1, first para. (NNRTIs are largely specific for HIV-1 RT)).

16. In view of the distinct mechanisms of action of NRTIs and NNRTIs, and the specific mechanism of NNRTI mediated RT inhibition (*i.e.*, direct binding to a hydrophobic pocket in the p66 subunit of RT), one of skill in the art would have had no reasonable expectation, based on the teachings of Ghori, that NNRTIs are generally effective inhibitors of any RT, particularly the reverse transcriptase catalytic subunit of human telomerase. In fact, the general knowledge (*see* paragraphs 14-15 above) would have suggested that NNRTIs would be largely ineffective against RTs other than HIV-1 RT. Therefore, persons of skill in the art would have lacked any expectation, based on Ghori, that NNRTIs, such as nevirapine, efavirenz, delavirdine, and compounds in the class of 5,11-dihydro-6h-dipyrido[3,2-b:2',3'-e][1,4]diazepines, would be useful for treating cell proliferation in tumor pathologies.

17. Thirdly, Damm et al., "A Highly Selective Telomerase Inhibitor Limiting Human Cancer Cell Proliferation," *EMBO J.* 20(24):6958–68 (2001) ("Damm") (attached hereto as Exhibit 8), which identifies a class of small molecules exhibiting selective inhibition of telomerase activity without RT inhibition (*see* Figure 1C), clearly demonstrates that telomerase is distinct from other DNA and RNA polymerases, including HIV RT. Thus, a compound with known specific inhibitory activity for telomerase cannot be expected to inhibit RTs generally.

18. Finally, inhibition of telomerase activity is known to induce senescence and cell death after a long lag period required for the attrition of telomeres (*see* Damm at p. 6958, col. 2, last para.). In contrast, the above referenced application demonstrates NNRTI-mediated differentiation of tumor cells cannot be attributed to the inhibition of telomerase activity, because the differentiation appears too rapidly to be linked to telomerase inhibition (*see e.g.*, Example 4 and Figure 4 showing nevirapine induced differentiation of myoblasts C2C7 after 90 hours, Example 4 and Figure 5, showing the nevirapine induced differentiation of teratocarcinoma F9 cells after 72 hours, and Example 5, Figure 6, showing nevirapine induced differentiation of AML cells after 5 days). This rapid induction of cell differentiation following NNRTI exposure clearly suggests such differentiation is mediated by a mechanism other than telomerase inhibition.

19. For the reasons set forth in paragraphs 12–18 above, one of skill in the art would not conclude, based on Ghori's demonstration that certain NRTIs inhibit telomerase activity and slow cellular proliferation, that NNRTIs—a structurally distinct class of compounds with a distinct mechanism of action—would likewise exert similar effects, be useful for counteracting the loss of cellular differentiation, and treating cell proliferation in tumor pathologies.

20. I hereby declare that all statements made herein of my own knowledge are true and that all statements made on information and belief are believed to be true; and further that these statements were made with the knowledge that willful false statements and the like so made are punishable by fine or imprisonment, or both, under section 1001 of Title 18 of the United States Code, and that such willful false statements may jeopardize the validity of the application or any patent issuing thereon.

Date: August 16, 2010

François Ichas, Ph.D.

Exhibit 1: Curriculum Vitae

Dr François Ichas

Date of birth: 2 May 1969, France
Nationality : French
Professional address :
INSERM U916 "VINCO" - Validation et Identification de Nouvelles Cibles en Oncologie
Institut Bergonié - 229 cours de l'Argonne - 33076 Bordeaux cedex - France
Tél : 05.56.33.04.26 Fax : 05.56.33.32.06 E-mail : francois.ichas@inserm.fr

Scientific Education

- 1987-1996 : Medicine School "Paul Broca" University Victor Segalen-Bordeaux 2, Bordeaux
- 1996 : Certificate of Clinical and Therapeutical Synthesis. Doctoral School of University Victor Segalen-Bordeaux 2
- 1996 : Thesis of University Bordeaux 2, Biomedical Sciences
- 2001 : Post-doctoral degree (authorization to direct researches - HDR), University of Bordeaux 2

Employment

- 1990-1993: Student in Biology (Lab of Histo-Embryology, University of Bordeaux 2). Profs. R. Maraud & R. Stoll
- 1993: FEBS short-term fellowship - University of Oxford, Dept. of Human Anatomy (Lab. of Developmental Biology, University of Oxford, UK). Encadrement: Pr. C.D. Stern
- 1993-1997 : Student (Thesis) in Mitochondrial Biophysics (GESBI, Bordeaux 2 University, France). Prof. J.P. Mazat
- 1994-1995 : Research Associate of the American Heart Association - University of Virginia (Dept. of Neuroscience, University of Virginia, Charlottesville, USA). Dr. J.D. Lechleiter
- 1997-1999 : Post-Doctoral researcher - Human Frontier University of Padova, Italy (Dept. of Biomedical Sciences, CNR-University of Padova, Italy). Profs. P. Bernardi & T. Pozzan
- 1999 : Research Associate INSERM (INSERM EMI-U.9929, Victor Segalen/Bordeaux 2 University). Director: Prof, J.P. Mazat
- 2000 : Group Leader in the European Institute of Biology and Chemistry (IECB)– Bordeaux, France
- 2003-2007 : Research Director – Director of the INSERM E.347 team
- 2004 : Translational research - CLCC Bergonié (Regional anti-cancer center) / INSERM
- 2007- : Department Director –INSERM U916 "VINCO" Validation and Identification of New Targets in Oncology

Valorization and transfer activities

- Collaborations with many pharmaceutical companies:
  - Janssen, Johnson & Johnson, Lafon, Organon, Pierre Fabre, Servier, Sanofi-aventis.
- Founder in 2003 of a biotech company « Fluofarma SA », specialized in High Content Screening (Oncology / Neuobiology). CSO.

Expertise and Honors

- 1993 : FEBS & Development (the Company of Biologists Ltd.) Summer Fellowships Unoviersty of Oxford, UK.
- 1994-1995 : Research scientist contract - American Heart Association University of Virginia, USA
- 1997-1999 : Human Frontier & Marie Curie (TMR) Research Felloships University of Padova, Italy
- 1998 : Laureate of the Bioenergeticist Prize 98 - Biophysical Society - 98 Biophysical Meeting (USA, Kansas City); Finalist of the Amersham/Science (AAAS) Molecular Biologist Contest 98
- 2000 : Editor of the Editorial Board of the International Journal "Cell Calcium"; Invited Editor for the special "Cell Calcium" entitled "Mitochondrial Calcium Signaling" (volume 28, December 2000)

Publications

Synthesis and study of antiproliferative activity of novel thienopyrimidines on glioblastoma cells.
Pédeboscq S, Gravier D, Casadebaig F, Hou G, Gissot A, De Giorgi F, Ichas F, Cambar J, Pometan JP.
Eur J Med Chem. 2010 Jun;45(6):2473-9. Epub 2010 Feb 18.
Recombinant differential anchorage probes that tower over the spatial dimension of intracellular signals for high content screening and analysis.
Schembri L, Zanese M, Depierre-Plinet G, Petit M, Elkaoukabi-Chaibi A, Tauzin L, Florean C, Lartigue L, Medina C, Rey C, Belloc F, Reiffers J, Ichas F, De Giorgi F.
Anal Chem. 2009 Dec 1;81(23):9590-8.
Outer membrane VDAC1 controls permeability transition of the inner mitochondrial membrane in cellulo during stress-induced apoptosis.
Tomasello F, Messina A, Lartigue L, Schembri L, Medina C, Reina S, Thoraval D, Crouzet M, Ichas F, De Pinto V, De Giorgi F.
Cell Res. 2009 Dec;19(12):1363-76. Epub 2009 Aug 11.

Anticancer drugs exert differential apoptotic and cytotoxic effects on glioblastoma primary cultures with various EGFR and bcl-2 profiles.
Pédeboscq S, L'Azou B, Passagne I, De Giorgi F, Ichas F, Liguoro D, Pometan JP, Cambar J.
J Exp Ther Oncol. 2009;8(2):105-16.
An intracellular wave of cytochrome c propagates and precedes Bax redistribution during apoptosis.
Lartigue L, Medina C, Schembri L, Chabert P, Zanese M, Tomasello F, Dalibart R, Thoraval D, Crouzet M, Ichas F, De Giorgi F.
J Cell Sci. 2008 Nov 1;121(Pt 21):3515-23. Epub 2008 Oct 7.
Cytotoxic and apoptotic effects of bortezomib and gefitinib compared to alkylating agents on human glioblastoma cells.
Pédeboscq S, L'Azou B, Passagne I, De Giorgi F, Ichas F, Pometan JP, Cambar J.
J Exp Ther Oncol. 2008;7(2):99-111.
Spatial relational memory requires hippocampal adult neurogenesis.
Dupret D, Revest JM, Koehl M, Ichas F, De Giorgi F, Costet P, Abrous DN, Piazza PV.
PLoS ONE. 2008 Apr 9;3(4):e1959.
High content analysis of gamma-secretase activity reveals variable dominance of presenilin mutations linked to familial Alzheimer's disease.
Florean C, Zampese E, Zanese M, Brunello L, Ichas F, De Giorgi F, Pizzo P.
Biochim Biophys Acta. 2008 Aug;1783(8):1551-60. Epub 2008 Apr 3.
Localization of Fas/CD95 into the lipid rafts on down-modulation of the phosphatidylinositol 3-kinase signaling pathway.
Bénéteau M, Pizon M, Chaigne-Delalande B, Daburon S, Moreau P, De Giorgi F, Ichas F, Rebillard A, Dimanche-Boitrel MT, Taupin JL, Moreau JF, Legembre P.
Mol Cancer Res. 2008 Apr;6(4):604-13.
Protein arginine (N)-methyl transferase 7 (PRMT7) as a potential target for the sensitization of tumor cells to camptothecins.
Verbiest V, Montaudon D, Tautu MT, Moukarzel J, Portail JP, Markovits J, Robert J, Ichas F, Pourquier P.
FEBS Lett. 2008 Apr 30;582(10):1483-9. Epub 2008 Mar 31.
Tyrosine hydroxylase and dopamine transporter expression in lactotrophs from postlactating rats: involvement in dopamine-induced apoptosis.
Jaubert A, Drutel G, Leste-Lasserre T, Ichas F, Bresson-Bepoldin L.
Endocrinology. 2007 Jun;148(6):2698-707. Epub 2007 Mar 15.
The HA tag is cleaved and loses immunoreactivity during apoptosis.
Schembri L, Dalibart R, Tomasello F, Legembre P, Ichas F, De Giorgi F.
Nat Methods. 2007 Feb;4(2):107-8. No abstract available.
Signaling pathway involved in the pro-apoptotic effect of dopamine in the GH3 pituitary cell line.
Jaubert A, Ichas F, Bresson-Bepoldin L.
Neuroendocrinology. 2006;83(2):77-88. Epub 2006 Jun 20.
Amplification of Fas-mediated apoptosis in type II cells via microdomain recruitment.
Legembre P, Daburon S, Moreau P, Ichas F, de Giorgi F, Moreau JF, Taupin JL.
Mol Cell Biol. 2005 Aug;25(15):6811-20.
Hepatitis C virus core triggers apoptosis in liver cells by inducing ER stress and ER calcium depletion.
Benali-Furet NL, Chami M, Houel L, De Giorgi F, Vernejoul F, Lagorce D, Buscail L, Bartenschlager R, Ichas F, Rizzuto R, Paterlini-Bréchot P.
Oncogene. 2005 Jul 21;24(31):4921-33.
Oligomeric Bax is a component of the putative cytochrome c release channel MAC, mitochondrial apoptosis-induced channel.
Dejean LM, Martinez-Caballero S, Guo L, Hughes C, Teijido O, Ducret T, Ichas F, Korsmeyer SJ, Antonsson B, Jonas EA, Kinnally KW.
Mol Biol Cell. 2005 May;16(5):2424-32. Epub 2005 Mar 16.
New functions of an old protein: the eukaryotic porin or voltage dependent anion selective channel (VDAC).
De Pinto V, Messina A, Accardi R, Aiello R, Guarino F, Tomasello MF, Tommasino M, Tasco G, Casadio R, Benz R, De Giorgi F, Ichas F, Baker M, Lawen A.
Ital J Biochem. 2003 Mar;52(1):17-24. Review.
RGD-functionalized spherulites as targeted vectors captured by adherent cultured cells.
Chenevier P, Delord B, Amédée J, Bareille R, Ichas F, Roux D.
Biochim Biophys Acta. 2002 Dec 16;1593(1):17-27.
Selective targeting of synthetic antioxidants to mitochondria: towards a mitochondrial medicine for neurodegenerative diseases?
Dessolin J, Schuler M, Quinart A, De Giorgi F, Ghosez L, Ichas F.
Eur J Pharmacol. 2002 Jul 5;447(2-3):155-61.
The permeability transition pore signals apoptosis by directing Bax translocation and multimerization.
De Giorgi F, Lartigue L, Bauer MK, Schubert A, Grimm S, Hanson GT, Remington SJ, Youle RJ, Ichas F.
FASEB J. 2002 Apr;16(6):607-9.

Electrical coupling and plasticity of the mitochondrial network.
De Giorgi F, Lartigue L, Ichas F.
Cell Calcium. 2000 Nov-Dec;28(5-6):365-70.
The mitochondrial permeability transition.
Bernardi P, Colonna R, Costantini P, Eriksson O, Fontaine E, Ichas F, Massari S, Nicolli A, Petronilli V, Scorrano L.
Biofactors. 1998;8(3-4):273-81. Review.
A ubiquinone-binding site regulates the mitochondrial permeability transition pore.
Fontaine E, Ichas F, Bernardi P.
J Biol Chem. 1998 Oct 2;273(40):25734-40.

Modulation of cell calcium signals by mitochondria.
Jouaville LS, Ichas F, Mazat JP.
Mol Cell Biochem. 1998 Jul;184(1-2):371-6.
From calcium signaling to cell death: two conformations for the mitochondrial permeability transition pore. Switching from low- to high-conductance state.
Ichas F, Mazat JP.
Biochim Biophys Acta. 1998 Aug 10;1366(1-2):33-50.
A model of mitochondrial Ca(2+)-induced Ca2+ release simulating the Ca2+ oscillations and spikes generated by mitochondria.
Selivanov VA, Ichas F, Holmuhamedov EL, Jouaville LS, Evtodienko YV, Mazat JP.
Biophys Chem. 1998 May 5;72(1-2):111-21.
Regulation of the permeability transition pore in skeletal muscle mitochondria. Modulation By electron flow through the respiratory chain complex i.
Fontaine E, Eriksson O, Ichas F, Bernardi P.
J Biol Chem. 1998 May 15;273(20):12662-8.
Mitochondria are excitable organelles capable of generating and conveying electrical and calcium signals.
Ichas F, Jouaville LS, Mazat JP.
Cell. 1997 Jun 27;89(7):1145-53.
Microtubule-active drugs suppress the closure of the permeability transition pore in tumour mitochondria.
Evtodienko YV, Teplova VV, Sidash SS, Ichas F, Mazat JP.
FEBS Lett. 1996 Sep 9;393(1):86-8.
Propofol and cellular calcium homeostasis.
Sztark F, Ichas F, Mazat JP, Dabadie P.
Anesthesiology. 1995 Dec;83(6):1386. No abstract available.
Synchronization of calcium waves by mitochondrial substrates in Xenopus laevis oocytes.
Jouaville LS, Ichas F, Holmuhamedov EL, Camacho P, Lechleiter JD.
Nature. 1995 Oct 5;377(6548):438-41.
Differential effects of verapamil and quinine on the reversal of doxorubicin resistance in a human leukemia cell line.
Bennis S, Ichas F, Robert J.
Int J Cancer. 1995 Jul 28;62(3):283-90.
Effects of the anaesthetic propofol on the calcium-induced permeability transition of rat heart mitochondria: direct pore inhibition and shift of the gating potential.
Sztark F, Ichas F, Ouhabi R, Dabadie P, Mazat JP.
FEBS Lett. 1995 Jul 10;368(1):101-4.
Action of testosterone on the estradiol-induced feminization of the male chick embryo.
Faucounau N, Ichas F, Stoll R, Maraud R.
Anat Embryol (Berl). 1995 Apr;191(4):377-9.
Action of testosterone on the anti-müllerian activity of the chick embryonic testis assayed in vivo by organotypic grafting.
Ichas F, Faucounau N, Stoll R, Maraud R.
Anat Embryol (Berl). 1994 Sep;190(3):297-9.
Mitochondrial calcium spiking: a transduction mechanism based on calcium-induced permeability transition involved in cell calcium signalling.
Ichas F, Jouaville LS, Sidash SS, Mazat JP, Holmuhamedov EL.
FEBS Lett. 1994 Jul 11;348(2):211-5.

Exhibit 2: Grimaudo et al., "Apoptotic Effects of Thiazolobenzimidazole Derivatives on Sensitive and Multidrug Resistant Leukaemic Cells," *Eur. J. Cancer* 37(1):122–30 (2001).

Display Settings: Abstract

Eur J Cancer. 2001 Jan;37(1):122-30.

Apoptotic effects of thiazolobenzimidazole derivatives on sensitive and multidrug resistant leukaemic cells.

Grimaudo S, Raimondi MV, Capone F, Chimirri A, Poretto F, Monforte AM, Simoni D, Tolomeo M.

Divisione di Ematologia e Servizio A.I.D.S., Facolta' di Medicina, Universita' di Palermo, Palermo, Italy. dusonc@unipa.it

Abstract

We investigated the cytotoxic activity of eight thiazolobenzimidazole derivatives on sensitive HL60 and multidrug-resistant (MDR) (HL60R) leukaemia cell lines. The antitumour effects of these compounds were compared with those of RS-TBZ, a thiazolobenzimidazole derivative, previously described in our reports, that was able to induce apoptosis more markedly in MDR cells than in the parental sensitive cell lines. Only two compounds in this study proved to have interesting effects: (a) the S-enantiomer of TBZ, that was able to induce apoptosis in MDR cells in a slightly more selective manner than TBZ (racemic form); and (b) TBZ-4-OCH3 (TBZ-4-OCH3), that showed cytotoxic and apoptotic effects on sensitive and resistant leukaemia cells greater than TBZ, without cytotoxic effects on normal haemopoietic progenitor cells. Moreover, we observed that TBZ-4-OCH3 was also active in cells expressing Bcr-Abl, an oncogene that confers resistance to apoptosis induced by several stimuli, including cytotoxic agents. The inhibition of caspase-9 and caspase-3 by specific polypeptide inhibitors decreased the apoptotic effects of TBZ-4-OCH3 in HL60 cells indicating that apoptosis induced by this compound was, at least partly, caspase-mediated. On the contrary, the blocking of FL-associated cell surface antigen (Fas) using a specific Fas -blocking monoclonal antibody did not affect the level of apoptosis induced by TBZ-4-OCH3 suggesting that the Fas pathway was not involved. In addition, the caspase 8 inhibitor was unable to inhibit the apoptotic activity of TBZ-4-OCH3. The very low toxicity shown by TBZ-4-OCH3 in normal haemopoietic progenitor cells and its high activity in sensitive and MDR neoplastic cells suggest a possible clinical use for this new compound.

PMID: 11165139 [PubMed - indexed for MEDLINE]

Apoptotic effects of thiazolobenzimidazole derivatives on sensitive and multidrug resistant leukaemic cells

S. Grimaudo [a,*], M.V. Raimondi [a], F. Capone [a], A. Chimirri [b], F. Poretto [a], A.M. Monforte [c], D. Simoni [d], M. Tolomeo [a]

[a]

have recently observed that the 2,6-difluorophenyl-thiazolobenzimidazole derivative called TBZ (RS-TBZ) was able to induce apoptosis selectively in the P-glycoprotein (Pgp)-expressing multidrug resistant (MDR) HL60R cell line [12]. This property was particularly interesting considering that in our study several classical antineoplastic agents were unable to induce apoptosis in HL60R cells when used at concentrations able to overcome the effects of Pgp. However, TBZ had a low cytotoxic activity: in fact it was active only at concentration of approximately 50 μM. Thus, in this work, we investigated the apoptotic activity in neoplastic cells of novel thiazolobenzimidazole derivatives in order to identify compounds more active than TBZ. The toxic effects on haemopoietic normal cells were also investigated.

2. Materials and methods

2.1. Cell culture

Continuous neoplastic cells (HL60, HL60R, K562 and K562ADR) were grown in Roswell Park Memorial Institute (RPMI) 1640 (Gibco Grand Island, NY, USA) containing 10% fetal calf serum (FCS) (Gibco), 100 U/ml penicillin (Gibco), 100 μg/ml streptomycin (Gibco), and 2 mM L-glutamine (Sigma Chemical Co., St Louis, MO, USA) in a 5% CO_2 atmosphere at 37°C. MDR HL60R and K562ADR cells were selected from parental sensitive HL60 and K562 cells by continuous exposure to increasing concentrations of daunorubicin (HL60R) or doxorubicin.

2.2. Chemicals

Daunorubicin, etoposide and mitoxantrone were purchased from Sigma Chemical Company. The caspase inhibitors Ac-DEVD-CHO (acetyl-Asp-Glu-Val-Asp-aldehyde), Ac-Z-LEHD-fmk (Z-Leu-Glu(Ome)-His-Asp(Ome)-fmk), Ac-IETD-CHO (N-acetyl-Ile-Glu-Thr-Asp-CHO) (aldehyde) and Z-VAD-fmk (benzyl-oxycarbonyl-Val-Ala-Asp-fluoromethyl ketone) were purchased from Alexis Biochemicals (Laufelfingen, Switzerland). The Fas agonistic antibody CH11 and the anti-Fas Ab ZB4 were purchased from Upstate Biotechnology (Lake Placid NY, USA). All other reagents were analytical grade.

2.3. Synthesis of thiazolobenzimidazole derivatives (TBZs)

The one-pot synthesis of 1H, 3H-thiazolo[3,4-a]benzimidazoles (TBZs) was carried out by a condensation–cyclisation reaction between o-phenylenediamine 1, aromatic aldehydes 2 and mercaptoacetic acid 3 in refluxing benzene (18a,b) as shown in Fig. 1.

In order to explore the influence of molecular modifications on biological activity, we synthesised derivatives with substituents on the C-1 phenyl ring having different electronic, steric and lipophilic properties. The compounds were obtained in good yields and characterised by spectroscopic methods.

2.4. Drug preparation

Each thiazolobenzoimidazole derivative was dissolved in dimethylsulphoxide (DMSO) in a stock solution at a concentration of 20 mM, stored at −20°C and protected from the light. In each experiment, DMSO never exceeded 0.5% and this percentage did not interfere with cell growth.

2.5. Cytotoxicity assays

To evaluate the number of live and dead neoplastic cells, the cells were stained with trypan blue and counted on a haemocytometer. To determine the growth inhibitory activity of the drugs tested, 2×10^5 cells were plated into 25 mm wells (Costar, Cambridge, UK) in 1 ml of complete medium and treated with different concentrations of each drug. After 48 h of incubation, the number of viable cells was determined and expressed as a per cent of control proliferation. To evaluate the cytotoxic effects on the haemopoietic progenitor cells, mononucleated cells obtained from bone marrow aspirates of five normal volunteers were treated with different concentrations of each drug. The *in vitro* clonal assays for haemopoietic progenitor cells were performed as described in Ref. [13]. Briefly, 3–5 ml bone marrow were diluted in RPMI 1640, layered over Ficoll-Hypaque gradients (density, 1.077), centrifuged at 400*g* for 30 min, and the interface mononuclear cells collected. The interface cells were washed three times in phosphate buffered saline (PBS), counted, and resuspended at a concentration of 1×10^5 in modified Eagle medium (MEM) containing 0.9% methylcellulose, 30% FCS, 10^{-5} M 2-mercaptoethanol, 5% phytohemoagglutinin lymphocyte culture medium (PHA–LCM), and 1 IU human erythropoietin in 15-mm plastic dishes. After 14 days of culture at 37°C in an environment of 5% CO_2 and 100% humidity, the number of colony forming unit (CFU)-multipotential (GEMM), CFU-granulocyte-macrophage (GM), and CFU-erythroid (E) was evaluated.

2.6. Flow cytometry analysis of the cell cycle and apoptosis

The cells were washed once in ice-cold PBS and resuspended at 1×10^6 ml in a hypotonic fluorochrome solution containing propidium iodide (Sigma) 50 μg/ml in 0.1% sodium citrate plus 0.03% (v/v) nonidet P-40 (Sigma). After a 30 min incubation, the samples were

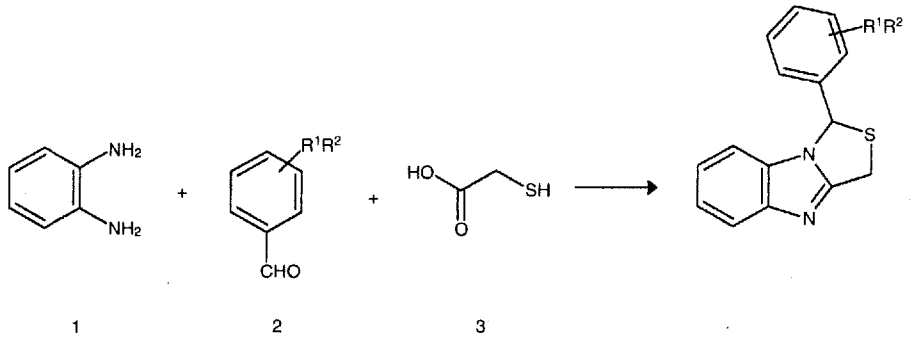

1 2 3

	R^1	R^2
TBZ-H	H	H
TBZ-2,6-Cl_2	2-Cl	6-Cl
TBZ-2,3-$(OCH_3)_2$	2-OCH_3	3-OCH_3
TBZ-3-OCH_3	3-OCH_3	H
TBZ-2-F	2-F	H
RS-TBZ	2-F	6-F
S-TBZ	2-F	6-F
R-TBZ	2-F	6-F
TBZ-4-OCH_3	4-OCH_3	H

Fig. 1. Chemical structure of synthesised thiazolobenzimidazole derivatives.

filtered through Nylon cloth, and their fluorescence was analysed as single-parameter frequency histograms using a fluorescent activated cell sorter (FACScan) flow cytometer. Apoptosis was determined by evaluating the percentage of hypoploid nuclei accumulated in the sub-G_0G_1 peak after labelling with propidium iodide [13].

2.7. Morphological evaluation of apoptosis and necrosis

Drug-induced apoptosis and necrosis were determined morphologically after labelling with acridine orange and ethidium bromide [14]. The cells (2×10^5) were centrifuged (300*g*) and the pellet was resuspended in 25 μl of the dye mixture. Ten microlitres of the mixture was examined in oil immersion with a 100× objective using a fluorescence microscope. Live cells were determined by the uptake of acridine orange (green fluorescence) and exclusion of ethidium bromide (red fluorescence). Live and dead apoptotic cells were identified by perinuclear condensation of chromatin stained by acridine orange or ethidium bromide, respectively, and by the formation of apoptotic bodies. Necrotic cells were identified by uniform labelling of the cells with ethidium bromide.

3. Results

3.1. Cytotoxicity assay

The chemical structure of the new thiazolobenzoimidazole derivatives used in this study are shown in Fig. 1. The stability and the solubility in DMSO was examined and no difference was observed between the new derivatives and TBZ (RS-TBZ). Table 1 shows the cytotoxic activity, expressed as inhibitory concentration (IC) 50 and IC90, of these compounds in sensitive HL60 and MDR HL60R cells. TBZ-4-OCH_3 (TBZ-4-OMe), characterised by the presence of a methoxy group at the 4-position of the C-1 phenyl substituent, was the most active compound in both the sensitive and resistant cell lines. Compounds TBZ-2,3-$(OCH_3)_2$ and TBZ-2,6-Cl_2 showed a slightly higher cytotoxic activity in HL60 cells compared with RS-TBZ, but were less effective in the resistant HL60R cells. The R-enantiomer of TBZ was more active than RS-TBZ in both the sensitive and resistant cells, while the S-enantiomer was more active in the HL60R cell line but less active in the sensitive cells.

3.2. Effects of TBZ derivatives on normal haematopoietic precursors

To evaluate the myelotoxicity induced by TBZ derivatives, we studied the effects of RS-TBZ, R-TBZ, S-TBZ and TBZ-4-OCH_3 on the growth of human haemopoietic progenitors CFU-GEMM, CFU-GM and CFU-E by clonal assay (Fig. 2). At the concentrations active on HL60 and HL60R cells, the racemic TBZ and the R- and S- enantiomers did not show any toxicity on CFU-GEMM and CFU-GM, while, a considerable toxicity was observed on erythroid precursors when these drugs were used at concentrations greater than 75 μM. Interestingly, TBZ-4-OCH_3 did not show any inhibition of myeloid and erythroid precursors when used at concentrations greater than those active in HL60 or HL60R cells (25 μM).

3.3. Apoptosis and cell cycle

Fig. 3(a) and (b) shows the apoptotic effects of RS- S- and R-TBZ used at concentrations of 50 μM, 75 μM and 100 μM in HL60 and HL60R cells. At all concentrations used, S-TBZ was the less active in HL60 cells, but it showed an apoptosis-inducing activity similar to RS- and R-TBZ in the MDR HL60R cells.

TBZ-4-OCH_3 was the thiazolobenzoimidazole derivative that was more active in inducing apoptosis in HL60 and HL60R cell lines. It was approximately 24-fold more active than R-TBZ in HL60 cells and approximately 5-fold more active than RS-, S and R-TBZ in the HL60R cells, respectively (Fig. 3c). Flow cytometry assay shows an evident apoptotic pre-G_0G_1-peak with a decrease of cells in the G_0G_1-phase in the HL60 and HL60R cells treated with 5 or 10 μM TBZ-4-

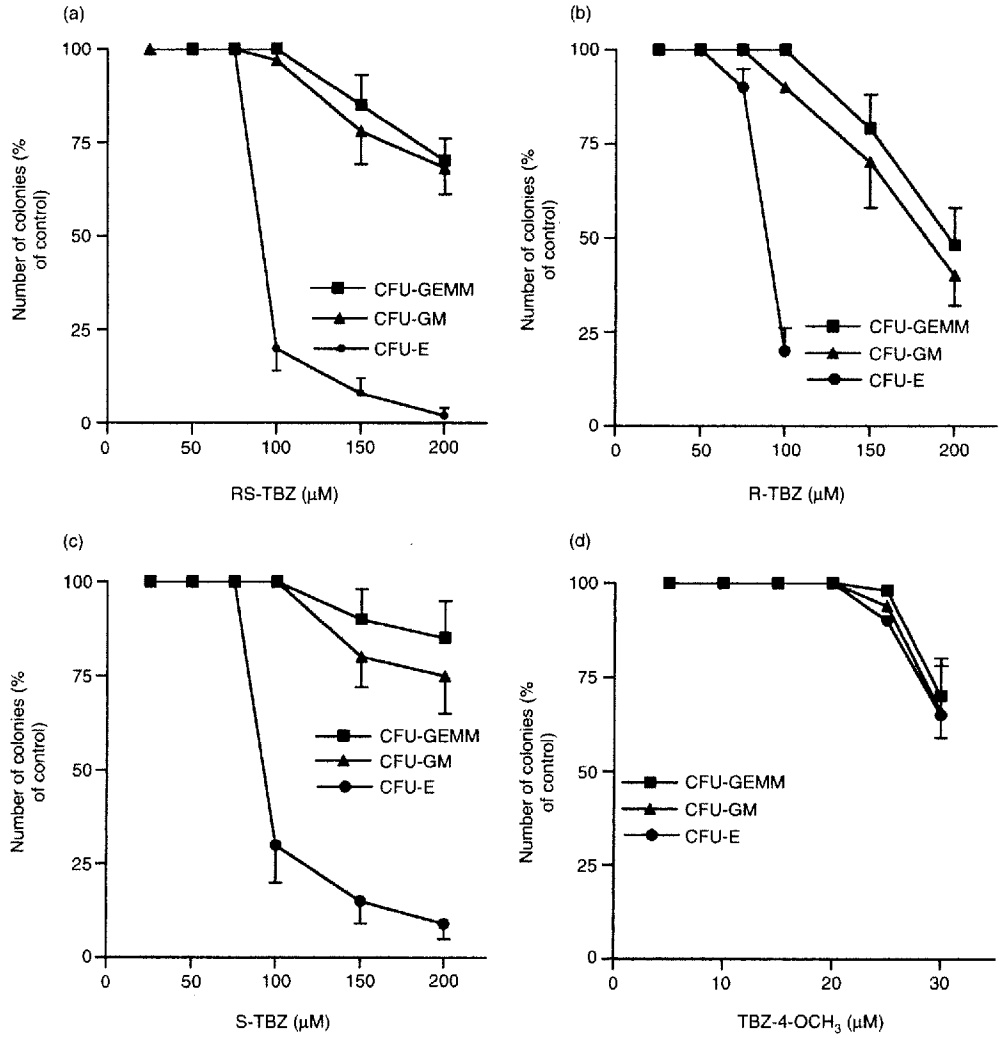

Fig. 2. Effects of (a) RS-TBZ; (b) R-TBZ; (c) S-TBZ and (d) TBZ-4-OCH_3 on colony forming unit (CFU) GEMM, CFU-GM and CFU-E. Results are means ±standard deviation (S.D.) of five experiments performed on mononucleated cells obtained from bone marrow aspirates of five normal volunteers. CFU-GEMM, colony forming unit-multipotential; CFU-GM, colony forming unit-granulocyte macrophage; CFU-E, colony forming unit-erythroid.

OCH_3 (Fig. 4). Interestingly, TBZ-4-OCH_3 was also able to induce apoptosis in the K562 cells, a fusion product of the bcr and c-Abelson genes (Bcr-Abl)-expressing cell line that is resistant to apoptosis caused by several cytotoxic agents. As shown in Table 2, chemotherapeutic drugs commonly used in the treatment of leukaemia, such as daunorubicin, etoposide and mitoxantrone, were able to induce apoptosis in K562 cells only at concentrations many times greater than those effective in the HL60 cells. On the contrary, the activity of TBZ-4-OCH_3, in the K562 cells and in the MDR counterpart K562ADR was similar to that observed in HL60 and HL60R cells (Fig. 3c and d). These data indicate that the apoptosis-inducing activity of TBZ-4-OCH_3 is unaffected by the presence of the *Bcr-Abl* oncogene in the neoplastic target cells. Moreover, we examined whether TBZ-4-OCH_3 was able to reverse the MDR in HL60R and K562ADR cells. We treated these MDR cell lines with different subtoxic concentrations of TBZ-4-OCH_3 (0.1, 0.5 or 1 μM) and, after 2 h, with daunorubicin (0.1 μg/ml for HL60R and 0.25 μg/ml for K562ADR). TBZ-4-OCH_3 did not modify the resistance (in terms of cytotoxicity and apoptosis) to daunorubicin. On the contrary, verapamil used at a concentration of 5 μg/ml, or cyclosporin A (2 μg/ml) were able to sensitise MDR cells to the cytotoxic effects of daunorubicin (data not shown).

3.4. *Effects of Fas and caspase inhibitors on the apoptosis induced by TBZ-4-OCH_3*

Previously, we observed that HL60 is a cell line that expresses the cell death receptor Fas and these cells undergo apoptosis after treatment with the agonistic

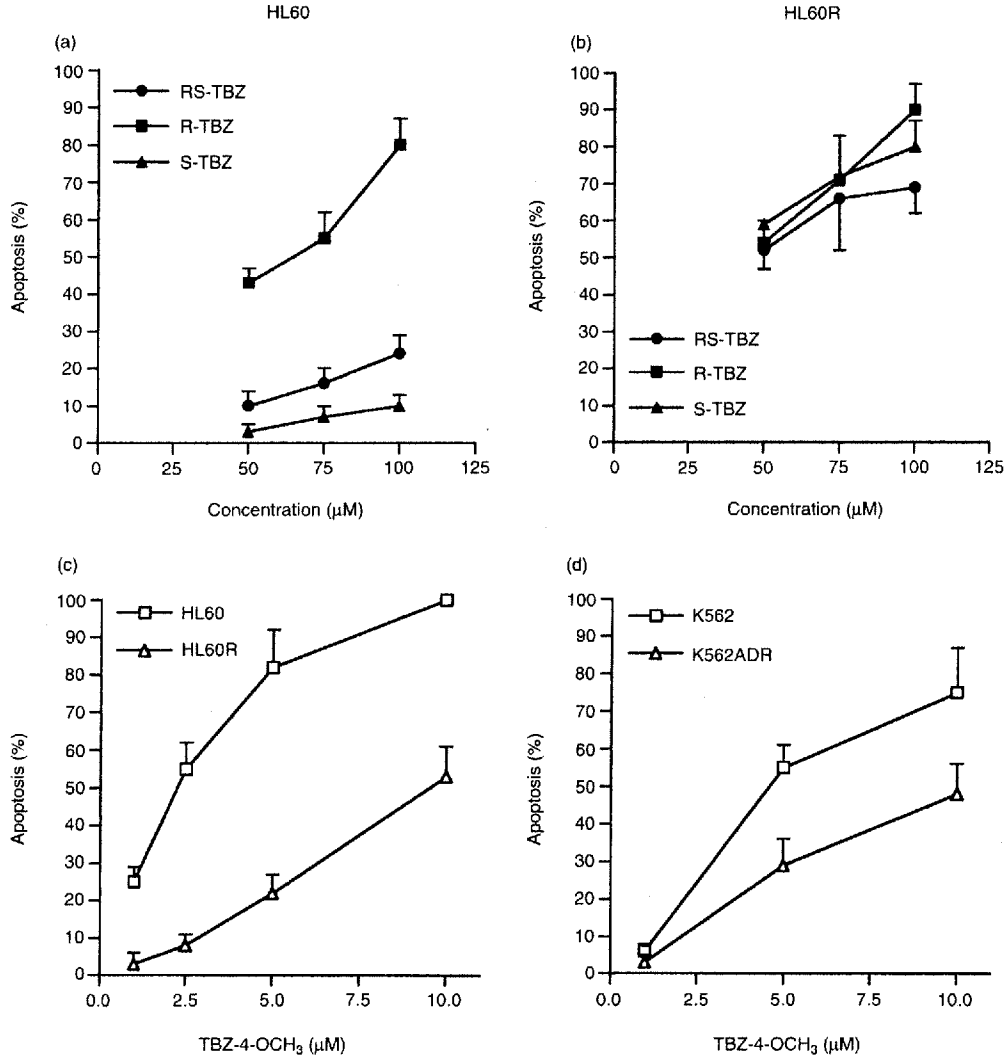

Fig. 3. Apoptosis-inducing activity, evaluated by morphological examination of RS-TBZ, R-TBZ, S-TBZ and TBZ-4-OCH_3 in HL60 and HL60R cell lines (a, b and c). (d) Apoptosis-inducing activity of TBZ-4-OCH_3 in K562 and K562ADR cells. Results are means ±standard deviations (S.D.) of at least five experiments.

anti-Fas monoclonal antibody CH11 [15]. To understand if TBZ-4-OCH_3-induced apoptosis was Fas-mediated, we treated HL60 cells with a Fas-blocking monoclonal antibody (ZB4) or with the caspase 8 inhibitor Ac-IETD-CHO, and, after 2 h with 2.5 μM TBZ-4-OCH_3. As shown in Fig. 5, these inhibitors were unable to inhibit TBZ-4-OCH_3-induced apoptosis which was, on the contrary, partially inhibited by the pan-caspase inhibitor Ac-Z-VAD-fmk, by the caspase 9 inhibitor Ac-Z-LHED-fmk and by the caspase 3 inhibitor Ac-DEVD-CHO.

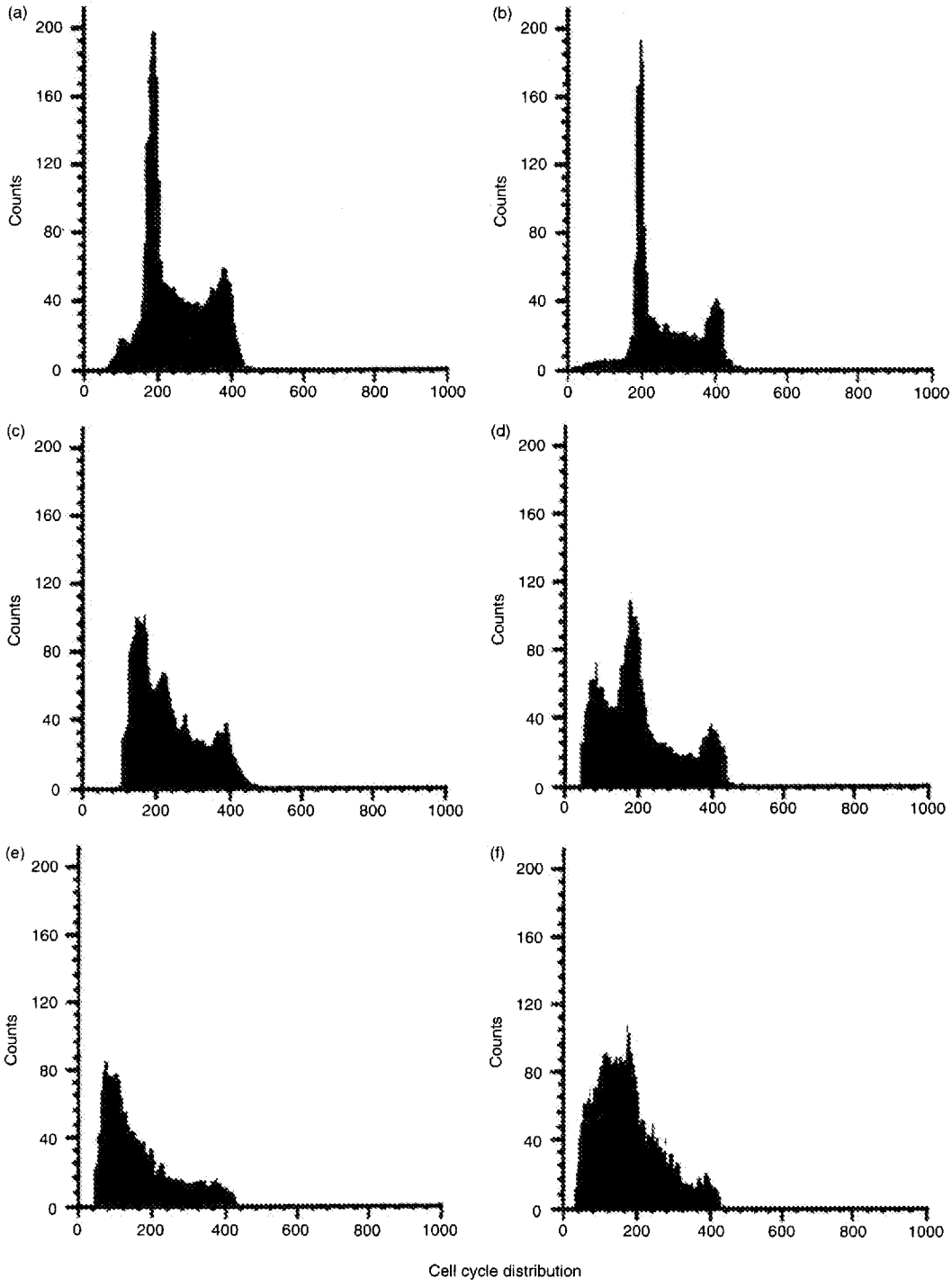

Fig. 4. Flow cytometric assay of cell cycle distribution of HL60 and HL60R cells after 48 h exposure to TBZ-4-OCH_3. (a) Untreated HL60 cells; (b) untreated HL60R cells; (c) HL60 cells treated with 5 μM TBZ-4-OCH_3; (d) HL60R cells treated with 5 μM TBZ-4-OCH_3; (e) HL60 cells treated with 10 μM TBZ-4-OCH_3 and (f) HL60R cells treated with 10 μM TBZ-4-OCH_3.

Table 1
IC50 and IC90 of different thiazolobenzimidazole derivatives in sensitive HL60 and in multidrug resistant HL60R cell lines

	HL60		HL60R	
	IC50 (μM)	IC90 (μM)	IC50 (μM)	IC90 (μM)
TBZ-H	75 (±8)	180 (±13)	120 (±18)	210 (±11)
TBZ-2,6-Cl_2	25 (±4)	100 (±10)	100 (±12)	250 (±25)
TBZ-2,3-$(OCH_3)_2$	23 (±3)	100 (±9)	120 (±20)	280 (±23)
TBZ-3-OCH_3	40 (±16)	240 (±17)	75 (±8)	270 (±11)
TBZ-2-F	80 (±6)	250 (±17)	130 (±16)	300 (±22)
RS-TBZ	50 (±9)	150 (±13)	55 (±5)	100 (±7)
S-TBZ	75 (±10)	250 (±22)	25 (±3)	75 (±9)
R-TBZ	25 (±4)	85 (±12)	20 (±3)	60 (±8)
TBZ-4-OCH_3	1 (±0.2)	5 (±0.2)	3 (±0.4)	10 (±2)

Evaluation after 48 h of treatment. Results are means ±S.D. of at least five experiments.

IC50, inhibitory concentration required for 50% inhibition; IC90, inhibitory concentration required for 90% inhibition; S.D., standard deviation.

Table 2
Apoptosis inducing activity evaluated as AC70 (drug concentration able to induce 70% apoptosis) of TBZ-4-OCH_3 and other antitumoral drugs in HL60 and K562 cell lines

	AC70 (μM)		
	HL60	K562	R[a]
Daunorubicin	0.028 (±0.005)	0.56 (±0.1)	20
Etoposide	0.1 (±0.02)	100 (±20)	1000
Mitoxantrone	0.005 (±0.001)	0.5 (±0.09)	100
TBZ-4-OCH_3	3.8 (±0.7)	8 (±1.6)	2.1

Evaluation after 48 h of treatment. Results are means ±S.D. of at least five experiments. S.D., standard deviation.

[a] Ratio between AC70 in K562 cells and AC70 in HL60 cells.

4. Discussion

TBZ is an anti-HIV thiazolobenzoimidazole derivative able to inhibit the HIV-1 reverse transcriptase [16–19]. We had previously observed that TBZ was active as an antitumoral agent both in sensitive and MDR cell lines when used at concentrations higher (75–100 μM) than those required to exert its antiviral activity (1 μM). Furthermore, TBZ has been shown to inhibit the growth of leukaemic HL60 cells with a recruitment in the G_0G_1 phase of the cell cycle. Moreover, it induced a more marked apoptosis in MDR HL60R cells compared with the sensitive parental HL60 cell line [12]. In this study, the antitumour activity of novel thiazolobenzoimidazole derivatives was investigated, which were synthesised with the aim of identifying more active TBZ analogues. The compounds TBZ-2,6-Cl_2 and TBZ-2,3-$(OCH_3)_2$, were more active than RS-TBZ in HL60-sensitive cells, but were less effective in the MDR HL60R cells. The R and S enantiomers of TBZ showed a similar cytotoxicity in the HL60R cells, while, in the sensitive HL60 cells, the activity of these enantiomers was markedly different, especially in terms of the induction of apoptosis. In fact, the S-enantiomer completely failed to induce apoptosis when used at a concentration of 100 μM. In contrast, the R-enantiomer exhibited a similar apoptotic activity in the HL60 cells to that observed in the HL60R cells.These data indicate

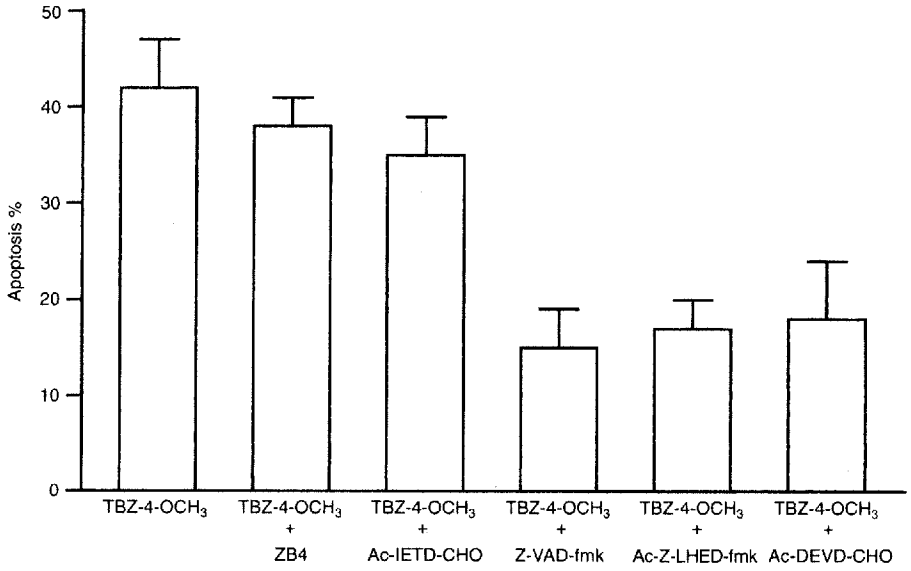

Fig. 5. Effects of the Fas-blocking monoclonal antibody ZB4, the caspase-8 inhibitor Ac-IETD-CHO, the pan-caspase inhibitor Z-VAD-fmk, the caspase-9 inhibitor Ac-Z-LEHD-fmk, and the caspase-3 inhibitor Ac-DEVD-CHO on the apoptotic-inducing activity of TBZ-4-OCH_3 in HL60 cells. Cells were incubated with 200 μM of each caspase inhibitor or with 0.5 μg/ml of ZB4 and, after 2 h, with 5 μM TBZ-4-OCH_3. Evaluation was after 24 h of treatment. Results are means ±standard deviation (S.D.) of at least five experiments.

that the selective apoptosis-inducing activity of RS-TBZ in MDR cells depends only on the presence of the S-component of the racemic compound.

The derivative TBZ-4-OCH_3 was the most active compound identified in this study. It showed an IC50 25 times lower than TBZ-2,6-Cl_2 and 23 times lower than TBZ-2,3-$(OCH_3)_2$, in HL60 cells and approximately 7 and 8 times lower than the R- and S-TBZ derivatives, respectively, in the HL60R cells. TBZ-4-OCH_3 induced cytotoxicity in HL60 cells at concentrations comparable with those required for TBZ to exert its antiviral activity (1 μM). Moreover, TBZ-4-OCH_3 did not show any toxicity in normal haemopoietic progenitor cells, even when used at high concentrations (25 μM). We also observed that TBZ-4-OCH_3 exerts its antitumour activity by primarily inducing programmed cell death in the target cells. This activity is, at least in part, caspase-mediated, as shown by the ability of caspase inhibitors to reduce the percentage of apoptotic cells. In particular, caspase 9 and caspase 3 seem to be involved in the TBZ-4-OCH_3-induced apoptosis. On the contrary, apoptosis was not modified by the inhibitor of caspase 8. Moreover, the use of a Fas receptor blocking monoclonal antibody did not inhibit apoptosis, confirming that the Fas pathway is not involved in the programmed cell death induced by TBZ-4-OCH_3. Another important property of this compound was its activity in cells expressing the Philadelphia chromosome such as the K562 cell line. The Philadelphia chromosome is the product of a reciprocal exchange between the long arms of chromosomes 9 and 22. This fusion event results in a hybrid gene in which the amino terminal sequence of the *bcr* gene on chromosome 22 is fused to the second exon of the *c-abl* gene on chromosome 9 [20]. The resulting Bcr–Abl protein product is an oncoprotein that confers resistance to apoptosis induced by many anticancer drugs such as etoposide, actinomycin D, cycloheximide and dexamethasone [3,21–24]. We observed that TBZ-4-OCH_3 induced apoptosis in K562 cells when used at a concentration only 2.1 higher than the concentration effective in HL60 cells. These data are significant considering that drugs commonly used in the treatment of leukaemia such as daunorubicin, etoposide and mitoxantrone are active in terms of apoptosis, in K562 cells at concentrations many times higher than the concentrations that are active in HL60 cells.

In conclusion, two interesting thiazolobenzoimidazole derivatives have been identified: the S-TBZ, characterised by a selective action in MDR cells greater than that previously described for the racemic TBZ, and the TBZ-4-OCH_3 that showed a potent antitumour activity in sensitive and MDR leukaemia cells with very low toxic effects in normal haemopoietic progenitor cells. Like TBZ, these thiazolobenzoimidazole derivatives exert their antitumour effects by activating the programmed cell death pathway. At the moment, the mechanisms of the selective activity in MDR cells shown by S-TBZ are not known; however, this property may be useful in the treatment of MDR malignancies to selectively kill only Pgp-expressing neoplastic cells while preserving Pgp-negative normal cells.

References

1. Collins RJ, Harmon BV, Souvlis T, Pope JH, Kerr JFR. Effects of cycloheximide on B-chronic lymphocytic leukaemic and normal lymphocytes in vitro: induction of apoptosis. *Br J Cancer* 1991, **64**, 518–522.
2. Walker PR, Smith C, Youdale T, Leblanc J, Whitfield JF, Sikorska M. Topoisomerase II-reactive drugs induce apoptosis in thymocytes. *Cancer Res* 1991, **51**, 1078–1084.
3. Martins LM, Mesner PW, Kottke TJ, *et al.* Comparison of caspase activation and subcellular localization in HL-60 and K562 cells undergoing etoposide-induced apoptosis. *Blood* 1997, **11**, 4283–4296.
4. Vial JP, Belloc F, Dumain P, *et al.* Study of the apoptosis induced in vitro by antitumoral drugs on leukaemic cells. *Leukemia Res* 1997, **21**, 163–172.
5. Salvesen GS, Dixit VM. Caspases: intracellular signaling by proteolysis. *Cell* 1997, **91**, 443–446.
6. Alnemri ES. Mammalian cell death proteases: a family og highly conserved aspartate specific proteases. *J Cell Biochem* 1997, **64**, 33–42.
7. Decaudin D, Geley S, Hirsch T, *et al.* Bcl-2 and Bcl-xL antagonize the mitochondrial dysfunction preceding nuclear apoptosis induced by chemotherapeutic agents. *Cancer Res* 1997, **57**, 62–67.
8. Nagata S, Golstein P. The Fas death factor. *Science* 1995, **267**, 1449–1455.
9. Friesen C, Herr I, Krammer PH, Debatin K-M. Involvement of the CD95 (APO-1/Fas) receptor/ligand system in drug-induced apoptosis in leukemia cells. *Nature Med* 1996, **5**, 574–577.
10. Muller M, Strand S, Hug H, *et al.* Drug-induced apoptosis in hepatoma cells is mediated by the CD95 (APO-/Fas) receptor/ligand system and involves activation of wild-type p53. *J Clin Invest* 1997, **99**, 403–413.
11. Fulda S, Sieverts H, Friesen C, Herr I, Debatin KM. The CD95 (APO-/Fas) system mediates drug-induced apoptosis in neuroblastoma cells. *Cancer Res* 1997, **57**, 3823–3829.
12. Grimaudo S, Tolomeo M, Chimirri A, Zappala M, Gancitano RA, D'Alessandro N. Selective induction of apoptosis in multidrug resistant HL60R cells by the thiazolobenzoimidazole derivative 1-(2,6-difluorophenyl)-1H,3H-thiazolo 3,4-a(benzimidazole) (TBZ). *Eur J Cancer* 1998, **11A**, 1756–1763.
13. Darziynkiewick Z, Bruno S, Del Bino G, *et al.* Features of apoptotic cells measured by flow cytometry. *Cytometry* 1992, **13**, 795–798.
14. Duke RC, Cohen JJ. Morphological and biochemical assays of apoptosis. In Coligan JE, Kruisbeak AM, *et al.*, eds. *Current Protocols in Immunology*. New York, John Wiley & Sons, 1992, 3.17.1.
15. Tolomeo M, Grimaudo S, Cannizzo G, *et al.* Implication of Fas/APO-1 and NF-kB in resistance to drug-induced apoptosis in MDR leukemic cells. *Haematologica* 1999, **84**, 291.
16. Hizi A, Tal R, Shaharabany M, *et al.* Specific inhibition of the reverse transcriptase of human immunodeficiency virus type 1 and the chimeric enzymes of human immunodeficiency virus type 1 and type 2 nonnucleoside inhibitors. *Antimicrob Agents Chemother* 1993, **37**, 1037–1042.
17. Artico M. Non nucleoside anti-HIV reverse transcriptase inhibitors (NNRTIs); a chemical survey from lead compounds to select drugs for clinical trials. *Il Farmaco* 1996, **51**, 305–331.
18. Chimirri A, Grasso S, Molica C, *et al.* Structural features and anti-HIV activity of the isomers of 1-(2′,6′-difluorophenyl)-

1H,3H-thiazolo(3,4-a)benzimidazole, a potent non-nucleoside HIV-1 reverse transcriptase inhibitor. *Antiviral Chem Chemother* 1997, **8**, 83–90.

19. Chimirri A, Grasso S, Monforte AM, Monforte P, Zappala' M. Anti-HIV agents II: synthesis and in vitro anti-HIV activity of novel 1H,3H-thiazolo(3,4-a)benzimidazoles. *Il Farmaco* 1991, **46**, 925–933.
20. Groeffen J, Heistenkamp N. The BCR/ABL hybrid gene. In Goldman JM, ed. *Chronic Myeloid Leukemia.* London, Bailliere Tindall, 1987, 983–999.
21. Bedi A, Zehnbauer A, Barber J, Sharkis S, Jones R. Inhibition of apoptosis by BCR-ABL in chronic myeloid leukemia. *Blood* 1994, **83**, 2038–2040.
22. McGahon A, Bissonette RP, Schmitt M, Cotter K, Green DR, Cotter TG. Bcr-Abl maintains resistance of chronic myelogenous leukemia cells to apoptotic cell death. *Blood* 1994, **83**, 1179–1187.
23. McGahon JA, Brown DG, Martin SJ, *et al.* Downregulation of Bcr-Abl in K562 cells restores susceptibility to apoptosis: characterization of the apoptotic death. *Cell Death Different* 1997, **4**, 95–104.
24. Bedi A, Barber JP, Bedi GC, *et al.* BCR–ABL-mediated inhibition of apoptosis with delay of G2/M transition after DNA damage: a mechanism of resistance to multiple anticancer agents. *Blood* 1995, **86**, 1148–1158.

Exhibit 3: White et al., "Telomerase Inhibitors," *Trends in Biotech.* 19(3):114–120 (2001).

14 Hidalgo, E. and Demple, B. (1994) An iron–sulfur center essential for transcriptional activation by the redox-sensing SoxR protein. *EMBO J.* 13, 138–146
15 Ding, H. *et al.* (1996) The redox state of the [2Fe–2S] clusters in SoxR protein regulates its activity as a transcription factor. *J. Biol. Chem.* 271, 33173–33175
16 Gaudu, P. and Weiss, B. (1996) SoxR, a [2Fe–2S] transcription factor, is active only in its oxidized form. *Proc. Natl. Acad. Sci. U. S. A.* 93, 10094–10098
17 Hidalgo, E. and Demple, B. (1997) Spacing of promoter elements regulates the basal expression of the *soxS* gene and converts SoxR from a transcriptional activator into a repressor. *EMBO J.* 16, 1056–1065
18 Outten, C.E. *et al.* (1999) DNA distortion mechanism for transcriptional activation by ZntR, a Zn(II)-responsive MerR homologue in *Escherichia coli*. *J. Biol. Chem.* 274, 37517–37524
19 Ding, H.G. and Demple, B. (1997) *In vivo* kinetics of a redox-regulated transcriptional switch. *Proc. Natl. Acad. Sci. U. S. A.* 94, 8445–8449
20 Gaudu, P. *et al.* (1997) Regulation of the *soxRS* oxidative stress regulon. Reversible oxidation of the Fe–S centers of SoxR *in vivo*. *J. Biol. Chem.* 272, 5082–5086
21 Hidalgo, E. *et al.* (1997) Redox signal transduction: mutations shifting [2Fe–2S] centers of the SoxR sensor-regulator to the oxidized form. *Cell* 88, 121–129
22 Kobayashi, K. and Tagawa, S. (1999) Isolation of reductase for SoxR that governs an oxidative response regulon from *Escherichia coli*. *FEBS Lett.* 451, 227–230
23 Liochev, S.I. and Fridovich, I. (1992) Fumarase C, the stable fumarase of *Escherichia coli*, is controlled by the *soxRS* regulon. *Proc. Natl. Acad. Sci. U. S. A.* 89, 5892–5896
24 Nunoshiba, T. *et al.* (1995) Roles of nitric oxide in inducible resistance of *Escherichia coli* to activated murine macrophages. *Infect. Immun.* 63, 794–798
25 Nunoshiba, T. *et al.* (1993) Activation by nitric oxide of an oxidative-stress response that defends *Escherichia coli* against activated macrophages. *Proc. Natl. Acad. Sci. U. S. A.* 90, 9993–9997
26 Ding, H. and Demple, B. (2000) Direct nitric oxide signal transduction via nitrosylation of iron–sulfur centers in the SoxR transcription activator. *Proc. Natl. Acad. Sci. U. S. A.* 97, 5146–5150
27 Demple, B. and Halbrook, J. (1983) Inducible repair of oxidative DNA damage in *Escherichia coli*. *Nature* 304, 466–468
28 Christman, M.F. *et al.* (1985) Positive control of a regulon for defenses against oxidative stress and some heat-shock proteins in *Salmonella typhimurium*. *Cell* 41, 753–762
29 Christman, M.F. *et al.* (1989) OxyR, a positive regulator of hydrogen peroxide-inducible genes in *Escherichia coli* and *Salmonella typhimurium*, is homologous to a family of bacterial regulatory proteins. *Proc. Natl. Acad. Sci. U. S. A.* 86, 3484–3488
30 Hausladen, A. *et al.* (1996) Nitrosative stress: activation of the transcription factor OxyR. *Cell* 86, 719–729
31 Altuvia, S. *et al.* (1997) A small, stable RNA induced by oxidative stress: role as a pleiotropic regulator and antimutator. *Cell* 90, 43–53
32 Gonzalez-Flecha, B. and Demple, B. (1999) Role for the *oxyS* gene in regulation of intracellular hydrogen peroxide in *Escherichia coli*. *J. Bacteriol.* 181, 3833–3836
33 Altuvia, S. *et al.* (1998) The *Escherichia coli* OxyS regulatory RNA represses *fhlA* translation by blocking ribosome binding. *EMBO J.* 17, 6069–6075
34 Zhang, A. *et al.* (1998) The OxyS regulatory RNA represses *rpoS* translation and binds the Hfq (HF-I) protein. *EMBO J.* 17, 6061–6068
35 Storz, G. *et al.* (1990) Transcriptional regulator of oxidative stress-inducible genes: direct activation by oxidation. *Science* 248, 189–194
36 Toledano, M.B. *et al.* (1994) Redox-dependent shift of OxyR DNA contacts along an extended DNA-binding site: a mechanism for differential promoter selection. *Cell* 78, 897–909
37 Gonzalez-Flecha, B. and Demple, B. (1997) Transcriptional regulation of the *Escherichia coli oxyR* gene as a function of cell growth. *J. Bacteriol.* 179, 6181–6186
38 Gonzalez Flecha, B. and Demple, B. (1997) Homeostatic regulation of intracellular hydrogen peroxide concentration in aerobically growing *Escherichia coli*. *J. Bacteriol.* 179, 382–388
39 Zheng, M. *et al.* (1998) Activation of the OxyR transcription factor by reversible disulfide bond formation. *Science* 279, 1718–1721
40 Åslund, F. *et al.* (1999) Regulation of the OxyR transcription factor by hydrogen peroxide and the cellular thiol disulfide status. *Proc. Natl. Acad. Sci. U. S. A.* 96, 6161–6165

Telomerase inhibitors

Laura K. White, Woodring E. Wright and Jerry W. Shay

There has been a vast increase in telomerase research over the past several years, with many different pre-clinical approaches being tested for inhibiting the activity of this enzyme as a novel therapeutic modality to treat malignancy. In this review, we will provide some basic background information about telomeres and telomerase and then discuss the pros, cons and challenges of the approaches that are currently under investigation, and what we might expect in the future of this emerging field.

Laura K. White
Woodring E. Wright*
Jerry W. Shay*
Depts of Internal Medicine and Cell Biology, The University of Texas Southwestern Medical Center at Dallas Dallas, Texas 75390-9039
*e-mail: woodring.wright@UTSsouthwestern.edu
*e-mail: Jerry.Shay@UTSouthwestern.edu

Telomeres are repetitive DNA sequences at the ends of linear chromosomes that protect the termini from being recognized as double-strand breaks. Without telomeres, the ends of the chromosomes would be 'repaired', leading to chromosome fusion and massive genomic instability. In humans, the telomeres typically contain 5–15 kb pairs of repeating TTAGGG sequences. With each cell division, telomeres shorten by 50–200 bp because the lagging strand of DNA synthesis is unable to replicate the extreme 3′ end of the chromosome (the 'end replication problem'; Fig. 1). Normal cultured human cells have a limited replication potential in culture. As first described by Hayflick[1], normal cells in culture replicate until they reach a discrete point at which population growth ceases. This is termed the Phase III or M1 stage and is caused by the shortening of a few telomeres to a size that leads to a growth arrest called 'cellular senescence'. A popular misconception is that cellular senescence leads to cell death rather than to a stable non-dividing state. This stage can be bypassed *in vitro* by abrogation of the function of the *p53* and *pRB* human tumor suppressor genes[2]. The cells can then replicate until the telomeres have become critically shortened, which produces the M2 or crisis stage. As opposed to M1, the net growth arrest in the M2 or crisis stage is caused by a balance between the cell proliferation and cell death rate. At this stage, when most of the telomeres are extremely short, end-to-end fusions and chromosome breakage-fusion cycles cause marked chromosomal abnormalities and apoptosis. Under rare circumstances a cell can escape M2 and

0167-7799/01/$ – see front matter PII: S0167-7799(00)01541-9

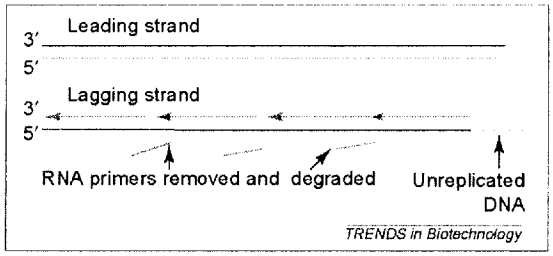

Fig. 1. End replication problem. DNA replication starts by the unwinding of double stranded DNA at the origin of replication. Synthesis of the new strands of DNA proceeds in the 5′ to 3′ direction. The leading strand is continuous, but the lagging strand is synthesized as a series of short segments of DNA (Okazaki fragments) onto the ends of RNA primers. The RNA primers are removed and DNA polymerase fills in the gaps, which are then ligated (not shown). The extreme 3′ end is not replicated leading to DNA loss and the 'end replication problem'. The leading strand might also be processed to give a short overhang to which end-protecting factors could bind.

become immortal by stabilizing the length of its telomeres. This almost always occurs through the activation of the enzyme telomerase[3,4].

Telomerase is a unique ribonucleoprotein enzyme that is responsible for adding the telomeric repeats onto the 3′ ends of chromosomes[5] (Fig. 2). It has two major components as well as many associated proteins that are critical for proper function. The first major component is a functional or template RNA, the human telomerase RNA (hTR), which contains an 11 bp sequence that serves as the template on which telomeric repeats are added to the chromosome. The second major component is the human telomerase reverse transcriptase (hTERT) catalytic subunit. The ability of cells to express telomerase activity is limited by the presence or absence of hTERT because all human somatic cells constitutively contain hTR (Ref. 6).

Telomerase activity has been found in ~85–90% of all human tumors but not in adjacent normal cells[4]. It has thus been hypothesized that for a tumor cell to undergo sustained proliferation beyond the limits of cellular senescence, it must reactivate telomerase or an alternative mechanism in order to maintain telomeres. This makes telomerase a target not only for cancer diagnosis but also for the development of novel therapeutic agents. There are several considerations about telomerase as an anticancer target that need to be addressed. First, there will be an expected lag phase between the time telomerase is inhibited and the time when the telomeres of the cancer cells shorten sufficiently to produce detrimental effects on cellular proliferation. This lag phase will vary depending on the initial telomere length. There is, at least in theory, the possibility that cancer cells might become resistant to telomerase inhibitors or develop alternative mechanisms of telomere maintenance independent of telomerase, which has been seen in experimentally immortalized human cell lines[7]. Finally, inhibitors of telomerase would potentially have effects on other human somatic cells that express telomerase, such as hematopoietic stem cells, germline cells and cells of the basal layer of the epidermis and intestinal crypts[8]. We believe that these effects might be minor because stem cells of renewal tissues typically have much longer telomeres than cancer cells have and the deepest stem cells only proliferate intermittently. During the time that these cells are quiescent, telomere shortening does not occur and telomerase activity is negligible. The expected effects of telomerase inhibition on cancer cells as well as telomerase-positive normal cells are illustrated in Fig. 3.

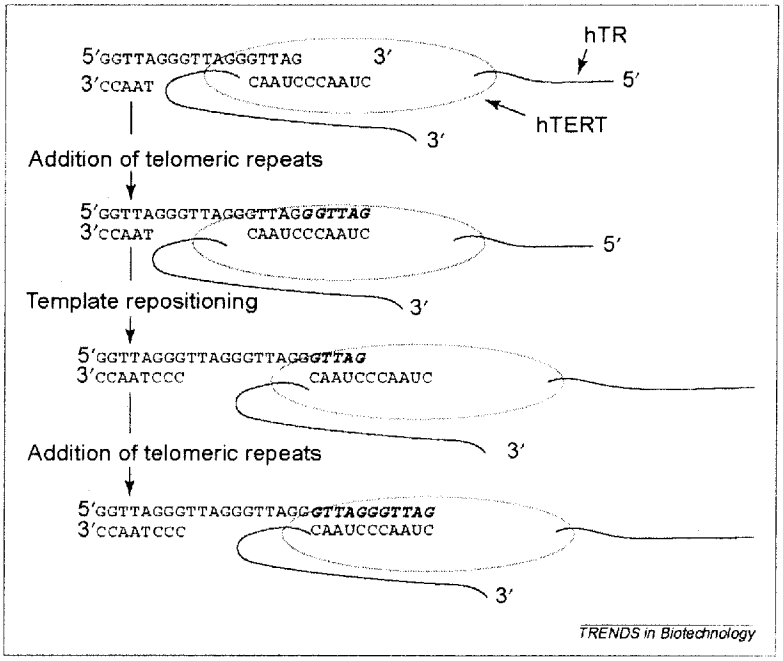

Fig. 2. The addition of telomeric repeats. Telomerase adds hexameric TTAGGG repeats by attaching to the end of the chromosome and then utilizing its internal template to specify the sequence of added nucleotides. As evidenced by telomerase repeat addition processivity, it then is able to reposition downstream and re-anchor its template for the addition of more telomeric repeats.

There have also been concerns that inhibiting telomerase might lead to an increase in malignancy by enhancing the genomic instability of cells. These concerns have risen from the mTR$^{-/-}$ knockout mice which, as compared with the mTR$^{+/+}$ model, has an increased incidence of malignancies in both early and late generation cohorts[9]. There is no evidence to suggest that this would be true in humans. Mouse telomeres are much longer than even the longest human telomeres and do not appear to have a role in signaling senescence. Human cells that lack cell cycle checkpoints with some terminally short telomeres die, whereas similar mouse cells show little evidence of any significant block to further proliferation[10]. It is therefore difficult to interpret any effects on genomic instability or tumorigenesis that telomerase inhibition in human cells will have based on previous mouse experiments.

To confirm that a telomerase inhibitor is acting specifically through a telomere-dependent mechanism, certain criteria should almost always be met: (1) inhibitors should reduce telomerase activity but initially should not affect cell growth rates; (2) addition of inhibitors should lead to progressive telomere shortening with each cell division; (3) addition of inhibitors should eventually cause cells to die or undergo growth arrest; (4) the time necessary to observe decreased proliferation should vary depending on initial telomere length; and (5) chemically related molecules that do not inhibit telomerase activity should not cause decreased cell proliferation or telomere shortening.

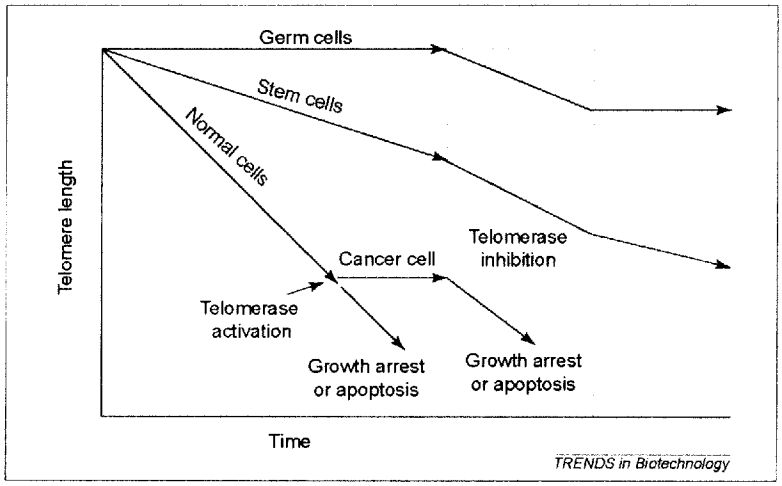

Fig. 3. Effects of telomerase inhibition on the telomere lengths and proliferative capacity of both cancer cells and telomerase-positive normal human somatic cells and germ line cells.

The telomerase holoenzyme complex presents multiple potential sites for the development of inhibitors. These include the functional RNA or hTR, the catalytic reverse transcriptase subunit hTERT, the primer anchoring site, holoenzyme assembly and the factors involved in recruiting telomerase to the telomere. In the past several years there have been more than 100 manuscripts published on telomerase inhibitors. However, only a handful of these reports fulfill the criteria for telomerase inhibitors outlined above. In this article, we will review some of the different approaches to telomerase inhibition that are currently under investigation (Box 1).

Targeting the RNA component of telomerase

Antisense oligodeoxynucleotides

Antisense oligodeoxynucleotides (ODN) are an area of heightened interest in the field of telomerase inhibition. These drugs consist of short stretches of DNA that are complementary to a target RNA. The mechanism of action for most applications is to hybridize to their complementary RNA by Watson–Crick base pairing and inhibit the translation of the RNA by a passive and/or active mechanism. The passive inhibition occurs simply by the competitive binding of the ODN to the RNA, whereas the active mechanism recruits RNaseH to degrade the mRNA once the RNA–ODN hybridization occurs[11]. Therapeutic uses of these molecules are currently under investigation in many different fields of research including oncology, cardiovascular disease and infectious diseases, with one drug currently approved for use in cytomegalovirus retinitis[11].

Box 1. Approaches for targeting telomerase in cancer therapy

- Oligonucleotides – antisense hTR template
- Hammerhead ribozymes – hTR template
- Small molecules
  - G-quadruplex stabilizers
  - Combinatorial libraries
  - Compound collections
- Catalytic (hTERT) component
  - Reverse transcriptase inhibitors
  - Dominant-negative hTERT
  - Immunotherapy

Telomerase presents itself as an intriguing target for these drugs because it possesses a functional RNA component as part of its structure. The template region of hTR must be exposed to add new telomeric repeats onto the chromosome, making this an accessible target for the ODN. Thus, rather than using ODNs to inhibit translation, ODNs directed against the hTR template are designed to directly inhibit telomerase activity. ODNs present several problems in drug development. The first is cellular delivery because, without a transfecting agent, these drugs do not easily enter cells in culture. *In vivo*, they have been found to cross the cell membrane by a poorly understood endocytic mechanism. Once inside the cell they are subjected to degradation by a variety of exo- and endonucleases. Chemical modifications to the ODNs have been implemented that might reduce their degradation but might also reduce the specificity of binding to the target sequence.

A variety of studies have been published on the inhibition of telomerase using antisense approaches directed both at the template and at non-template regions of hTR. The first report was by Feng *et al.*[6] who used a construct expressing an antisense transcript to the first 185 nucleotides of the RNA and introduced them into HeLa cells. In this study, 33 out of 41 clones underwent crisis after 23–26 doublings. The clones that entered crisis had reduced telomerase activity, as well as shorter telomeres compared with the clones that contained vector alone. Since that first study there have been many reports on antisense ODN inhibitors of telomerase. Many of these have reported a reduction in telomerase activity in cancer cells treated in culture, however, most have not documented reduction in telomere length with continued treatment[12–14]. Another concern is that in some cases the cells underwent slowed growth or apoptosis without the time lag that would have been expected if the mechanism of action was specific to telomerase and telomere erosion[15–17].

There have been several studies describing the use of a 2′,5′-oligoadenylate (2-5A) moiety attached to the ODN to increase the activity of the ODN against telomerase[16–18]. The addition of the 2-5A recruits RNaseL along with RNaseH to degrade the targeted RNA once the ODN has hybridized. RNaseL is part of the mammalian antiviral defense. It is an endoribonuclease that functions in the interferon regulated 2-5A system. Upon binding to 2-5A, it is converted to an active form that cleaves the single-standed RNA to which it is targeted. Kondo *et al.*[16] used this approach to target malignant glioma cells and showed that five hours after treating the cells

with a 2′-5A antisense moiety directed at a non-template region, hTR was not detectable by reverse transcriptase (RT) PCR. After continuous treatment with the antisense drug over a 14-day period, 79% of the cells underwent apoptosis. This striking effect on cell growth is unlikely to be explained by telomere erosion because the cells would not have undergone sufficient cell divisions to significantly shorten their telomeres. Kushner *et al.*[17] described a similar effect of a 2′-5A antisense ODN directed against hTR in human ovarian cancer cell lines. They also showed a profound early cell death after only seven days of treatment with the antisense ODN as compared with control ODN. These chemistries have subsequently been tested *in vivo* in a nude mouse using a human prostate cancer xenograft. A 2′-5A anti-hTR 19mer was injected directly into the tumor over a period of seven days, resulting in an increase in tumor volume of only 14% as compared with 215% for the control[18]. Analyses of the tumors treated with the 2′-5A antisense showed many apoptotic cells, and analyses of the cells in culture showed activation of the caspase family. The mechanism of action of these processes and their specificity to telomerase is still unknown. There has been no long-term follow up on the cells that did not apoptose to determine whether they became resistant to the ODN. In addition, there are no reports on the effects these drugs have on telomerase-positive normal somatic cells.

Another class of oligonucleotides being studied are peptide nucleic acids (PNAs). PNAs are analogs of RNA and DNA, in which the pentose-phosphate backbone is replaced by an oligomer of *N*-(2-aminoethyl) glycine, making them resistant to degradation by endo- and exonucleases. This neutral backbone additionally enhances the affinity and specificity of hybridization to the RNA targets. Human telomerase can be inhibited in cells in culture by PNA oligonucleotides complementary to the telomere-templating region of hTR (Ref. 9). When delivered to immortalized SV40 human cell lines in culture using electroporation over 11–16 doublings, the cells showed reduced telomerase activity, shortening of telomere lengths, and growth inhibition after an initial lag phase[20]. Although the pharmacokinetics and uptake of these drugs *in vivo* is largely unknown, they present an exciting new class of oligonucleotide agents.

The most extensively studied modified ODNs are the chimeric 2′-*O*-methyl RNA and 2′ methoxyethoxy RNAs. These modifications to the sugar moieties of the RNA bases flanking the antisense DNA, along with substituting phosphorothioate linkages for phosphodiester bonds, confers greater specificity to the RNA target and also greater resistance to nucleases. One downside of the chimeric ODNs is that with this modification, RNaseH cannot be activated and the ODN acts only through a passive mechanism of competitive binding to the target sequence.

In one study, the 2′-*O*-methyl chemistry was administered to immortalized human breast epithelial cells in culture, using both match and mismatch 13mers that were complementary to the hTR template region over a 120-day period[21]. Cells given the match ODNs demonstrated inhibition of telomerase activity, and after an initial period of normal growth, shortening of telomeres and eventual cell death via apoptosis was observed. The control cells and cells that were given the mismatch ODNs did not exhibit any significant alterations in telomere biology or other phenotypic changes. Furthermore, when the match ODNs were removed from the cells in culture, the surviving cells regained their baseline telomerase activity, proliferation rate returned to normal, and the telomeres grew back to their original lengths, supporting the conclusion that their mechanism of action is through a competitive inhibition of the telomerase enzyme. During this study, there was no evidence of any emergence of an alternative pathway for telomere elongation.

Hammerhead ribozymes

Hammerhead ribozymes are small RNA molecules that possess specific endoribonuclease activity. They consist of a catalytic core flanked by anti-sense sequences that function in the recognition of the target site. Yokoyama *et al.*[22] used three different ribozyme constructs targeting the 3′ end of different sequences in hTR and introduced them into an endometrial cancer cell line. The ribozyme targeting the template region proved to be the most efficacious in reducing telomerase activity and additionally led to telomere shortening over a four-week period. No change in proliferation rate was seen in these cells over this time period. A similar study using a ribozyme targeting the hTR template in melanoma cells, showed a reduction in telomerase activity with a reported slowing in doubling time. However, after >20 passages, the cells exhibited no reduction in telomere length and were still proliferating[23]. This strategy for telomerase inhibition might prove to be a useful tool if investigators are able to demonstrate the expected effects on telomere biology with specific targeting of the telomerase RNA.

Inhibition of the telomerase catalytic protein subunit (hTERT)

Dominant negative hTERT

Dominant negative hTERT constructs (mutants that are catalytically inactive but still able to bind and sequester hTR) effectively inhibit telomerase both *in vitro* and *in vivo*. By introducing cDNA that contains point mutations in the reverse transcriptase motifs of hTERT into both a human epidermoid tumor cell line and an immortalized embryonic kidney cell line, Zhang *et al.*[24] demonstrated an inhibition of telomerase activity as well as a reduction in telomere length. The epidermoid tumor cells, which had very short telomeres (1–4 kb), showed early morphologic changes and the population underwent growth arrest with all the plated cells dead at 32 days. By contrast, the embryonic kidney cells have a significant clone-to-clone

variability in telomere length (3–12 kb). Clones chosen with long telomeres (10–12 kb) continued to proliferate at the same rate as the control and wild-type hTERT infected cells until their telomeres shortened to ~4 kb. At this point, the clones lost the dominant-negative protein and reactivated telomerase resulting in a stabilization of telomere length. Considering data from other reports on inhibitors that cause progressive telomere shortening, it is probable that these clones would have undergone an apoptotic cell death at a point when their telomeres became critically short if the dominant-negative mutants remained active.

Hahn *et al.*[25] described the expression of a catalytically inactive hTERT subunit in a variety of human immortalized cells and cancer cells using a retroviral vector. The dominant-negative mutant was created by substituting the aspartic acid and valine residues at positions 710 and 711 with alanine and isoleucine, respectively. Multiple cell clones infected with the DN-hTERT had undetectable telomerase activity with gradual telomere shortening and eventual growth arrest and cell death. The clones infected with wild-type hTERT and empty vectors retained telomerase activity and no effects were seen on telomere length or proliferation when compared with control clones. In addition, GM847 cells, an immortal cell line that maintains its telomeres by an alternative mechanism, were tested with these constructs. The GM847 clones that were infected with the DN-hTERT remained telomerase negative with no effects on cell growth or telomere length, whereas the GM847 clones that were infected with the wild-type hTERT became positive for telomerase activity but maintained their heterogeneous telomere length and growth rate. To further test the hypothesis that the inhibition of telomerase will decrease tumorigenicity of cells *in vivo*, late passage 36M ovarian cancer cells were injected into immunodeficient nude mice. The cells containing the wild-type hTERT and control vectors readily produced tumors whereas the cells with the DN-hTERT failed to form tumors. These results validate the targeting of hTERT as a potentially powerful site for anti-cancer drug design.

Reverse transcriptase inhibitors

Reverse transcriptase inhibitors (RTIs) are predominantly used in the treatment of HIV. They are able to incorporate into the viral DNA and block chain elongation using the reverse transcriptase enzyme. Telomerase, because of its RNA-dependent DNA polymerase activity, has been studied as a potential use for these agents in cancer therapeutics. The results of these investigations thus far have been inconsistent. 3′-azido-3′-deoxythymidine (AZT) has been the most extensively studied of the RTIs. Several investigators have tested AZT in concentrations ranging from 100 μM to 1.75 mM, according to the IC_{50} for the cell lines used.

They were able to demonstrate telomerase inhibition and slowed growth of cells in culture; however, they have not demonstrated telomere erosion or eventual growth arrest of the cells after prolonged exposure[26–28]. Strahl and Blackburn showed progressive telomere shortening of two immortalized human lymphoid lines using dideoxyguanosine inhibitors but no effects on cell viability after prolonged exposure were observed[29]. It is unlikely that these analogs are functioning through a selective inhibition of telomerase because their reduced proliferation is occurring in the setting of sufficiently long telomeres. A plausible explanation might be that the RTIs have a toxic effect on the cells, perhaps by inhibiting mitochondrial DNA replication leading to the observed reduction in telomerase activity, which is dose dependent. Work in this field is continuing and might shed some light on their precise effects on telomere biology.

Immunotherapy

Recently, there has been exciting work in the field of antigen-specific immune responses in tumor cells. Previous studies have focused on expression of tumor-associated antigens that are restricted to only a few tumor types, making progress in this field slow and tedious. The discovery of tumor-associated antigens that are universal to a broad range of tumor types would greatly enhance the efforts to target these antigens in strategies such as vaccination and in generation of effective anti-tumor cytotoxic T lymphocyte (CTL) responses.

Telomerase is present in the majority of human tumors and is, therefore, a good candidate as a universal tumor-associated antigen. Vonderheide *et al.*[30] identified a hTERT-derived peptide, I540, that binds to human leukocyte antigen (HLA)-A2.1. This major histocompatibility complex (MHC) class I allele is expressed by nearly 50% of the population, making it an attractive target. They generated CTL from CD8+ T cells from the peripheral blood of normal HLA-A2.1 donors by priming with the peptide pulsed autologous dendritic cells. They then showed a specific CTL response in cells expressing hTERT. This response was shown in a variety of tumor cells and was not present in either telomerase negative cells or in cells negative for the HLA-A2.1 allele.

Similarly, Minev *et al.*[31] identified two hTERT peptides containing known binding motifs to the HLA-A2.1 allele, p540 and p865, which were able to generate a specific CTL response in HLA-A2.1 positive tumor cells of prostate, lung, breast, colon and melanoma. Neither of these studies found a CTL effect on telomerase positive CD34+ hematopoietic cells. This might be because of the relatively low level of telomerase expression in these cells compared with tumor cells, and the fact that they do not continuously express telomerase. Whether other normal somatic cells that express telomerase will be affected by the CTL response remains to be determined.

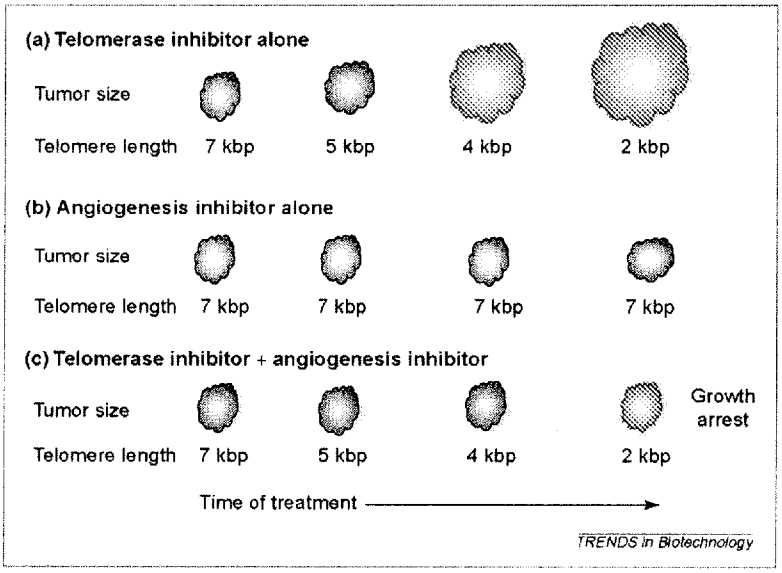

Fig. 4. Model of telomerase inhibition in conjunction with angiogenesis inhibitors. (a) Treatment with telomerase inhibitor alone. The cells continue to proliferate as telomere lengths shorten. Once the telomeres reach a critically short length, the cells will growth arrest or apoptose. This lag phase of continued cell proliferation and tumor growth will vary depending on initial telomere length. (b) Tumor treated with an angiogenesis inhibitor alone. The tumor's growth is balanced by apoptosis but telomeres remain unchanged from their initial lengths. (c) Treatment with a combination of telomerase inhibitor and angiogenesis inhibitor. The tumors do not increase in size as growth is balanced by apoptosis as in (b) above. However, when telomeres reach a critical length, there is eventual growth arrest and apoptosis.

The early *in vitro* work on the immunogenicity of hTERT peptides provides a novel avenue of telomerase inhibition because no lag period would be required before cell death. Much work remains to be done in this field because the *in vivo* efficacy of delivering these vaccines to trigger immunity and the elicitation of CTL responses gave inconclusive results in recent clinical trials using melanoma-associated peptides[32].

G-quadruplex stabilization

The 3′ overhang of telomeres are rich in guanine units and have been shown *in vitro* to produce tetra-stranded DNA structures termed G-quadruplexes. These G-quadruplex conformations inhibit telomerase activity and, therefore, drugs that stabilize these tetraplexes could conceivably be effective chemotherapeutic agents. There have been many reports of compounds that inhibit telomerase through the stabilization of the G-quadruplexes in cell extracts and cell culture. Some of these potential compounds include porphyrin derivatives, acridine derivatives, 2,6-diamidoanthraquinones and fluorenone-based compounds[33–36]. Although this might be a viable approach for telomerase inhibition, none of the published work to date provides data regarding telomere shortening with these agents. Until more is known about the effects of these small molecules on telomere biology, it remains to be determined whether they will be a reasonable strategy for telomerase inhibition.

Small molecule inhibitors

A rapidly emerging area for discovering potential candidate telomerase inhibitors is through the rapid screening of small molecules using NCI-COMPARE analyses or other large-scale screening models. The NCI COMPARE bioinformatics approach incorporates a strategy of testing and categorizing drugs based on their chemical structures relative to a known 'seed' compound[37]. There are efforts under way to identify prospective telomerase inhibitors using this system, with several potentially promising rhodacyanine derivatives discovered thus far[38]. The mechanism of action of these molecules is not known at this time but could be through disruption of the anchoring of telomerase to the telomere, disruption of the telomerase holoenzyme assembly or G-quartet stabilization. This and other small-molecule screening strategies using combinatorial libraries are likely to yield new classes of telomerase inhibitors.

Conclusions and future perspectives

We have discussed the major avenues of targeting telomerase in human cancer cells; the question, however, still remains whether telomerase will be a viable approach to treating cancer. Would inhibition of the enzyme in the classical sense, which would require a lag phase before any detrimental effects on the cells, be a reasonable strategy in patients with a large tumor burden? Probably not. Most likely, the use of telomerase inhibitors in this situation would be as an adjuvant treatment in combination with surgery, radiation treatment and chemotherapy with standard agents, as well as new agents such as angiogenesis inhibitors (Fig. 4). It is also possible that telomerase inhibitors could be used following standard therapies in which there is no clinical evidence of disease to treat possible micrometastases, and thus prevent cancer relapse. In these situations, which would probably require prolonged treatment, it will be imperative that the drugs have a low toxicity profile and are easily administered.

The other avenue of telomerase inhibition is by targeting telomerase-expressing cells as a means to kill the cells. Immunotherapy directed against telomerase positive cells, as well as strategies using a suicide gene promoter targeted to hTERT-expressing cells (unpublished results) are currently under investigation. These modalities have the advantage of abolishing the lag phase that is required with the classic mode of telomerase inhibition. However, these treatments might also prove to be more toxic to normal somatic cells expressing telomerase.

Will telomerase inhibitors become a common weapon in the armory against cancer? Will there be emergence of alternative mechanisms of telomere maintenance? What will the effects of telomerase inhibition be on normal hematopoietic and germline cells? These and other questions will only be answered when these drugs are moved into clinical trials.

References

1 Shay, J.W. and Wright, W.E. (2000) Haylick, his limit, and cellular aging. *Nature Review: Mol. Cell Biol.* 1, 72–76
2 Shay, J.W. *et al.* (1991) A role for both RB and p53 in the regulation of human cellular senescence. *Exp. Cell Res.* 196, 33–39
3 Wright, W.E. and Shay, J.W. (1992) The two stage mechanism controlling cellular senescence and immortalization. *Exp. Gerontol.* 27, 383–389
4 Kim, N.W. *et al.* (1994) Specific association of human telomerase activity with immortal cells and cancer. *Science* 266, 2011–2015
5 Greider, C.W. and Blackburn, E.H. (1985) Identification of a specific telomere terminal transferase activity in *Tetrahymena* extracts. Cell *43*, 405–413
6 Feng, J. *et al.* (1995) The RNA component of human telomerase. *Science* 269, 1236–1241
7 Bryan, T.M. *et al.* (1995) Telomere elongation in immortal human cells without detectable telomerase activity. *EMBO J.* 14, 4240–4248
8 Wright, W.E. *et al.* (1996) Telomerase activity in human germline and embryonic tissues and cells. *Dev. Genet.* 18, 173–179
9 Artandi, S.E. and DePinho, R.A. (2000) Mice without telomerase: what can they teach us about human cancer? *Nat. Med.* 6, 852–855
10 Wright, W.E. and Shay, J.W. (2000) Telomere dynamics in cancer progression and prevention: fundamental differences in human and mouse telomere biology. *Nat.Med.* 6, 849–851
11 Galderisi, U. *et al.* (1999) Antisense oligonucleotides as therapeutic agents. *J. Cell Physiol.* 181, 251–257
12 Ohnuma, T. *et al.* (1997) Inhibitory effects of telomere-mimic phosphorothioate oligonucleotides on various human tumor cells *in vitro*. *Anticancer Res.* 17, 2455–2458
13 Glukhov, A.I. *et al.* (1998) Inhibition of telomerase activity of melanoma cells *in vitro* by antisense oligonucleotide. *Biochem. Biophys. Res. Commun.* 248, 368–371
14 Bisoffi, M. *et al.* (1998) Inhibition of human telomerase by a retrovirus expressing telomeric antisense RNA. *Eur. J. Cancer* 34, 1242–1249
15 Mata, J.E. *et al.* (1997) A hexameric phosphorothioate oligonucleotide telomerase inhibitor arrests growth of Burkitt's lymphoma cells *in vitro* and *in vivo*. *Toxicol. Appl. Pharmacol.* 144, 189–197
16 Kondo, S. *et al.* (1998) Targeted therapy of human malignant glioma in a mouse model by 2-5A antisense directed against telomerase RNA. *Oncogene* 16, 3323–3330
17 Kushner, D.M. *et al.* (2000) 2-5A antisense directed against telomerase RNA produces apoptosis in ovarian cancer cells. *Gynecol. Oncol.* 76, 183–192
18 Kondo, Y. *et al.* (2000) Treatment of prostate cancer *in vitro* and *in vivo* with 2-5A-anti-telomerase RNA component. *Oncogene* 19, 2205–2211
19 Norton, J.C. *et al.* (1996) Inhibition of human telomerase activity by peptide nucleic acids. *Nat. Biotechnol.* 14, 615–619
20 Shammas, M.A. *et al.* (1999) Telomerase inhibition by peptide nucleic acids reverses 'immortality' of transformed human cells. *Oncogene* 18, 6191–6200
21 Herbert, B.S. *et al.* (1999) Inhibition of human telomerase in immortal human cells leads to progressive telomere shortening and cell death *Proc. Natl. Acad. Sci. U. S. A.* 96, 14276–14281
22 Yokoyama, Y. *et al.* (1998) Attenuation of telomerase activity by a hammerhead ribozyme targeting the template region of telomerase RNA in endometrial carcinoma cells. *Cancer Res.* 58, 5406–5410
23 Folini, M. *et al.* (2000) Inhibition of telomerase activity by a hammerhead ribozyme targeting the RNA component of telomerase in human melanoma cells. *J. Invest. Dermatol.* 114, 259–267
24 Zhang, X. *et al.* (1999) Telomere shortening and apoptosis in telomerase-inhibited human tumor cells. *Genes Dev.* 13, 2388–2399
25 Hahn, W.C. *et al.* (1999) Inhibition of telomerase limits the growth of human cancer cells. *Nat. Med.* 5, 1164–1170
26 Strahl, C. and Blackburn, E.H. (1996) Effects of reverse transcriptase inhibitors on telomere length and telomerase activity in two immortal human cell lines. *Mol. Cell. Biol.* 16, 53–56
27 Melana, S.M. *et al.* (1997) Inhibition of cell growth and telomerase activity of breast cancer cells *in vitro* by 3′-azido-3′-deoxythymidine. *Clin. Cancer Res.* 4, 693–696
28 Murakami, J. *et al.* (1998) Inhibition of telomerase activity and cell proliferation by a reverse transcriptase inhibitor in gynaecological cancer cell lines. *Eur. J. Cancer* 35, 1027–1034
29 Gomez, D.E. *et al.* (1998) Irreversible telomere shortening by 3′-azido-2′,3′-dideoxythymidine (AZT) treatment. *Biochem. Biophys. Res. Commun.* 246, 107–110
30 Vonderheide, R.H. *et al.* (1999) The telomerase catalytic subunit is a widely expressed tumor-associated antigen recognized by cytotoxic T lymphocytes. *Immunity* 10, 673–679
31 Minev, B. *et al.* (2000) Cytotoxic T cell immunity against telomerase reverse transcriptase in humans. *Proc. Natl. Acad. Sci. U. S. A.* 97, 4796–4801
32 Rosenberg, S.A. *et al.* (1998) Immunologic and therapeutic evaluation of a synthetic peptide vaccine for the treatment of patients with metastatic melanoma. *Nat. Med.* 4, 321–327
33 Harrison, R.J. *et al.* (1999) Human telomerase inhibition by substituted acridine derivatives. *Bioorg. Med. Chem. Lett.* 9, 2463–2468
34 Sun, D. *et al.* (1997) Inhibition of human telomerase by a G-quadruplex-interactive compound. *J. Med. Chem.* 40, 2113–2116
35 Perry, P.J. *et al.* (1999) 2,7-Disubstituted amidofluorenone derivatives as inhibitors of human telomerase. *J. Med. Chem.* 42, 2679–2684
36 Read, M.A. *et al.* (1999) Molecular modeling studies on G-quadruplex complexes of telomerase inhibitors: structure-activity relationships. *J. Med. Chem.* 42, 4538–4546
37 Paull, K.D. *et al.* (1989) Display and analysis of patterns of differential activity of drugs against human tumor cell lines: development of mean graph and COMPARE algorithm. *J. Natl. Cancer Inst.* 81, 1088–1092
38 Naasani, I. *et al.* (1999) FJ5002: A potent telomerase inhibitor identified by exploiting the disease-oriented screening program with COMPARE analysis. *Cancer Res.* 59, 4004–4011

Exhibit 4: Strahl and Blackburn, "Effects of Reverse Transcriptase Inhibitors on Telomere Length and Telomerase Activity in Two Immortalized Human Cells Lines," *Mol. Cell. Biol.* 16(10):53–65 (1996).

MOLECULAR AND CELLULAR BIOLOGY, Jan. 1996, p. 53–65
0270-7306/96/$04.00+0

Vol. 16, No. 1

Effects of Reverse Transcriptase Inhibitors on Telomere Length and Telomerase Activity in Two Immortalized Human Cell Lines

CATHERINE STRAHL AND ELIZABETH H. BLACKBURN*

Department of Microbiology and Immunology and Department of Biochemistry and Biophysics, University of California, San Francisco, San Francisco, California 94143-0414

Received 17 May 1995/Returned for modification 6 July 1995/Accepted 10 October 1995

The ribonucleoprotein telomerase, a specialized cellular reverse transcriptase, synthesizes one strand of the telomeric DNA of eukaryotes. We analyzed telomere maintenance in two immortalized human cell lines: the B-cell line JY616 and the T-cell line Jurkat E6-1, and determined whether known inhibitors of retroviral reverse transcriptases could perturb telomere lengths and growth rates of these cells in culture. Dideoxyguanosine (ddG) caused reproducible, progressive telomere shortening over several weeks of passaging, after which the telomeres stabilized and remained short. However, the prolonged passaging in ddG caused no observable effects on cell population doubling rates or morphology. Azidothymidine (AZT) caused progressive telomere shortening in some but not all T- and B-cell cultures. Telomerase activity was present in both cell lines and was inhibited in vitro by ddGTP and AZT triphosphate. Prolonged passaging in arabinofuranyl-guanosine, dideoxyinosine (ddI), dideoxyadenosine (ddA), didehydrothymidine (d4T), or phosphonoformic acid (foscarnet) did not cause reproducible telomere shortening or decreased cell growth rates or viabilities. Combining AZT, foscarnet, and/or arabinofuranyl-guanosine with ddG did not significantly augment the effects of ddG alone. Strikingly, with or without inhibitors, telomere lengths were often highly unstable in both cell lines and varied between parallel cell cultures. We propose that telomere lengths in these T- and B-cell lines are determined by both telomerase and telomerase-independent mechanisms.

Telomeres, the ends of eukaryotic chromosomes, are characterized by an array of tandemly repeated short DNA repeat units (3), with the sequence TTAGGG in humans and other mammals (33). These essential telomeric sequences are added to chromosomal DNA ends by telomerase (14; reviewed in reference 4), a cellular ribonucleoprotein reverse transcriptase which uses a sequence within its RNA moiety to template the repeats added to chromosome ends (15, 31, 40, 41). The specialized DNA-protein complexes formed by these repeats (6, 13) are thought to be important for still poorly understood interactions within the nucleus that affect nuclear division and chromosome maintenance (5) and protect the ends of chromosomes from fusion (30) and potential degradation by exonucleases (13).

During successive rounds of DNA replication, an inevitable progressive loss of genetic information is predicted to occur, because DNA polymerase is unable to complete synthesis of the ends of linear DNA (reviewed in references 3 and 10). By polymerizing DNA onto the chromosome termini, telomerase counterbalances this terminal DNA attrition. Functional telomerase has been demonstrated to be essential for normal telomere maintenance in the ciliated protozoan *Tetrahymena thermophila* and the yeasts *Kluyveromyces lactis* and *Saccharomyces cerevisiae*. In *T. thermophila*, a particular mutant RNA, which prevents correct telomerase polymerization in vitro (12), causes telomere shortening and senescence (11a, 12, 46). Similarly, deleting or disrupting the RNA moiety of telomerase in the budding yeasts *K. lactis* and *S. cerevisiae* or the *EST1* gene in *S. cerevisiae* causes progressive telomere shortening and cellular senescence (28, 31, 41). These results established that in these organisms, which can grow indefinitely, telomere maintenance is essential for long-term viability and telomerase is required for normal telomere maintenance. However, preventing normal telomerase-mediated maintenance has also revealed telomerase-independent mechanisms for telomere maintenance in yeasts. In *est1*$^-$ cells that survive deletion of the *EST1* gene, *RAD52*-dependent recombination takes place between internal and terminal telomeric repeat tracts separated by the Y′ class of subtelomeric elements, regenerating sufficient terminal telomeric repeat tracts for chromosomal maintenance (27). The *K. lactis* genome lacks internal telomeric repeat tracts, precluding the type of pathway seen in *est1*$^-$ *S. cerevisiae* cells. Instead, deletion of the telomerase RNA gene, *TER1*, of *K. lactis* has uncovered a second pathway of non-telomerase-mediated telomeric DNA replenishment, involving recombination and/or gene conversions between terminal telomeric repeats in the *ter1*$^-$ survivors (31a). Heterologous telomeres introduced into *S. cerevisiae* also exhibit recombination between the introduced telomeric sequences (44). These results raised the possibility that non-telomerase-mediated pathways play important roles in other systems.

Telomerase activity has been detected in various immortalized human and mouse cell lines, as well as tumor and germ line cells and some normal somatic cell types (6a, 36; reviewed in reference 10). In early studies, it was found that certain primary human somatic cells in culture lacked detectable telomerase activity (8) and that telomeres from these cells decreased in length during cell divisions (8, 17; reviewed in reference 10). These cells eventually reached a state in which they ceased to divide ("crisis"), but in the tiny fraction of cells that for unknown reasons survive crisis and become "immortal," telomerase activity became detectable. In the subsequent cell divisions, telomere lengths stabilized and sometimes increased (8, 23). Therefore, it was proposed that telomerase activity may be required for cell immortalization in vitro and that interfering with telomere length regulation by inhibiting telomerase may be a basis for cancer therapy (9, 17).

* Corresponding author. Mailing address: Department of Microbiology and Immunology, Department of Biochemistry and Biophysics, Box 0414, University of California, San Francisco, San Francisco, CA 94143-0414. Phone: (415) 476-4912. Fax: (415) 476-8201.

In several studies, attempts have been made to relate telomere lengths to in vitro telomerase activity and cell growth. However, various contradictory results have prevented the emergence of any straightforward relationship between these properties. Although telomerase activity has been detected by in vitro assays of extracts from many immortalized cell lines (8, 22), an immortal human fibroblast cell line with no detectable telomerase activity has been reported (34). An artificially constructed marked telomere and a natural telomere analyzed in this cell line showed highly variable and unstable lengths as the cells were propagated, yet the chromosome bearing the marked telomere was stable and there was no correlation of loss rates of this chromosome with shortening of its marked telomere (34). The lack of detectable telomerase and the patterns of telomere length variability strongly suggested that a non-telomerase-mediated mechanism was acting to maintain the telomeres in this cell line.

Telomeres in cancer cells are often significantly shorter than in normal somatic tissue (9, 11, 18, 21, 39). Hence, it was suggested that because of their increased numbers of divisions, cancer cells that may initially lack telomerase lose more telomeric repeats than do surrounding somatic tissue cells and that when telomerase is reactivated in these cancer cells, telomere lengths stabilize, albeit at a shorter length (8, 9). However, in some tumor samples, the reported telomere lengths were much greater than those of normal surrounding tissues, while other tumor samples showed no changes compared with normal donor cells (19, 35, 39). Reports of telomere lengths in immortalized cell lines have given variable results. Rogalla et al. (37) reported decreased mean telomere length in immortalized cells compared with cells from the originating tumor. On the other hand, telomeres in some immortalized HeLa cell lines can be very long (>20 kb) (11). While many malignant tumors have detectable telomerase activity, some do not (19, 22). Nilsson et al. (35) reported that malignant hematopoietic (acute leukemia) cells could be either positive or negative for telomerase activity but that the telomere lengths were no different in both classes. All these results suggest that the relationship between telomerase activity and telomere length is not a simple one.

Our initial goal was to determine whether telomere length maintenance could be perturbed in immortalized human cells expressing telomerase activity and, if so, whether this would lead to cellular senescence. We have shown previously that telomerase activity from *T. thermophila* can be inhibited in vitro by chain-terminating nucleoside triphosphate analogs known to inhibit retroviral reverse transcriptases. Some of these analogs, including azidothymidine (AZT), caused telomere shortening in vivo in *T. thermophila* (42). AZT also inhibited the developmentally programmed de novo telomere addition of this organism.

Here we report the effects of several inhibitors of retroviral reverse transcriptases on the telomere length and cell growth properties of two immortalized human lymphoid cell lines, the B-cell line JY616, derived from a B-cell lymphoma, and the T-cell line Jurkat E6-1, derived from a human T-cell leukemia. While telomeres in both cell lines reproducibly were progressively shortened by prolonged passaging in the nucleoside analog dideoxyguanosine (ddG), there was no detectable senescence or change in cell growth rates. In addition, passaging in the presence of 100 μM AZT caused marked progressive telomere shortening over several weeks in some but not all T- and B-cell cultures, again without changing cell growth rates. We show that telomerase activity is present in both cell lines and is inhibited strongly by ddGTP and less strongly by AZT-5′-triphosphate (AZT-TP). Hence, we propose that the in vivo shortening of telomeres in the presence of ddG or AZT may be attributable to inhibition of telomerase activity by these analogs within the cell.

These studies also revealed unexpectedly high degrees of telomere length variation between parallel cell cultures and dynamic changes in telomere lengths during logarithmic-phase growth in both the T- and B-cell lines with or without inhibitors. We propose that telomeres in the two immortalized lymphoid cell lines examined here are acted on by a combination of telomerase and telomerase-independent mechanisms.

MATERIALS AND METHODS

Manufacturers of reverse transcriptase inhibitors. Arabinofuranyl-guanosine (Ara-G; discontinued), ddI, and ddG were obtained from Calbiochem. ddA, ddGTP, ddTTP, foscarnet, didehydrothymidine (d4T) and dimethyl sulfoxide (DMSO) were obtained from Sigma. AZT was obtained from Bochringer-Mannheim. AZT-TP supplied as a 1-mg/ml solution in sterile water, was obtained from Raymond F. Schinazi through the AIDS Research and Reference Reagent program, Division of AIDS, National Institute of Allergy and Infectious Diseases.

Cell culture. JY616 cells, an immortalized human B-cell lymphoma cell line generously supplied by Joel Goodman, Department of Microbiology and Immunology, University of California, San Francisco, were maintained in RPMI 1640–0.025 M *N*-2-hydroxyethylpiperazine-*N*′-2-ethanesulfonic acid (HEPES)–10% fetal calf serum supplemented with 100 U of penicillin per ml plus 100 μg of streptomycin per ml or with 50 μg of gentamicin per ml at 37°C under 5% CO_2. For each experiment, culture aliquots were maintained in parallel as separate passaging lineages (for exceptions, see below) after the initial aliquoting of the stock culture. Cultures were grown in six-well plates, 5 ml per well in duplicate, with analogs added to the medium to final working concentrations immediately before passaging. Cells were counted with a hemacytometer and transferred every 7 to 10 days (five to seven mean population doublings [MPDs]), with 3×10^4 cells per well seeded into fresh medium containing analog or control medium. In some cases, cell viability was checked before harvesting by using trypan blue stain during counting. For all cultures counted in this way, the average viability was greater than 90%. Remaining cells were pelleted and stored at −80°C until processed for analysis of DNA. All cultures in a given experiment were initially split from the same cell stock. In some cases, cultures were lost over time because of contamination or problems with the growth media. In these cases, the cultures were reseeded at the appropriate density with cells from the corresponding duplicate culture. Only contiguous passages of each culture have been used in this work. Jurkat E6-1 cells (ATCC TIB152), an immortal human T-cell leukemia cell line generously supplied by Art Weiss, Department of Medicine, University of California, San Francisco, were maintained essentially identically to the B cells, in RPMI 1640 (no HEPES)–10% fetal calf serum, with penicillin-streptomycin or gentamicin, seeded at 6×10^4 cells per well. All cultures were split from the same cell stock at the start of the experiment, with two exceptions: RPMI-only control B4 was lost because of contamination at passage 3, and RPMI-only control A4 was lost at passage 4. Both were replaced with the corresponding passage of RPMI-only control A1 and subsequently carried as separate cultures, as noted in the legend to Fig. 9.

To determine the highest concentration of each inhibitor that was nontoxic and that did not affect cell viability or growth, each cell line was cultured in duplicate as described above in various concentrations (in twofold dilutions) of the inhibitor for 1 week (five to seven MPDs). The highest concentration of each analog which did not cause a decrease in cell growth rate measured after 1 week or cause changes in cell morphology was chosen for use throughout the duration of the experiment. For the JY616 line, these concentrations were 10 μM ddG, 100 μM AZT, 12 μM Ara-G, 10 μM ddA, 300 μM foscarnet, 50 μM d4T, 2.5 μM ddI, and DMSO at a final concentration of 0.01% as the solvent control for ddG and Ara-G. Two RPMI medium-only cultures were also maintained as controls. For the Jurkat cell line, the subcytotoxic inhibitor concentrations determined in this way were 30 μM ddG, 100 μM AZT, 0.05 μM Ara-G, 37.5 μM ddA, 600 μM foscarnet, 75 μM d4T, and DMSO at a final concentration of 0.008% as the solvent control for ddG and Ara-G. Eight RPMI medium-only cultures were also maintained as controls.

Genomic DNA was prepared by incubating cell pellets in 3 ml of lysis buffer (0.1 M NaCl, 10 mM Tris [pH 8.0], 25 mM EDTA [pH 8.0], 0.5% sodium dodecyl sulfate [SDS], 0.1 mg of proteinase K [Boehringer Mannheim] per ml) overnight at 55°C, followed by phenol extraction and ethanol precipitation. DNA pellets were resuspended in TE (10 mM Tris [pH 7.6], 1 mM EDTA [pH 8.0]), and restriction digests were done with either *Rsa*I plus *Hin*fI as described previously (9) for JY616 cells except those shown in Fig. 1B and C or *Mse*I plus *Mnl*I for the JY616 cells shown in Fig. 1B and C and all Jurkat E6-1 cells. *Mse*I plus *Mnl*I was determined empirically to give shorter and therefore clearer terminal restriction fragments from these cell lines than *Rsa*I plus *Hin*fI in Southern blots with hybridization to a telomeric probe. Approximately 1 μg of digested DNA per lane was loaded onto a 0.8% agarose gel. Southern blotting was performed by standard methods (38), and blots were hybridized with the α-^{32}P-labeled oligo-

nucleotide $(TTAGGG)_3$ at 42°C for 3 to 18 h. Prior to restriction digestion, a sample of each DNA was electrophoresed to verify its integrity. Telomere lengths were measured with an LKB 2202 Ultroscan densitometer, with the center of the peak taken as the mean telomeric restriction fragment length. For several data sets, telomere lengths were also calculated as described previously (17) following scanning of the Southern blot autoradiograms with a digital scanner (Alpha Innotech Corp.).

Preparation of S-100 cell extracts. Extracts were prepared essentially as described previously (8) with minor modifications. Briefly, approximately 6×10^8 cells growing in suspension were collected by centrifugation for 10 min at 3,000 rpm (1,500 × *g*) in a Sorvall GSA fixed-angle rotor, rinsed twice in cold phosphate-buffered saline (PBS) (without Ca^+ or Mg^+), and centrifuged for 3 min at 3,000 rpm (1,500 × *g*). The final pellet was rinsed in hypotonic lysis buffer (Hypo buffer, consisting of 10 mM HEPES [pH 8.0], 3 mM KCl, 1 mM $MgCl_2$, 1 mM dithiothreitol, 0.1 mM Pefabloc SC [Boehringer Mannheim], 10 U of RNasin (Promega) per ml, 1 mM leupeptin [Boehringer Mannheim], and 10 mM pepstatin A [Boehringer Mannheim]) and centrifuged at 1,800 rpm (600 × *g*) in a Sorvall HB-4 swinging-bucket rotor, and the final pellet was resuspended in 0.75 volume of Hypo buffer. After incubation on ice for 10 min, the cells were transferred to a 7-ml ice-cold Dounce homogenizer and homogenized on ice with a tight-fitting (B type) pestle. After a further 30 min on ice, the suspension was centrifuged for 10 min at 10,000 rpm (16,000 × *g*) in a Sorvall HB-4 swinging-bucket rotor (this step was omitted for the JY616 cells; instead, the extract remained on ice for an additional 20 min). The supernatant was harvested and centrifuged for 1 h at 48,000 rpm (100,000 × *g*) in a Beckman TL100 mini-ultracentrifuge TLA100.2 fixed-angle rotor at 4°C. The supernatant was harvested, and glycerol was added to a 20% final concentration for storage at −80°C until DEAE columns were prepared.

DEAE column chromatography of S-100 extracts. A 0.5-ml volume of DEAE-agarose (Bio-Rad Bio-Gel agarose, 100-200 mesh) was equilibrated in ice-cold Hypo buffer, and 0.5 ml of extract was loaded at 4°C. The column was washed with 2 volumes of Hypo buffer followed by 2 volumes of Hypo buffer plus 0.2 M NaCl and eluted with 1 ml of 0.3 M NaCl in Hypo buffer. The eluate was concentrated at 4°C in a Microcon 30 microconcentrator (Amicon) as specified by the manufacturer and brought up to a convenient working volume in 0.3 M NaCl in Hypo buffer, approximately a twofold concentration. Glycerol was added to 20% for storage at −80°C if assays were to be performed later.

Conventional telomerase assays. For the standard telomerase assay, DEAE-purified extract was diluted in Hypo buffer to a convenient working volume so that the final salt concentration was approximately 0.04 M NaCl. A 20-μl aliquot of this dilution was mixed with 20 μl of a 2× reaction mixture and incubated for 2 h at 30°C. The final concentrations in the 2× reaction mixture were 2 mM dATP, 2 mM TTP, 5 μM total dGTP including 50 μCi of [α-^{32}P]dGTP (800 Ci/mmol; Amersham), 2 μM $(TTAGGG)_3$, 3 mM $MgCl_2$, 1 mM spermidine, 5 mM 2-mercaptoethanol, 50 mM potassium acetate, and 50 mM Tris acetate (pH 8.5). In reaction mixtures containing ddGTP or AZT-TP, telomerase extract was added to the 2× cocktail on ice and this mixture was added to chilled reaction tubes containing analog. The reaction was then started by placing tubes at 30°C. For reaction mixtures in which the concentration of TTP was varied, TTP was omitted from the 2× cocktail and added separately to each reaction tube before addition of enzyme. RNase controls were done by adding 0.7 μl of RNase A (10 mg/ml) and 0.6 μl of 2-mercaptoethanol to the tube before addition of extract. The 40-μl reactions were stopped by adding 50 μl of 0.1-mg/ml RNase A in 20 mM Tris HCl [pH 7.5]–10 mM EDTA to each tube and incubating the tubes for 10 min at 37°C. Reaction mixtures were deproteinated by adding proteinase K (Boehringer Mannheim) at 0.3 mg/ml in 10 mM Tris HCl (pH 7.5)–0.5% SDS, 50 μl per tube, incubating the tubes at 37°C for 15 min, and performing phenol-chloroform extraction and ethanol precipitation with glycogen (Calbiochem) as the carrier. DNA products were separated on a 10% polyacrylamide–7 M urea sequencing gel at 1,700 V for 2 to 3 h with 0.6× Tris-borate-EDTA. Dried gels were exposed on a Molecular Dynamics phosphorimaging screen and analyzed on a Molecular Dynamics phosphorimager. Typical exposures were 1 week. Dried gels were also exposed on Kodak X-AR5 film for up to 30 days.

TRAP assays. TRAP assays were performed essentially as described by Kim et al. (22) with the following minor changes: cells were pelleted, resuspended in 300 μl of PBS, and frozen at −80°C. The cells were thawed and incubated on ice for 30 min in 60 μl of 5× TRAP lysis buffer {[2.5% 3-[(3-cholamidopropyl)dimethylammonia]-1-propanesulfonate [CHAPS], 50 mM Tris HCl [pH 7.5], 5 mM $MgCl_2$, 5 mM EGTA, 25 mM β-mercaptoethanol, 50% glycerol} plus 2 μl of 100 mM Pefabloc (Boehringer Mannheim). Cell debris was pelleted for 20 min at 16,000 × *g* at 4°C. Supernatants were aliquoted and flash frozen on dry ice before storage at −80°C.

Each telomerase reaction volume was 25 μl above the wax barrier (22), at an extract concentration corresponding to 100 cells per assay. Control assays were performed on samples of each cell type to determine that bands visualized on a 10% polyacrylamide–7 M urea sequencing gel were due to telomerase activity. These included preincubation for 20 min at 37°C with 10 μg of RNase A as a control for non-telomerase-mediated incorporation of the ^{32}P label or with RNase plus RNasin (40 U), phenol extraction of the cell extract before the assay, omission of the cell extract from the assay, and assaying with only the CX or the TS primer (22) (data not shown). Reaction products were labeled with [α-^{32}P]dGTP and [α-^{32}P]TTP. Each set of reactions included duplicate reaction mixtures containing 10 μg of RNase A in the 25 μl above the wax barrier to control for non-telomerase-produced background. One-tenth of each total reaction mixture (5 μl plus 5 μl of formamide loading dye) was run on the gel.

Duplicate reactions were performed to ensure reproducibility of the reaction and of gel loading. Gels were phosphorimaged for 1 to 2 days. They were then exposed to Kodak X-AR5 film for up to 1 week. For the quantitations of TRAP assays shown in Fig. 6, reaction products were separated on a denaturing 10% polyacrylamide gel and quantitated by phosphorimaging, measuring the total phosphorimage units (pixels) for each lane in a central region of the gel. The mean pixels of duplicate RNase-treated reactions were subtracted as background from the mean of each of the other duplicate reactions. The 0 μM inhibitor reactions were considered to be 100% total telomerase activity, and the results were plotted as a percentage of total incorporation against the concentration of inhibitor (micromolar) present in the telomerase reactions.

RESULTS

ddG causes progressive telomere shortening in two immortalized cell lines. Duplicate cultures of the immortalized JY616 B-cell line were tested with several viral reverse transcriptase inhibitors (24): the nucleoside analogs AZT, Ara-G, ddG, ddI, ddA, d4T and a nonnucleoside viral reverse transcriptase inhibitor, foscarnet (a triphosphate analog). Concentrations of each inhibitor used were determined in initial tests (see Materials and Methods). For each inhibitor, the concentration chosen was the highest that did not cause a significant change in cell growth rate or morphology over five to seven population doublings. For each culture, every 5 to 7 days, cells were counted to determine cell growth rates (as MPDs), cell morphologies were monitored, and cells were passaged quantitatively to maintain them in logarithmic growth conditions. Telomere length distributions were analyzed at a series of time points during the serial passaging. Lengths of terminal restriction fragments (TRFs), determined by Southern blotting analyses with a telomeric sequence probe, were used as the measure of telomere lengths, as described previously (18). Consistent with previous measurements of telomere lengths in human cells (17, 18, 26), the data presented here indicate that the great majority of length fluctuations were attributable to different numbers of telomeric TTAGGG repeats rather than to different complex sequences added to ends, since we used frequently cutting restriction enzymes to measure TRFs.

Figure 1A shows the results of one experiment with JY616 cells. After 10 weeks of passaging in the presence of ddG (plus the 0.01% DMSO added as the solvent for ddG or Ara-G), a marked telomere shortening (a ~3.2-kb drop in mean TRF length) was seen compared with the control 0.01% DMSO culture (a ~1.2-kb drop) (Fig. 1A, compare lane 9 with lane 12). However, over the 10-week passaging period, the mean telomere length also declined in all the cultures in this experiment (e.g., a ~2.2-kb drop in RPMI medium alone), although the change after 10 weeks was greatest with ddG present (Fig. 1A, compare lane 9 with lanes 3, 6, 12, and 15; also see Fig. 3, JY4 panel).

Because the decline in telomere length in cells grown without inhibitors was unexpected, the experiments were repeated with the JY616 B-cell line and a different cell line, the Jurkat E6-1 T-cell line. Three separate additional complete experiments, each with duplicate culture sets, were performed with the JY616 cells. In each experiment, an initial stock of each cell line was split into multiple culture aliquots, which were maintained in parallel in log-phase growth conditions by serial passaging in the presence of each reverse transcriptase inhibitor or in control medium lacking an inhibitor. Analogs were tested individually or in certain combinations. Figures 1B and C and Fig. 2 show representative data from one set of Southern blotting analyses, in which JY616 cells were passaged in either medium alone (RPMI panel), 0.01 or 0.03% DMSO, or various inhibitors as indicated on the panels. The Southern blots

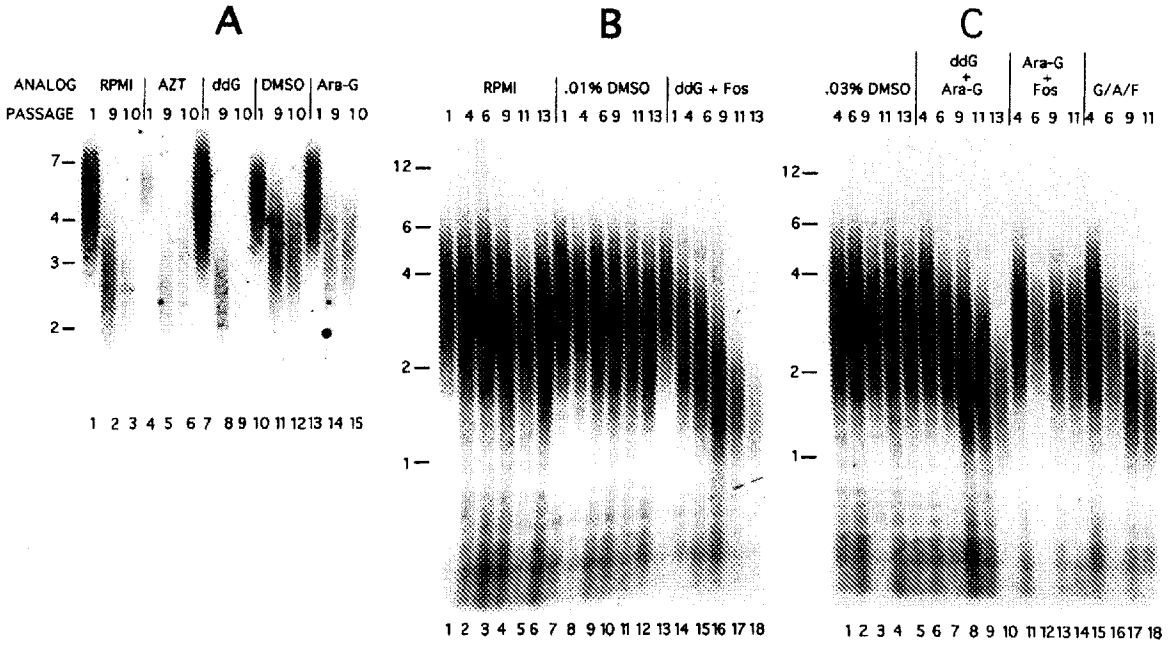

FIG. 1. Telomere lengths of JY616 cells grown in the presence of ddG and other analogs. DNAs from serial passages of JY616 cells grown in the absence or presence of analogs or DMSO were restriction digested with *Rsa*I and *Hin*fI (A) or *Mse*I and *Mnl*I (B and C), run on a 0.8% agarose gel, and Southern blotted with the ^{32}P-labeled human telomeric oligonucleotide $(TTAGGG)_3$ as a probe. Numbers above each lane represent the week of passage for the sample. Size markers (in kilobases) are shown to the left of each panel. RPMI lanes are medium-only controls for AZT cultures. DMSO was the solvent for ddG and Ara-G, and DNA preparations from cells grown in medium containing 0.01% DMSO (lanes 10 to 12 in panel A and lanes 7 to 12 in panel B) were used as controls for ddG- or Ara-G-containing cultures; 0.03% DMSO (lanes 1 to 5) in panel C was the control for these two analogs in combination. (A) Lanes: 1 to 3, RPMI medium-only control; 4 to 6, 100 μM AZT; 7 to 9, 10 μM ddG plus 0.01% DMSO; 10 to 12, 0.01% DMSO (control for ddG plus DMSO); 13 to 15, 12 μM Ara-G. (B and C) A separate experiment in which analogs were used in combination, starting from a different stock culture of JY616 cells from that used in panel A. (B) Lanes: 1 to 6, RPMI medium-only control; 7 to 12, 0.01% DMSO as control for ddG plus foscarnet or Ara-G plus foscarnet; 13 to 18: 10 μM ddG plus 300 μM foscarnet. (C) Lanes: 1 to 5, 0.03% DMSO as control for ddG plus Ara-G; 6 to 10, 10 μM ddG plus 12 μM Ara-G; 11 to 14: 12 μM Ara-G plus 300 μM foscarnet; 15 to 18, 10 μM ddG plus 12 μM Ara-G plus 300 μM foscarnet (G/A/F).

shown in Fig. 1B and C were probed with the telomeric ^{32}P-labeled oligonucleotide $(TTAGGG)_3$, and telomeric mean lengths and distributions were measured by scanning densitometry of the autoradiograms. Figure 2 graphically shows the mean telomere length data over time from this representative set of passaging series, along with the corresponding number of MPDs for each culture.

In every experiment, 10 μM ddG reproducibly caused progressive telomere shortening beyond that seen in control cultures lacking ddG. Figure 3 shows the results for 26 separate passaging series in which telomere lengths were compared at the beginning of the passaging and after the number of MPDs indicated for each culture. The only case in which more telomere shortening occurred than in the parallel culture maintained in ddG was in one culture containing AZT (Fig. 3, JY5 panel). However, in these and all other JY616 cultures, the MPD rates remained similar to each other and did not change significantly over any of the passaging series (see Fig. 2 and 7 for examples; also see below).

In similar experiments, the same inhibitors were tested individually on Jurkat T cells. Again, the highest concentration of each analog which did not cause cytotoxicity after five to seven MPDs was chosen for use as described in Materials and Methods. The cytotoxicity levels for several of the analogs were markedly different for the JY616 B cells and the Jurkat T cells. However, although the concentrations of inhibitors used on the B- and T-cell lines in the time course experiments were different, they were functionally equivalent in terms of being twofold below their detectable cytotoxic levels.

Most of the analogs tested caused no reproducible telomere shortening in Jurkat cells, even after prolonged culture (~100 MPDs) in the presence of the analog (data not shown). As described below, Jurkat cell telomere length distributions were highly variable over time and between cultures. However, 30 μM ddG reproducibly caused telomere shortening in duplicate Jurkat T-cell cultures. In a typical result, at the beginning of the experiment the TRF lengths formed a broad distribution ranging from ~13 to ~2 kb, whereas after 142 MPDs in ddG, they ranged from ~8 to ~2 kb (data not shown). Again, in all cultures, cell growth rates remained unchanged throughout the entire passaging series.

Inhibition of telomerase activity in vitro by ddGTP and AZT-TP. Because ddG caused TRFs to shorten reproducibly in both the JY616 B-cell and Jurkat T-cell lines and, as described below, AZT had variable effects on telomere lengths, we tested whether telomerase activity from these cells was inhibited in vitro by ddGTP and AZT-TP. A new partial purification protocol for human telomerase and conventional in vitro telomerase reactions (see Materials and Methods) were used to assay for telomerase activity in both cell lines. The TTAGGG repeat elongation products of telomerase were fractionated by polyacrylamide gel electrophoresis. An RNase-sensitive, primer-dependent 6-nucleotide repeat banding pattern was seen for both cell lines (Fig. 4A, compare lanes 17 and R; Fig. 4B, compare lanes 19 and R). Thus, telomerase activity was present in both cell lines. In the reactions with the Jurkat cell fractions, in addition to the RNase-sensitive telomerase products, a few heavily labelled bands appeared at and above the

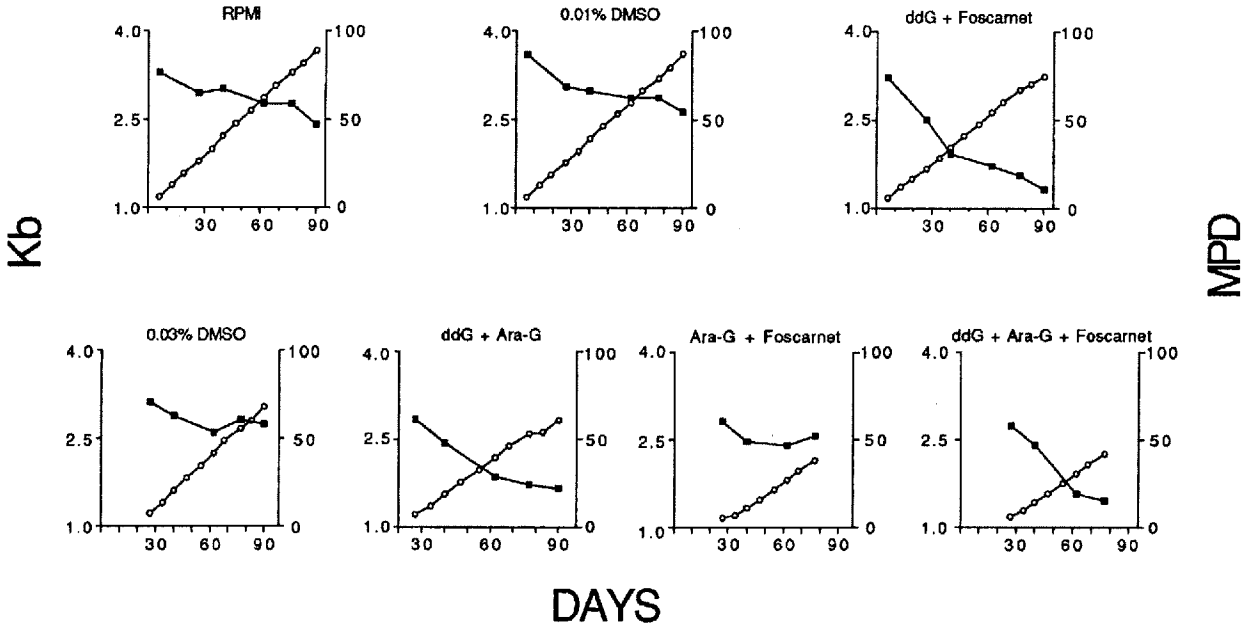

FIG. 2. Telomere lengths and growth rates of JY616 cells grown in the presence of combinations of analogs, DMSO, or medium-only controls. Densitometry analyses of Southern blots shown in Fig. 1B and C were performed. The center of the broad peak of telomeric DNA hybridization in each lane was used to calculate the average TRF length in kilobases for each cell population. MPDs (right y axis) are shown as open circles plotted against days in culture (x axis). Mean TRF lengths in kilobases (left y axis) are shown as solid squares plotted against days in culture (x axis).

position of the input telomeric repeat oligonucleotide primer (Fig. 4B). These bands were not RNase sensitive (Fig. 4B, compare lanes 19 and R) and therefore may result from addition of [^{32}P]dG residues to the DNA primer by terminal deoxynucleotidyl transferase, which is overexpressed in some acute lymphocytic T-cell leukemias (29).

ddGTP was an efficient in vitro inhibitor of both these human cell telomerase activities, causing 50% inhibition of overall product formation at 1 μM ddGTP in the presence of 5 μM dGTP, 2 mM TTP, and 2 mM dATP, as measured by phosphorimager analysis (Fig. 4A, lanes 1 to 6; Fig. 4B, lanes 1 to 8; Fig. 5A, left panel). Interestingly, in contrast to the effect of ddGTP on *T. thermophila* telomerase in vitro (14, 42), the inhibition of the telomerase activity from these human cells was not accompanied by alterations in the banding patterns of the products seen in gel electrophoresis (Fig. 4) or in a decreased ratio of longer to shorter products (Fig. 5B). Changes in the relative intensities of the bands corresponding to the positions of dG residues in the TTAGGG repeats, with a concomitant shift to shorter products, would have been expected for chain termination events. Hence, these results are consistent with those reported previously for human HeLa cell telomerase by Morin (32), who proposed that while ddGTP is efficiently recognized, it is not itself incorporated into the newly forming DNA. This differs from the incorporation of dideoxynucleotides and other chain-terminating analogs by *T. thermophila* telomerase (42).

AZT-TP inhibited telomerase activity from both the immortalized JY616 B-cell and Jurkat T-cell lines in vitro. As with ddGTP, overall product synthesis was decreased without a significant alteration of the banding pattern of elongation products (Fig. 4A, lanes 7 to 17; Fig. 4B, lanes 9 to 19). However, consistent with previous results from *T. thermophila* telomerase (42), AZT-TP was a much less potent inhibitor of telomerase from these human cell lines than was ddGTP, with

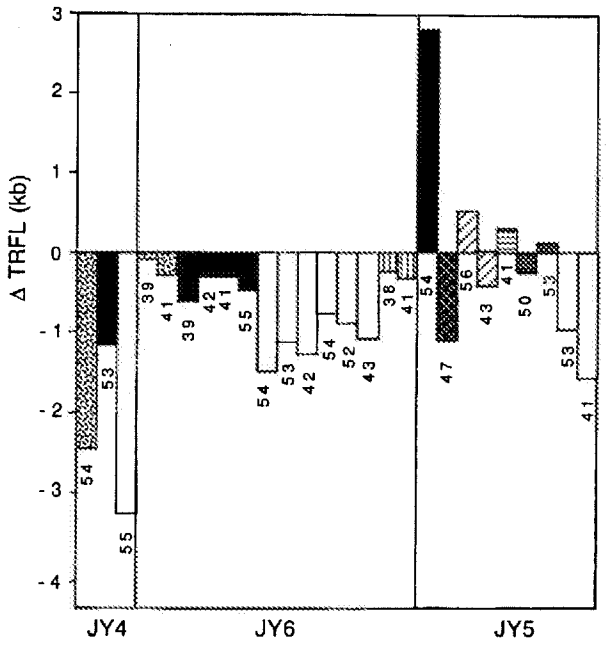

FIG. 3. Change in mean TRF lengths (Δ TRFL) of DNA from JY616 cells grown in the presence or absence of reverse transcriptase inhibitors. Telomere lengths (kilobases) for each of 26 cultures grown with or without analogs were measured by scanning densitometry at an early passage (1 to 3 weeks in culture) and at a later time point when each culture was approximately the same age. Changes in lengths are shown as histogram bars. The number of MPDs elapsed is shown under each bar. Histogram bars: stippled, RPMI medium alone; black cross-hatched, AZT; horizontally hatched, d4T; gray, foscarnet; diagonally hatched, Ara-G plus DMSO; vertically hatched, Ara-G plus foscarnet plus DMSO; black, DMSO; white, ddG plus DMSO. The three panels represent three separate experiments. JY4 is the experiment shown in Fig. 1A. Duplicate cultures are shown for several analogs and controls in experiments JY5 and JY6.

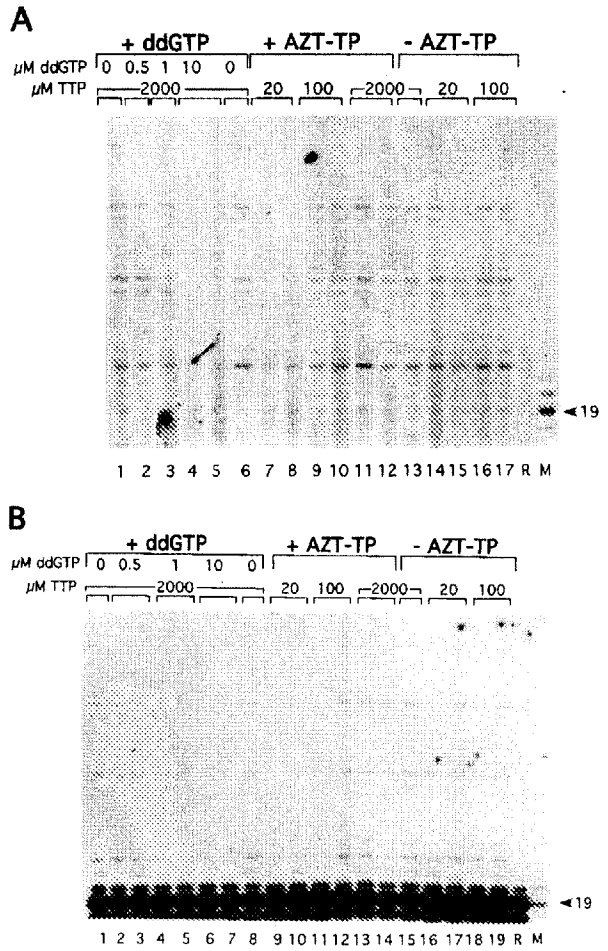

FIG. 4. Lymphoid cell telomerase activity. Telomerase reaction product profiles are shown from conventional telomerase assays (see Materials and Methods) with DEAE-purified S100 extracts from either JY616 cells (A) or Jurkat E6-1 cells (B), performed in the presence of the indicated concentrations of ddGTP (0, 0.5, 1, or 10 μM) plus 2,000 μM TTP or 100 μM AZT-TP with different concentrations of TTP (20, 100, or 2,000 μM). The reaction products were separated on denaturing 10% polyacrylamide gels. Concentrations of ddGTP and TTP are indicated above the lanes. Lane R in each panel indicates RNase-pretreated reactions. The input primer $(TTAGGG)_3$, labeled by addition of a dG residue with terminal deoxynucleotidyl transferase, is included as a 19-nt size marker (lane M and arrow).

100 μM AZT-TP causing significant inhibition (80%) of product synthesis only when the TTP concentration was lowered to 20 μM (Fig. 4A, lanes 7 and 8; Fig. 4B, lanes 9 and 10; Fig. 5A, right panel).

We tested whether telomerase activity extracted from cells that had undergone up to 38 passages in ddG or 16 passages in AZT had become resistant to either inhibitor. The in vitro TRAP assay (22) was used as described in Materials and Methods. Figure 6A shows an example of an autoradiogram of such TRAP assays, performed in the presence of different ddGTP concentrations, for telomerase from JY616 cells. The results of this and similar assays of JY616 cell telomerase, assayed after different numbers of passages in ddG or in control medium containing 0.01% DMSO, and Jurkat T-cell telomerase, after prolonged passaging in AZT or the control medium (see below), were plotted graphically (Fig. 6B and C). There was no loss of sensitivity to ddGTP or AZT-TP after passaging in the respective analog (Fig. 6B and C). Similar results were obtained with Jurkat cells after passaging for 91 days in ddG (data not shown). Hence, there was no evidence for any selection for a subset of cells whose telomerase had mutated to become resistant to either ddGTP or AZT-TP.

Highly variable telomere lengths in the B- and T-cell lines. A previous report (8) indicated that telomere lengths were relatively stable over many generations in an immortalized human embryonic kidney cell line (the HA1-IM 293 line). In contrast, highly variable and stochastic patterns of telomere length changes were apparent in both of the immortalized human cell lines analyzed here. In all the experiments performed, the cell growth conditions were closely controlled to maintain logarithmic growth rates. Despite these precautions, telomere length variability was very marked not only within a culture during its propagation for prolonged periods but also between cultures passaged in parallel. We observed large changes in mean telomere lengths as well as in length distributions, with different types of changes being characteristic for each cell line.

In JY616 cells, as shown in Fig. 1, the entire population of telomeric restriction fragments usually consisted of a single broad peak. Hence, at any one time point, telomeres fell primarily into a unimodal length distribution about a single common mean length. However, the mean telomere length both increased and decreased over time in many cultures, including those lacking any inhibitor. Furthermore, for the most part, these changes were different between duplicate cultures propagated in parallel after seeding with aliquots from the same initial stock culture. The only exceptions to this nonreproducibility were the B- and T-cell cultures grown in the presence of ddG, which invariably showed progressive telomere shortening, as described above. Figure 7 shows a sampling of the variety of telomere length dynamics observed in JY616 cells cultured for up to 281 days.

Many of the JY616 cultures exhibited both gradual (~10 to 40 bp/MPD) and rapid (~200 to 400 bp/MPD) stochastic decreases in telomere length. An example of progressive gradual decrease was seen in one AZT passaging series (Fig. 7, AZT panel). Between passages 5 and 19 (days 36 to 148), the mean TRF length gradually decreased by ~20 bp/MPD, leading to an overall telomere shortening of ~1.6 kb. In an experiment in which a culture was grown in 10 μM ddG for 281 days, as with all other ddG cultures, the telomeres shortened (Fig. 7, ddG panel). The rate of loss was ~73 bp/MPD between passages 5 and 9 (days 20 to 36) in this passaging series. At 120 days, the culture was split in two and the remainder of the passaging series was continued in either ddG alone or ddG plus 100 μM AZT. The telomeres remained short in both passaging series. The growth rates were slightly but not significantly different for the cultures in ddG alone versus those in ddG plus AZT (Fig. 7, 10 μM ddG panel). With Ara-G or foscarnet alone, as with AZT alone, telomere shortening was seen sporadically (although not reproducibly [see below]). However, adding Ara-G and/or foscarnet together with ddG caused no additive or synergistic effects on telomere shortening or changes in long-term cell growth rates (Fig. 2 and 3). One d4T culture showed small decreases and increases in mean telomere length during the entire experiment but no consistent long-term trend toward either shortening or lengthening (Fig. 7, d4T panel).

With foscarnet, in one culture between passages 5 to 15 (from days 36 to 117, corresponding to 66 MPDs), the mean TRF also decreased by ~15 bp/MPD (Fig. 7, left foscarnet panel), whereas in the duplicate foscarnet culture, there was a very gradual overall decrease of ~4 bp/MPD between passages

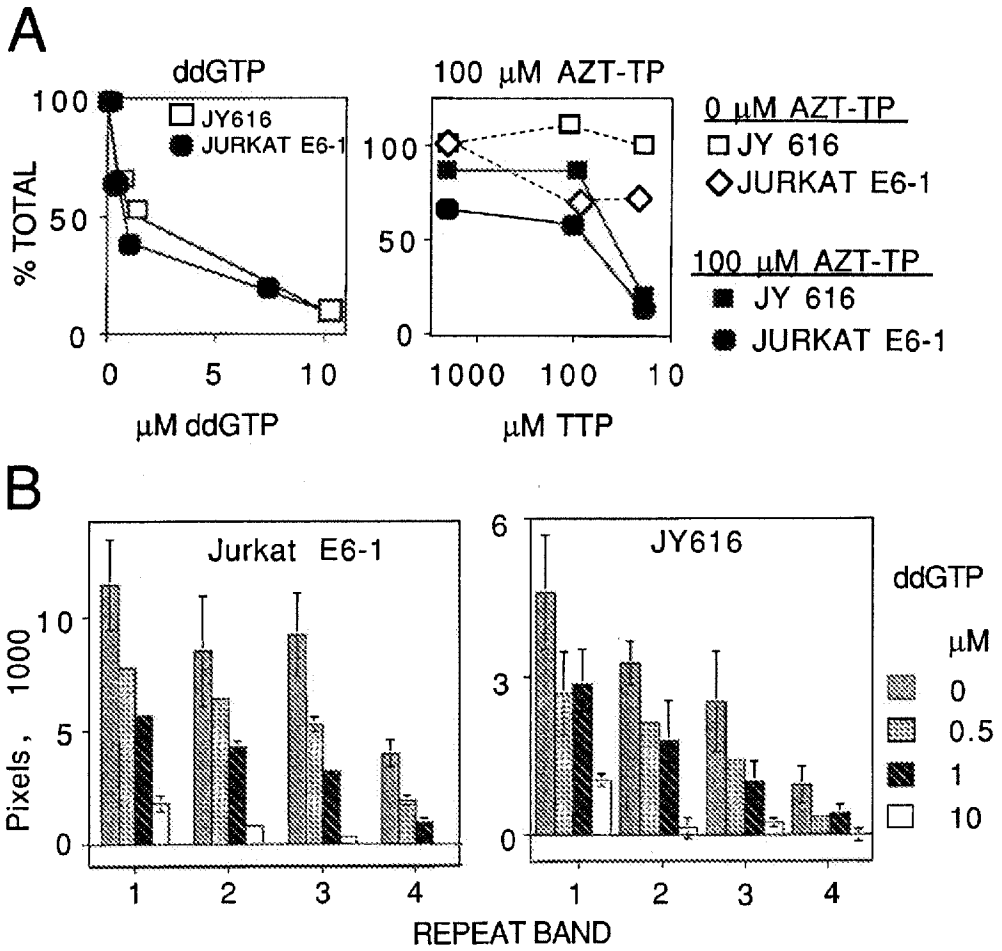

FIG. 5. Inhibition of lymphoid cell telomerase activity by ddGTP and AZT-TP. (A) Conventional telomerase assays were performed with DEAE-purified S-100 extracts from either JY616 or Jurkat E6-1 cells (see Materials and Methods). The intensities of the first four strong bands with 6-base periodicity above the input primer size were measured by phosphorimaging. After subtraction of backgrounds, the total phosphorimager units (pixels) of the sum of all four bands in each lane are plotted (*y* axis), setting the values for the control reactions at 100%. Data shown for Jurkat cell and JY616 cell telomerase reactions with ddGTP are the average for three experimental duplicate sets. Data for JY616 cell telomerase with AZT-TP represent one experimental duplicate set. (B) Quantitation of each of the first four strong bands with 6-base periodicity above the input primer size in the telomerase reaction product profiles. Conventional telomerase assays were performed as in panel A with different concentrations of ddGTP. Bands 1 and 4 are the shortest and longest product measured, respectively.

5 and 31 (Fig. 7, right foscarnet panel). Decreases in telomere lengths of ~50 bp/MPD have been reported in primary and immortalized human fibroblast cell lines lacking detectable telomerase (8, 17, 34). Thus, these gradual decreases in length in the JY616 cells were less than would have been predicted from the absence of telomerase-mediated maintenance.

Rapid stochastic decreases in mean TRF lengths were observed in some cultures of JY616 cells. In 12 μM Ara-G, in just one passage (between passages 9 and 10; days 64 to 76) the mean TRF length of the entire telomere population dropped by approximately 380 bp/MPD (Fig. 7, Ara-G panel). A less extreme drop was seen in another Ara-G culture (~75 bp/MPD over passages 6 to 8; days 43 to 58 [data not shown]).

Rapid stochastic increases in TRF length of some or all of the entire telomere population were also observed; in one example of JY616 cells passaged in DMSO, a mean TRF increase of ~240 bp/MPD for the entire telomere population was observed between the third and fifth passages (data not shown). In an interesting example (Fig. 7, left foscarnet panel), initially the majority of the population of telomeres steadily lost approximately 1 kb of telomeric DNA over 66 MPDs (~15 bp/MPD). Then in a single passage of 6.5 MPDs (between passages 14 and 15), a large telomere subpopulation suddenly gained almost 4 kb in length, an increase of ~600 bp/MPD. At this point, this cell culture abruptly exhibited a bimodal distribution of telomere lengths, after which the population of longer telomeres gradually shortened again. Southern blotting analysis of this passaging series is shown in Fig. 8. In contrast, the duplicate culture grown in foscarnet did not exhibit any notable changes in mean telomere length or length distribution (Fig. 7, right foscarnet panel).

With Jurkat T cells, in most cultures the mean TRF lengths increased dramatically as the cells were propagated in log-phase growth conditions (Fig. 9, lanes 1 to 5, 6 to 10, 21 to 25, and 26 to 30). As described above, the only reproducible exception to the general telomere lengthening was with ddG, in which telomeres invariably steadily shortened. In several cultures, the overall hybridization patterns also became more

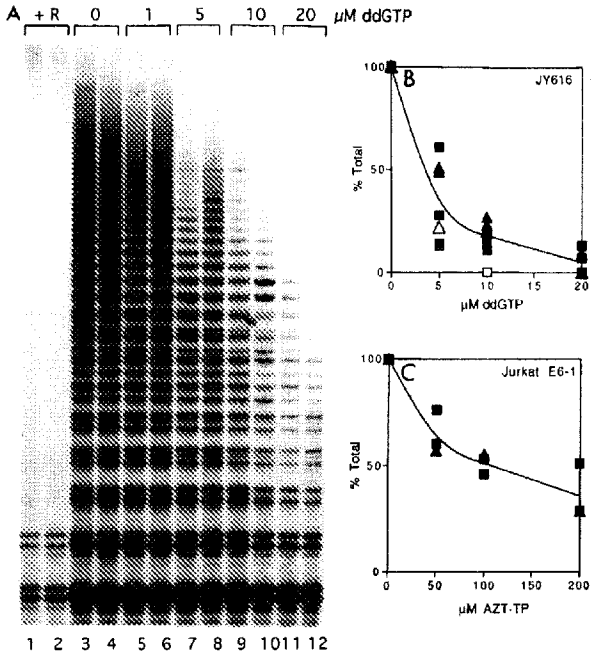

FIG. 6. Inhibition by ddGTP and AZT-TP of telomerase activity from cells passaged in the presence or absence of ddG or AZT. (A) Denaturing 10% polyacrylamide gel showing reaction products of TRAP assays (22) of telomerase performed with different ddGTP concentrations. TRAP assays (see Materials and Methods) were performed in duplicate on extracts from JY616 cells passaged in the presence of 0.01% DMSO for 30 weeks. The indicated concentrations of ddGTP were added to the telomerase reaction mixtures. These concentrations were previously determined to cause no inhibition of the PCRs when added to the PCR mixture only following the telomerase reaction (data not shown). RNase A was added to duplicate telomerase reaction mixtures as a control for non-telomerase-mediated incorporation of the ^{32}P label (+R lanes). The amount of extract used per reaction represented approximately 100 cells, with 1/10 of the total reaction mixture loaded onto a denaturing 10% polyacrylamide gel. (B and C) TRAP assays were performed in duplicate as in panel A, with approximately 100 cells per reaction, and contained the indicated concentrations of ddGTP or AZT-TP added to the telomerase reaction mixture. These concentrations were previously determined to cause no inhibition of the PCR. (B) JY616 cells grown in 10 μM ddG for one passage (□) and in 10 μM ddG for 12, 30, and 38 passages (■) or in 0.01% DMSO for one passage (△) or 30 passages (▲). (C) Jurkat E6-1 cells grown for 16 passages in 100 μM AZT (■) or RPMI control medium (▲). The two Jurkat cultures grown in AZT are each passage 16 of the same passaging series shown in Fig. 9, lanes 17 to 20 and 26 to 30, and the control RPMI culture is passage 16 of a passaging series similar to that shown in Fig. 9, lanes 7 to 10.

complex, suggesting that multiple subpopulations of telomeres with widely separated mean lengths were generated, each subpopulation having a relatively tight distribution about its mean length, so that the telomeres now fell into discrete length subsets (Fig. 9, lanes 9 and 10 and lanes 28 to 30). In one culture grown in 100 μM AZT, one modal telomere size class, which shortened in concert with the rest of the telomeres, decreased in mean TRF length from ~12 to ~8 kb over 15 passages, a shortening rate of ~50 bp/MPD (Fig. 9, lanes 16 to 20). The entire telomere population in this culture showed the same steady shortening over the entire 15 passages (92 MPDs) monitored. This shortening was clearly distinguishable from the length variations in control cultures: without AZT or ddG no similar steady shortening was seen in any of the total of 24 different Jurkat E6-1 cell-passaging series analyzed. In contrast, telomeres in the duplicate AZT culture (Fig. 9, lanes 26 to 30) showed the same general increase in telomere lengths as did several of the control cultures (compare with Fig. 9, lanes 21 to 25). However, the sensitivity to AZT-TP of telomerase activity from both cultures remained the same as that for the control culture (Fig. 6).

Extreme telomere shortening without cell senescence. The shortest mean TRF lengths occurred in JY616 cells grown in the presence of ddG or Ara-G. Examples were found in which the mean TRF lengths were ~1.1 kb (ddG, foscarnet, plus Ara-G), ~1.6 kb (ddG plus foscarnet), ~1.3 kb (another culture grown in ddG plus foscarnet), and ~1.4 kb (a culture grown in ddG plus foscarnet plus Ara-G) (Fig. 2 and 3 and data not shown). Furthermore, the broad band comprising the total telomeric fragment population was clearly visible down to 1.0 kb at these and several other points in these experiments (for example, Fig. 1B, lane 17 and Fig. 1C, lanes 10 and 18). Because the hybridization signal obtained with the short oligonucleotide probe $(TTAGGG)_3$ underestimates the numbers of telomere molecules in proportion to the shortness of the telomere tract (see references 8 and 26 for discussion), the mean telomere length was also calculated as described previously (17) to correct for this underestimate. As expected, even lower estimates were obtained for the mean telomere lengths (data not shown), and the very short (~1.0-kb) telomeric restriction fragments often made up a significant proportion of the total telomeres present in the cell population.

The TRFs include subtelomeric DNA, which contains tracts of degenerate, TTAGGG-cross-hybridizing sequences (1, 7). Because it is not known whether these act as functional TTAGGG tracts, the presence of these degenerate tracts normally prevents exact length determination of the functional tracts on natural human telomeres. An estimate for the minimum telomeric TTAGGG-hybridizing tracts in a human embryonic kidney cell line at crisis was made with the same *RsaI-HinfI* digestion of human genomic DNA used here, by quantitating the TTAGGG repeat hybridization signals as a function of TRF length. At crisis, the mean TRF length fell to its observed minimum of ~3.4 kb, and the average length of TTAGGG-hybridizing repeat tracts was ~1.5 kb in these cells (8). Hence, the shortest TRFs in the JY616 cells were considerably shorter than those reported previously for natural telomeres. This may reflect the different cell types used in the different studies or, possibly, differences in growth conditions between this and other studies.

In an experiment in which JY616 cell cultures were maintained in parallel in continuous log-phase growth by frequent passaging for up to 281 days in either RPMI medium alone, 0.01% DMSO, or various inhibitors, the shortest mean telomere lengths observed were in 12 μM Ara-G (~1.6 kb; Fig. 7), and 10 μM ddG (~1.7 kb; Fig. 7). After these shortest telomeres were observed, the mean telomeric fragment lengths increased slightly and then stabilized at ~2.1 and ~2.0 kb, respectively. These stabilized lengths represented relative net losses of ~0.9 and ~1.3 kb, respectively, from the measured starting lengths. The loss, gain, and stabilization of these telomeres were reminiscent of the dynamics seen in the small fraction of primary cells which overcome cell cycle controls to become immortalized (8, 23). However, in the situation reported here, these telomere length changes were not accompanied by any significant decreases in cell population doubling rates or increases in the percentage of trypan-blue-positive cells, which might have indicated increased cell death.

In all the experiments, in spite of the dramatic telomere losses in JY616 cells, no senescence phenotype was observed for the cell population, even after continuous logarithmic phase growth in the presence of 10 μM ddG for up to 238 mean population doublings (Fig. 1, 2, and 7 and data not shown). Likewise, Jurkat cells maintained in logarithmic-phase

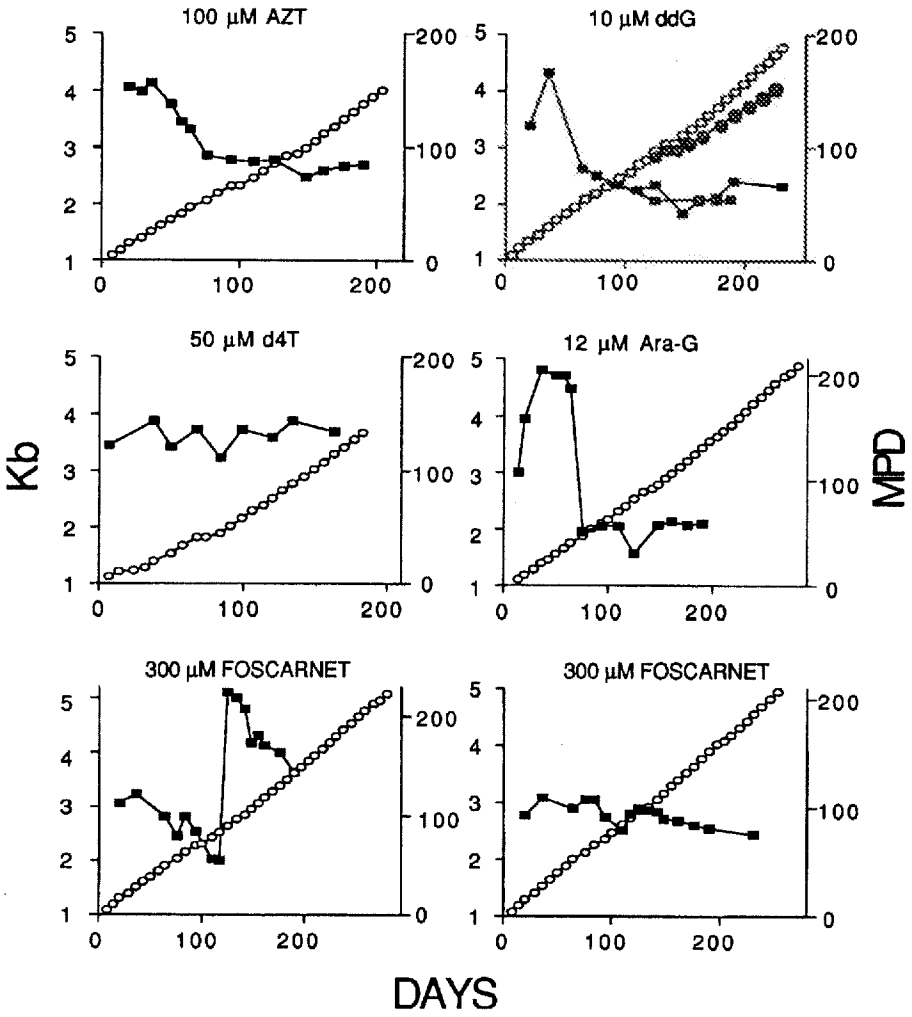

FIG. 7. Telomere lengths and growth rates of JY616 cells grown in the presence of analogs for up to 281 days. Growth rates and TRF lengths were calculated and plotted as in Fig. 2. MPDs (right *y* axis) are shown as open circles plotted against days in culture (*x* axis). Mean lengths of TRFs (in kilobases) (left *y* axis) are shown as solid squares plotted against days in culture (*x* axis). In the 10 μM ddG panel, the culture was split in two, and beginning at day 120, passaging was continued in 10 μM ddG alone (■, telomere lengths; ○, MPDs) or in 10 μM ddG plus 100 μM AZT (▨, telomere lengths; ◎, MPDs). In the left foscarnet panel, in which two distinguishable telomere subpopulations were seen, the mean length shown is that of the major subpopulation.

growth for ~100 MPDs in the presence or absence of inhibitors showed no decrease in growth rate or changes in cell morphology (data not shown). At the times during propagation when telomeres reached minimal lengths, as discussed above, there were no detectable changes in cell viabilities or population doubling rates. Hence, even extreme loss of telomeric DNA in these immortalized cell lines did not correlate with morphological changes, senescence, or cell death.

DISCUSSION

Human telomere shortening and telomerase inhibition by the nucleoside analog ddG. We have shown here that the nucleoside analog ddG reproducibly causes progressive telomere shortening in two immortalized human lymphoid cell lines, the B-cell line JY616 and the T-cell line Jurkat E6-1. This analog was the only reverse transcriptase inhibitor tested that consistently caused this effect in every culture duplicate of both cell lines. The progressive loss of telomeric DNA observed with ddG and in some cultures with AZT is predicted to occur in the absence of telomerase (reviewed in references 3 and 10) and resembles that initially seen after disruption of the telomerase RNA gene in *T. thermophila* and the budding yeasts *K. lactis* and *S. cerevisiae* (12, 31, 41, 46). Similar gradual shortening was reported in some subclones of an immortalized human fibroblast line which lacks detectable telomerase (34) and in human primary fibroblasts in culture, which also lacked detectable telomerase activity, as they approached senescence (8). However, telomerase activity was present in cell-free fractions of both the cell lines studied here and was efficiently inhibited in vitro by ddGTP. No effects on cell doubling rates, viability, or morphology occurred at the ddG concentrations used here, suggesting that other cellular DNA polymerases or DNA metabolic enzymes were not significantly perturbed. These results suggest that the progressive telomere shortening in all cultures grown in ddG is caused by inhibition of telomerase itself. The in vitro results further suggest that in human cells, ddG may cause its telomere-shortening effects by binding

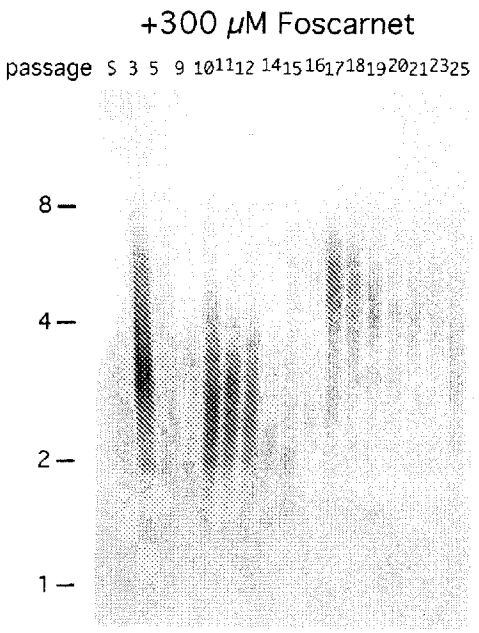

FIG. 8. Telomere lengths of JY616 cells grown in the presence of 300 μM foscarnet. DNAs from serial passages of JY616 cells grown in the presence of 300 μM foscarnet were restriction digested with *Rsa*I and *Hin*fI, separated on a 0.8% agarose gel, and Southern blotted with the ^{32}P-labeled human telomeric oligonucleotide $(TTAGGG)_3$ as the probe. Numbers above each lane represent the week of passage for each sample. S indicates DNA from the originating stock cell culture, not treated with analog. Kilobase size markers are shown to the left of the panel. The corresponding graph is shown in Fig. 7, left foscarnet panel.

to and competing for the nucleoside triphosphate-binding site of telomerase rather than by being incorporated and causing chain termination, since no evidence was found for incorporation of chain-terminating ddG residues in vitro. Hence, these findings provide evidence that telomere maintenance in human cells in culture can be perturbed by inhibition of telomerase activity by an exogenously added nucleoside analog.

In spite of significant telomere losses, the two established immortalized cell lines studied here continued to thrive. No senescence or changes in overall cell growth rates were observed even after continuous passaging under log-phase growth conditions for almost 1 year in the presence of ddG. Specifically, a significant finding was that no changes in doubling rates were detected at the points at which telomeres first reached minimum lengths. Telomerase remained sensitive to ddGTP in vitro. These results suggest that the degree of disruption of telomerase in these cell lines was insufficient to promote cellular senescence.

The ability of immortalized JY616 B cells to maintain telomeres at short lengths for prolonged periods in the presence of ddG, with no apparent decrease of population doubling rates, is consistent with observations in other systems suggesting that telomere length is regulated. Telomeres in many organisms do not normally fall below specific minimum lengths. During cell divisions in several of the same reverse transcriptase inhibitors tested here, *T. thermophila* telomeres decreased to a minimum threshold length below which no telomeres were detectable (42). Other studies of human telomeres are also indicative of a critical lower length limit below which telomere associations and fusions may increase (reviewed in reference 10). However, the exact minimum length for the TTAGGG repeat tract in human telomeres is unclear. In all the JY616 cultures, there appeared to be a minimum threshold length for the TRFs of ~1.0 kb. Hence, if the subtelomeric sequences in the TRFs of this cell line are similar to those in the embryonic kidney cell line analyzed by Counter et al. (8), this may represent as little as a few hundred base pairs of telomeric TTAGGG repeats. Such a short length is consistent with the very short telomeric TTAGGG repeat tracts reported at the end of an artificially constructed telomere in an immortalized human fibroblast cell line lacking detectable telomerase (34). Lacking associated tracts of degenerate TTAGGG-cross-hybridizing repeats, this telomere allowed accurate measurement of its minimal telomeric TTAGGG repeat tract length. At times, this was as little as a few hundred base pairs or less, with no apparent accompanying changes in cell growth rates or chromosome loss (34).

Analysis of telomere length regulation in cells of the yeast *K. lactis* synthesizing variant telomeric sequences has provided strong evidence that interactions with the telomeric DNA-protein complex regulate telomerase action at the chromosome end (31). The predicted consequence of this feedback mechanism is the selective addition of telomeric repeats to telomeres bearing shorter telomeric tracts, bringing their net lengths up to the level of the average population. While no direct information is available about the mechanism of such regulation in human cells, our results suggest that similar feedback could operate in the B- and T-cell lines maintained in ddG. In addition, as discussed below, sporadic mass shortening of the entire telomere population in several cultures also occurred, with no accompanying changes in cell population doubling rates or cell morphology and no evidence for senescence. The lack of senescence or cell death when the telomeres reached very short lengths and the stabilization of telomeres after that point suggest that to effectively overcome the regulation of telomere repeat addition, it will be necessary to perturb telomere length more severely than was accomplished by the inhibitors in this study.

Evidence for nonreciprocal recombination or gene conversion events. An unexpected outcome of the present studies was the high degree of variability in telomere lengths revealed in both of the human immortalized lymphoid cell lines analyzed. In the JY616 B-cell line, the stochastic changes in telomere lengths were usually concerted increases and decreases in mean length of the entire telomere population. These occurred either gradually or rapidly. Gradual concerted length changes are expected if the predominant telomere maintenance mechanism involves regulated additions by telomerase, countered by gradual telomere-shortening processes. In other human and nonhuman systems, telomeres are also globally regulated in concert (2, 8, 25, 43), with mean telomere length and length distribution being determined by the interactions of many genetic loci in *S. cerevisiae* (43; reviewed in reference 3). Over time, even slight perturbations of the relative rates of telomerase action versus DNA losses from the chromosome end will lead to gradual lengthening or shortening (reviewed in reference 3). While in the JY616 cells the trend was often toward gradual shortening (Fig. 1A, 7, and 8), this varied in rate even between duplicate cultures. In some but not all ddA and DMSO cultures, the mean TRF length increased gradually throughout the entire passaging (data not shown). These results suggest that the actions of telomerase and shortening mechanisms were modulated in a variable fashion. Since different cell culture aliquots showed marked differences in the lengths of the entire telomere population from culture to culture, small changes in cell conditions and possibly feedback between cells may have occurred in each cell population.

The sudden large drops in average telomere length, most

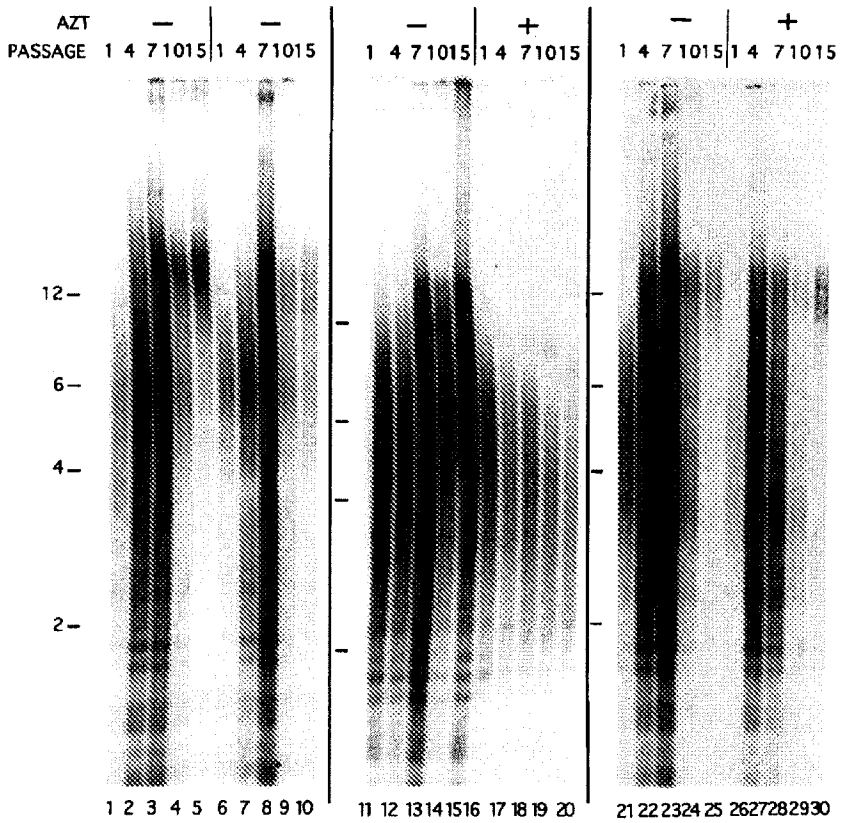

FIG. 9. Telomere length dynamics in Jurkat E6-1 cells grown in the absence or presence of 100 μM AZT. DNAs from serial passages of Jurkat E6-1 cell cultures grown in the absence (lanes 1 to 15 and 21 to 25) or presence (lanes 16 to 20 and 26 to 30) of 100 μM AZT were restriction digested with *MseI* and *MnlI*, separated on a 0.8% agarose gel, and Southern blotted with the ^{32}P-labeled human telomeric oligonucleotide $(TTAGGG)_3$ as the probe. Numbers above each lane represent the week of passage for each sample. Kilobase size markers are shown to the left of each panel. All cultures analyzed were split from the same cell stock at the start of the experiment (except that shown in lanes 6 to 10, which was subcultured at 3 weeks from the culture shown in lanes 11 to 15) and grown under identical conditions. Each set of lanes represents a separate culture; i.e., lanes 1 to 5, lanes 6 to 10, lanes 11 to 15, and lanes 21 to 25 represent four different medium-only control cultures, respectively. Lanes 17 to 20 and lanes 26 to 30 show two separate cultures grown in 100 μM AZT.

notably the ~380-bp/MPD drop in one JY616 cell culture grown in Ara-G, were much faster than predicted from lack of telomerase activity, which has been associated with loss rates of only ~50 bp per MPD (8, 17, 34). In addition, the ~600-bp/MPD length increase in one foscarnet culture (Fig. 7 and 8) was much greater than expected for telomerase action. Again, it was striking that in JY616 cells, usually the entire telomere population was shifted abruptly up or down in length.

The Jurkat E6-1 T-cell line showed even more complex and dynamic telomere length behavior. On the one hand, except in ddG, most telomeres in most T-cell cultures gradually lengthened during prolonged log-phase growth, with few if any telomeres detectable in the lower regions of the gels. On the other hand, the telomere population also stochastically showed sudden large changes in patterns of length distributions, with several discrete size classes often generated simultaneously. The observation of rapid, wide fluctuations in telomere lengths in an immortalized fibroblast cell line lacking detectable telomerase activity led Murnane et al. to propose that elongation of shortened telomeres can occur by nonreciprocal recombination (34). The large, rapid, stochastic increases and decreases in average telomere lengths in the B and T cells studied here are strikingly similar to the results with this fibroblast line. Telomere-telomere gene conversion and/or recombination events, often leading to massively lengthened telomeres, have been seen in *K. lactis* cells with telomerase RNA gene deletions (31a). The nontelomerase telomere maintenance pathways operative in the descendents of the survivors of the telomerase RNA deletion event and in the human fibroblast cell line lacking detectable telomerase (34) are adequate to support indefinite and relatively rapid cell population doubling rates.

To account for the surprising degree of telomere length variability in the immortalized human B and T cells analyzed here, we propose that in these cells, telomeres are maintained through a combination of telomerase and nontelomerase mechanisms acting on telomeric DNA. Our results indicate that the relative predominance of these mechanisms is characteristic of individual cell lines and may vary within a cell line at different times. Specifically, we propose that the large length changes characteristic of the Jurkat cell cultures and seen more rarely in the JY616 cultures result from extensive nonreciprocal recombination or gene conversions between telomeres. Such mechanisms could lead to periodic homogeneous lengthening or shortening of subsets of the telomeric population. These observations suggest for the first time for human cells that nontelomerase mechanisms can be a major determinant of telomere length, even in cells in which telomerase is active, and can obscure its action. Such pathways are potentially an impediment to therapeutic approaches involving targeting telomerase activity.

An important aspect of the present study is that the strong stochastic component of telomere length variation would not have been revealed if we had not passaged and analyzed duplicate and often multiple cultures in parallel from the same initial stock. The variability in telomere populations was particularly striking because cell growth conditions were carefully controlled: MPD rates were monitored closely by cell counting, and passaging was performed quantitatively and frequently to maintain logarithmic growth rates. However, even though measured MPD rates may be constant for long periods, a characteristic of immortalized mammalian cells maintained in culture is the wide range of doubling rates of individual cells in the population. One study has shown that slowly and rapidly dividing cells within an immortalized population growing at a steady overall rate constantly give rise to cells with highly heterogeneous division rates, whose doubling rates repeatedly tend toward that of the population as a whole (16). Hence, even though we observed constant MPD rates, the superposition of inherent clonal heterogeneity onto stochastic alterations in telomere lengths may have contributed significantly to the large jumps in length seen in the populations and subpopulations of telomeres.

Effects of AZT on telomere maintenance. Stochastic variations in cell populations with variable clonal cell division rates may underlie the differences we observed between duplicate cultures grown in AZT, the only other inhibitor besides ddG that caused significant progressive telomere shortening. Although the effects were not identical from one culture aliquot to another, when telomere shortening did occur in the presence of AZT, the trend was very consistent for many passagings. Although AZT-TP was only a relatively weak inhibitor of human T- and B-cell telomerase in the in vitro assays used here, such assays may not directly reflect the degree of the effects in the cell.

Our results suggest that AZT-TP may exert a direct effect on human telomerase and that AZT can perturb telomere maintenance in immortalized T cells. As AZT is used clinically in the treatment of AIDS (24), its effect on a T-cell telomerase is of particular interest. It has recently been shown that normal T cells express telomerase activity (6a). Since human immunodeficiency virus type 1 infection is accompanied by large amounts of new $CD4^+$ T-cell production (20, 45), sustaining this additional prolonged proliferation in response to human immunodeficiency virus type 1 infection may require telomerase activity. Therefore, although the predominance of different pathways for telomere maintenance may differ between cell types and immortalized cells in culture may differ from those in vivo, a possible clinical implication of these findings is that AZT may interfere with telomere maintenance and hence could compromise T-cell proliferation during human immunodeficiency virus type 1 infection in patients.

In summary, we have shown that ddG causes marked progressive telomere loss in immortalized cells in culture, probably from inhibition of telomerase activity, and our data suggest that AZT may have similar effects. However, overall cell growth rates were unchanged, and the results suggest that when telomeres become very short, they may be subject to regulation which counteracts further losses of telomeric DNA. These detailed studies of telomere length dynamics also uncovered a strong variable and stochastic component to telomere length regulation in the two immortalized cell lines analyzed. These insights into telomere length regulation may be relevant to therapeutic approaches against both cancer and human immunodeficiency virus type 1 infection.

ACKNOWLEDGMENTS

We thank Karen Kirk, Michael McEachern, and Renata Gallagher for critical comments on the manuscript and other laboratory members for helpful discussions; Joel Goodman and Art Weiss, University of California, San Francisco, for cell strains; and Raymond F. Schinazi, AIDS Research and Reference Reagent program, division of AIDS, NIAID, NIH, for AZT-5′-triphosphate.

This work was supported by grant GM26259 from the NIH to E.H.B. Laboratory facilities were provided in part by the Lucille P. Markey Charitable Trust.

REFERENCES

1. **Allshire, R. C., J. R. Gosden, S. H. Cross, G. Cranston, N. Rout, J. W. Sugawara, J. W. Szostak, P. Fantes, and N. D. Hastie.** 1988. Telomeric repeat from *T. thermophila* cross hybridizes with human telomeres. Nature (London) **332**:656–659.
2. **Bernards, A., P. A. M. Michels, C. R. Lincke, and P. Borst.** 1983. Growth of chromosome ends in multiplying trypanosomes. Nature (London) **303**:592–597.
3. **Blackburn, E. H.** 1991. Structure and function of telomeres. Nature (London) **350**:569–573.
4. **Blackburn, E. H.** 1993. Telomerase, p. 557–576. *In* R. F. Gesteland and J. F. Atkins (ed.), The RNA world. Cold Spring Harbor Laboratory Press, Cold Spring Harbor, N.Y.
5. **Blackburn, E. H.** 1994. Telomeres: no end in sight. Cell **77**:621–623.
6. **Blackburn, E. H., and S.-S. Chiou.** 1981. Non-nucleosomal packaging of a tandemly repeated DNA sequence at termini of extrachromosomal DNA coding for rRNA in *Tetrahymena*. Proc. Natl. Acad. Sci. USA **78**:2263–2267.

6a. **Broccoli, D., J. W. Young, and T. De Lange.** 1995. Telomerase activity in normal and malignant hematopoietic cells. Proc. Natl. Acad. Sci. USA **92**: 9082–9086.

7. **Brown, W. R. A., P. J. MacKinnon, A. Villasante, N. Spurr, V. J. Buckle, and M. J. Dobson.** 1990. Structure and polymorphism of human telomere-associated DNA. Cell **63**:119–132.
8. **Counter, C. M., A. A. Avilion, C. E. LeFeuvre, N. G. Stewart, C. W. Greider, C. B. Harley, and S. Bacchetti.** 1992. Telomere shortening associated with chromosome instability is arrested in immortal cells which express telomerase activity. EMBO J. **11**:1921–1929.
9. **Counter, C. M., H. W. Hirte, S. Bacchetti, and C. B. Harley.** 1994. Telomerase activity in human ovarian carcinoma. Proc. Natl. Acad. Sci. USA **91**: 2900–2904.
10. **de Lange, T.** 1994. Activation of telomerase in a human tumor. Proc. Natl. Acad. Sci. USA **91**:2882–2885.
11. **de Lange, T., L. Shiue, R. M. Myers, D. R. Cox, S. L. Naylor, A. M. Killery, and H. E. Varmus.** 1990. Structure and variability of human chromosome ends. Mol. Cell. Biol. **10**:518–527.

11a. **Gilley, D., and E. H. Blackburn.** 1996. Specific RNA residue interactions required for enzymatic functions of *Tetrahymena* telomerase. Mol. Cell. Biol. **16**:66–75.

12. **Gilley, D., M. S. Lee, and E. H. Blackburn.** 1995. Telomerase RNA residues play critical roles in active site function. Genes Dev. **9**:2214–2226.
13. **Gottschling, D. E., and V. A. Zakian.** 1986. Telomere proteins: specific recognition and protection of the natural termini of *Oxymicha* macronuclear DNA. Cell **47**:195–205.
14. **Greider, C. W., and E. H. Blackburn.** 1985. Identification of a specific telomere terminal transferase activity in *Tetrahymena* extracts. Cell **43**:405–413.
15. **Greider, C. W., and E. H. Blackburn.** 1989. A telomeric sequence in the RNA of *Tetrahymena* telomerase required for telomere repeat synthesis. Nature (London) **337**:331–337.
16. **Grundel, R., and H. Rubin.** 1988. Maintenance of multiplication rate stability by cell populations in the face of heterogeneity among individual cells. J. Cell Sci. **91**:571–576.
17. **Harley, C. B., A. B. Futcher, and C. W. Greider.** 1990. Telomeres shorten during ageing of human fibroblasts. Nature (London) **345**:458–460.
18. **Hastie, N. D., M. Dempster, M. G. Dunlop, A. M. Thompson, D. K. Green, and R. C. Allshire.** 1990. Telomere reduction in human colorectal carcinoma and with ageing. Nature (London) **346**:866–868.
19. **Hiyama, E., K. Hiyama, T. Yokoyama, Y. Matsuura, M. A. Piatyszek, and J. W. Shay.** 1995. Correlating telomerase activity levels with human neuroblastoma outcomes. Nat. Med. **1**:249–255.
20. **Ho, D. D., A. U. Neumann, A. S. Perelson, W. Chen, J. M. Leonard, and M. Markowitz.** 1995. Rapid turnover of plasma virions and CD4 lymphocytes in HIV-1 infection. Nature (London) **373**:123–126.
21. **Holzmann, K., N. Blin, C. Welter, K. D. Zang, G. Seitz, and W. Henn.** 1993. Telomeric associations and loss of telomeric DNA repeats in renal tumors. Genes Chromosomes Cancer **6**:178–181.
22. **Kim, N. W., M. A. Piatyszek, K. R. Prowse, C. B. Harley, M. D. West, P. L. C. Ho, G. M. Coviello, W. E. Wright, S. L. Weinrich, and J. W. Shay.** 1994. Specific association of human telomerase activity with immortal cells and

cancer. Science **266**:2011–2015.
23. **Klingelhutz, A. J., S. A. Barber, P. P. Smith, K. Dyer, and J. K. McDougall.** 1994. Restoration of telomeres in human papillomavirus-immortalized human anogenital epithelial cells. Mol. Cell. Biol. **14**:961–969.
24. **Larder, B. A.** 1993. Inhibitors of HIV reverse transcriptase as antiviral agents and drug resistance, p. 205–222. *In* A. M. Skalka and S. P. Goff (ed.), Reverse transcriptase. Cold Spring Harbor Laboratory Press, Cold Spring Harbor, N.Y.
25. **Larson, D. D., E. A. Spangler, and E. H. Blackburn.** 1987. Dynamics of telomere length variation in *Tetrahymena*. Cell **50**:477–483.
26. **Levy, M. Z., R. C. Allsopp, A. B. Futcher, C. W. Greider, and C. B. Harley.** 1992. Telomere end-replication problem and cell aging. J. Mol. Biol. **225**: 951–960.
27. **Lundblad, V., and E. H. Blackburn.** 1993. An alternative pathway for yeast telomere maintenance rescues *est1*$^-$ senescence. Cell **73**:347–360.
28. **Lundblad, V., and J. W. Szostak.** 1989. A mutant with a defect in telomere elongation leads to senescence in yeast. Cell **57**:633–643.
29. **McCaffrey, R., T. A. Harrison, R. Parkman, and D. Baltimore.** 1975. Terminal deoxynucleotidyl transferase activity in human leukemic cells and in normal human thymocytes. N. Engl. J. Med. **292**:775–780.
30. **McClintock, B.** 1939. The behavior of successive nuclear divisions of a chromosome broken at meiosis. Proc. Natl. Acad. Sci. USA **25**:405–416.
31. **McEachern, M., and E. H. Blackburn.** 1995. Runaway telomeres in telomerase RNA gene mutants of *Kluyveromyces lactis*. Nature (London) **276**: 403–409.
31a. **McEachern, M., and E. H. Blackburn.** Submitted for publication.
32. **Morin, G. B.** 1989. The human telomere terminal transferase enzyme is a ribonucleoprotein that synthesizes TTAGGG repeats. Cell **59**:521–529.
33. **Moyzis, R. K., J. M. Buckingham, L. S. Cram, M. Dani, L. L. Deaven, M. D. Jones, J. Meyne, R. L. Ratliff, and J. Wu.** 1988. A highly conserved repetitive DNA sequence, $(TTAGGG)_n$, present at the telomeres of human chromosomes. Proc. Natl. Acad. Sci. USA **85**:6622–6626.
34. **Murnane, J. P., L. Sabatie, B. A. Marder, and W. F. Morgan.** 1994. Telomere dynamics in an immortal human cell line. EMBO J. **13**:4953–4962.
35. **Nilsson, P., C. Mehle, K. Remes, and G. Roos.** 1994. Telomerase activity *in vivo* in human malignant hematopoietic cells. Oncogene **9**:3043–3048.
36. **Prowse, K. R., and C. W. Greider.** 1995. Developmental and tissue specific regulation of mouse telomerase and telomere length. Proc. Natl. Acad. Sci. USA **92**:4818–4822.
37. **Rogalla, P., B. Kazmierczak, C. Rohen, G. Trams, S. Bartnitzke, and J. Bullerdiek.** 1994. Two human breast cancer cell lines showing decreasing telomeric repeat length during early *in vitro* passaging. Cancer Genet. Cytogenet. **77**:19–25.
38. **Sambrook, J., E. F. Fritsch, and T. Maniatis.** 1989. Molecular cloning: a laboratory manual, 2nd ed. Cold Spring Harbor Laboratory Press, Cold Spring Harbor, N.Y.
39. **Schmitt, H., N. Blin, H. Zankl, and H. Scherthan.** 1994. Telomere length variation in normal and malignant human tissues. Genes Chromosomes Cancer **11**:171–177.
40. **Shippen-Lentz, D., and E. H. Blackburn.** 1990. Functional evidence for an RNA template in telomerase. Science **247**:546–552.
41. **Singer, M. S., and D. E. Gottschling.** 1994. *TLC1*$^-$ template RNA component of *Saccharomyces cerevisiae* telomerase. Science **266**:404–409.
42. **Strahl, C., and E. H. Blackburn.** 1994. The effects of nucleoside analogs on telomerase and telomeres in *Tetrahymena*. Nucleic Acids Res. **22**:893–900.
43. **Walmsley, R. M., and T. D. Petes.** 1985. Genetic control of chromosome length in yeast. Proc. Natl. Acad. Sci. USA **82**:506–510.
44. **Wang, S.-S., and V. A. Zakian.** 1990. Telomere-telomere recombination provides an express pathway for telomere acquisition. Nature (London) **345**: 456–458.
45. **Wei, X., S. K. Ghosh, M. E. Taylor, V. A. Johnson, E. A. Emini, P. Deutsch, J. D. Lifson, S. Bonhoeffer, M. A. Nowak, B. H. Hahn, M. S. Saag, and G. M. Shaw.** 1995. Viral dynamics in human immunodeficiency virus type 1 infection. Nature (London) **373**:117–122.
46. **Yu, G., J. D. Bradley, L. D. Attardi, and E. H. Blackburn.** 1990. *In vivo* alteration of telomere sequences and senescence caused by mutated *Tetrahymena* telomerase RNAs. Nature (London) **344**:126–131.

Exhibit 5: Murakami et al., "Inhibition of Telomerase Activity and Cell Proliferation by a Reverse Transcriptase Inhibitor in Gynaecological Cancer Cell Lines," *Eur. J. Cancer* 35(6):1027–34 (1999).

Pergamon

European Journal of Cancer, Vol. 35, No. 6, pp. 1027–1034, 1999

Printed in Great Britain
0959-8049/99/$ - see front matter

PII: S0959-8049(99)00037-4

Original Paper

Inhibition of Telomerase Activity and Cell Proliferation by a Reverse Transcriptase Inhibitor in Gynaecological Cancer Cell Lines

J. Murakami, N. Nagai, K. Shigemasa and K. Ohama

The Department of Obstetrics and Gynecology, Hiroshima University School of Medicine, 1-2-3 Kasumi, Minami-ku, Hiroshima 734, Japan

Telomerase is a ribonucleoprotein which has a RNA template to bind and extend telomere ends, so prolonging the life of tumour cells. The aim of this study was to determine whether transcriptase function of telomerase could be inhibited by the reverse transcriptase inhibitors (RTI); azydothymidine (AZT), dideoxyinosine (ddI) and AZT-5′ triphosphate(AZT-TP). We examined their effects on the proliferation of cancer cells and the antitumour effects of cisplatin *in vitro*. The three agents did not cause major changes in telomerase activity or telomere length in MCAS cells. However, in HEC-1 cells changes in telomerase activity and telomere length were observed that were dependent on the RTI concentration and duration of exposure. ddI and AZT-TP reduced telomerase activity and shortened the length of the telomere. In the presence of RTI, the antitumour effects of cisplatin were enhanced. This was particularly evident in HEC-1 cells where there was a marked reduction in cell proliferation, appearance of morphological changes and senescent-like cells in the presence of ddI or AZT-TP. In MCAS cells, *TP53* expression was increased by ddI and AZT-TP, while *p21* expression was unchanged. In HEC-1 cells the expression of both *TP53* and *P21* was increased by ddI. Continuous administration of RTI enhanced the cell growth inhibition of cisplatin. RTI also inhibited the proliferation of some cells.

Key words: telomerase, telomere, RTI, enhancement of cisplatin, inhibition of cell growth
Eur J Cancer, Vol. 35, No. 6, pp. 1027–1034, 1999

INTRODUCTION

TELOMERES ARE the extreme ends of chromosomes, and their length is continuously reduced because of incomplete replication at the time of cell division. As the telomere shortens with cell divisions, the chromosome becomes unstable and cell senescence occurs.

Telomerase is a ribonucleoprotein which has a RNA template, binds and extend telomere ends. Telomerase activity is not detected in many normal adult somatic cells, but it is detected in germ cells, stem cells and cancer cells. Telomerase activity is extremely high in human cancer, and many attempts have been made to utilise telomerase activity in the diagnosis and management of cancer [1–5].

Correspondence to J. Murakami.
Received 11 Sep. 1998; revised 4 Jan. 1999; accepted 22 Jan. 1999.

Telomerase activity generally correlates with growth rate [6] and reflects differences in proliferation between tumour and normal cells [7]. Therefore, it should be possible to inhibit cell proliferation by suppressing telomerase activity. Several reports have described attempts to inhibit telomerase activity using reverse transcriptase inhibitors [8–11]. Telomerase activity can be inhibited and the telomere length shortened by retrovirus reverse transcriptase inhibitors such as azidothymidine (AZT), dideoxyguanosine (ddG), dideoxyinosine (ddI), arabinofuranyl-guanosine (Ara-G) and AZT-5′ triphosphate (AZT-TP) [8, 10]. We reviewed agents which are actually used clinically at present or agents which are going to be released soon. In the present study we used reverse transcriptase inhibitors to inhibit the transcription function of telomerase and examined the effect on the proliferation of cancer cells *in vitro*. We also examined their effect

Table 1. Effect of RTI in MCAS and HEC-1 cells

Cell line	RTI	IC_{50} (μM)	Inhibition efficiency: Concentration (μM)	Inhibition efficiency: Cell growth (MTT assay) inhibition (%)
MCAS	AZT	900	100	22.5
	ddI	400	10	18.4
	AZT-TP	65	5.0	21.2
HEC-1	AZT	1100	90	24.4
	ddI	200	10	23.1
	AZT-TP	50	4.0	19.6

in vitro on the antitumour action of cisplatin, a drug widely used in the treatment of gynaecological and other tumours. Finally, we examined whether long-term administration of reverse transcriptase inhibitors affected expression of the *TP53* and *p21* gene since these genes are thought to play a role in tumour cell growth and senescence.

MATERIALS AND METHODS

Cell lines

The human MCAS ovarian mucinous cystadenocarcinoma cells and HEC-1 uterine endometrial carcinoma G2 cells were obtained from the Japanese Cancer Research Resources Cell Bank. These cells were maintained al 37°C under 5% CO_2 in RPMI 1640 (Gibco BRL, Grand Island, New York, U.S.A.) and 10% fetal calf serum supplemented with penicillin (100 U/mL), and streptomycin (100 μg/mL) or gentamicin (50 μg/mL). Cells were counted with a haemocytometer and passaged every 4 to 6 days (five to seven population doublings) by reseeding 5×10^4 cells per flask into fresh medium.

The nucleoside analogues, azidothymidine (AZT), dideoxyinosine (ddI) and AZT-5′-triphosphate (AZT-TP), were purchased from Sigma (St Louis, Missouri, U.S.A.). Cells were harvested cells at various time points, pelleted, frozen in liquid nitrogen and stored at − 80°C.

Telomeric repeat amplification protocol assay

Preparation of cell extracts. The telomeric repeat amplification (TRAP) assay and the quantification of telomerase activity were performed as descrived previously [12]. The TRAPeze telomerase detection kit (Geron, Maryland, U.S.A.) was used according to the manufacturers instructions (Oncor, Gaithersburg, Maryland, U.S.A.) with minor modifications [13]. Cells were lysed, incubated on ice for 30 min, and then the lysate was centrifuged at 15 000 × g for 20 min at 4°C. The resulting supernatant fluid was transferred to a microtube, frozen and stored at − 80°C. For the PCR reaction 1 to 2 μL of extract (5 μg of protein) was added to the 48 μL reaction mixture that contained 2 U Taq DNA polymerase. After incubation at room temperature for 30 min for the telomerase extension reaction, the samples were subjected to 31 cycles of 94°C for 30 sec, 50°C for 30 sec and 72°C for 45 sec. PCR products were electrophoresed, and the gel was stained with SYBR® Green 1 (Molecular Probes Inc., Oregon, U.S.A.). Ladder formation was observed under a 254 nm transilluminator.

TRAP assay quantification was done as previously described [13]. The intensity of bands with 6-base periodicity above the internal control band as assessed by the PhosphoImaging System (EDAS system) BioMax 1D software from Kodak (Rochester, New York, U.S.A.). After subtraction of background the sum of the total pixels for all bands was divided by the pixels of the internal control band to determined a relative telomerase activity.

Cell growth inhibition by anticancer agents

On day 0 exponentially growing cells were harvested with trypsin (0.05%): EDTA (0.02%) and resuspended to a final

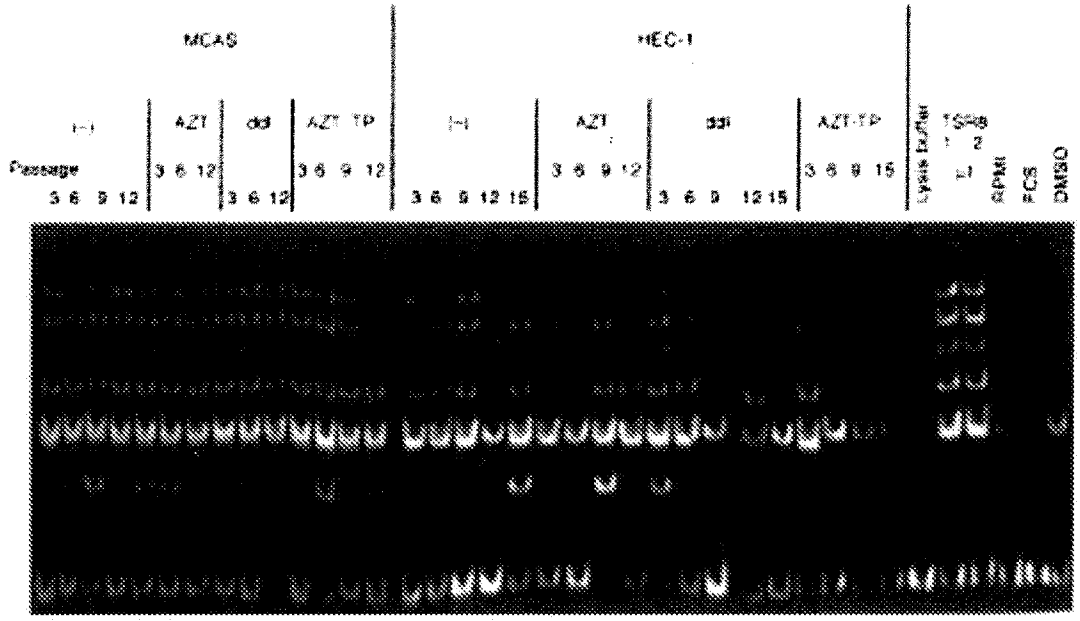

Figure 1. Inhibition of telomerase activity by RTIs. Telomerase activity was detected by the TRAP assay. TSR8 control template was used as a positive control and lysis buffer alone as a negative control. (−), medium without RTI. The band at the bottom is an internal control band of 36 bp.

concentration of 1.0×10^3 cells per mL in fresh medium with 1% FCS. Cell suspensions (100 μL) were dispensed into the individual wells of a 96-well tissue culture plate (Falcon, Franklin Lakes, New Jersey, U.S.A.). The cells were allowed to attach overnight, then cisplatin (50 μL) at different concentrations as added to individual wells. After 24-h incubation with the drug, this medium was replaced with fresh medium.

MTT assay

Viable cell growth was determined by a modified 3-(4,5-dimethylthiazol-2-yl), 5-diphenyltetrazolium bromide (MTT) assay as described previously [14]. 50 μL of MTT (1 mg per mL) was added to each well. The supernatant was removed after 4 h at 37°C. Acidified isopropanol (0.04 M HCl) (150 μL) was added and the solution was mixed thoroughly by repeated pipetting with a multichannel pipetter. The solution was maintained at room temperature for 15 min to solubilise the MTT-formazan product. Absorbance was measured with an ELISA plate reader at 570/630 nm (test/reference).

Southern blot analysis

Genomic DNA was prepared from normal and tumour tissue with a DNA Extraction Kit (Strategene, La Jolla, California, U.S.A.) and digested overnight with Hin I at 37°C. The resulting fragments (5 μg of DNA) underwent 0.7% agarose gel electrophoresis and then transferred to

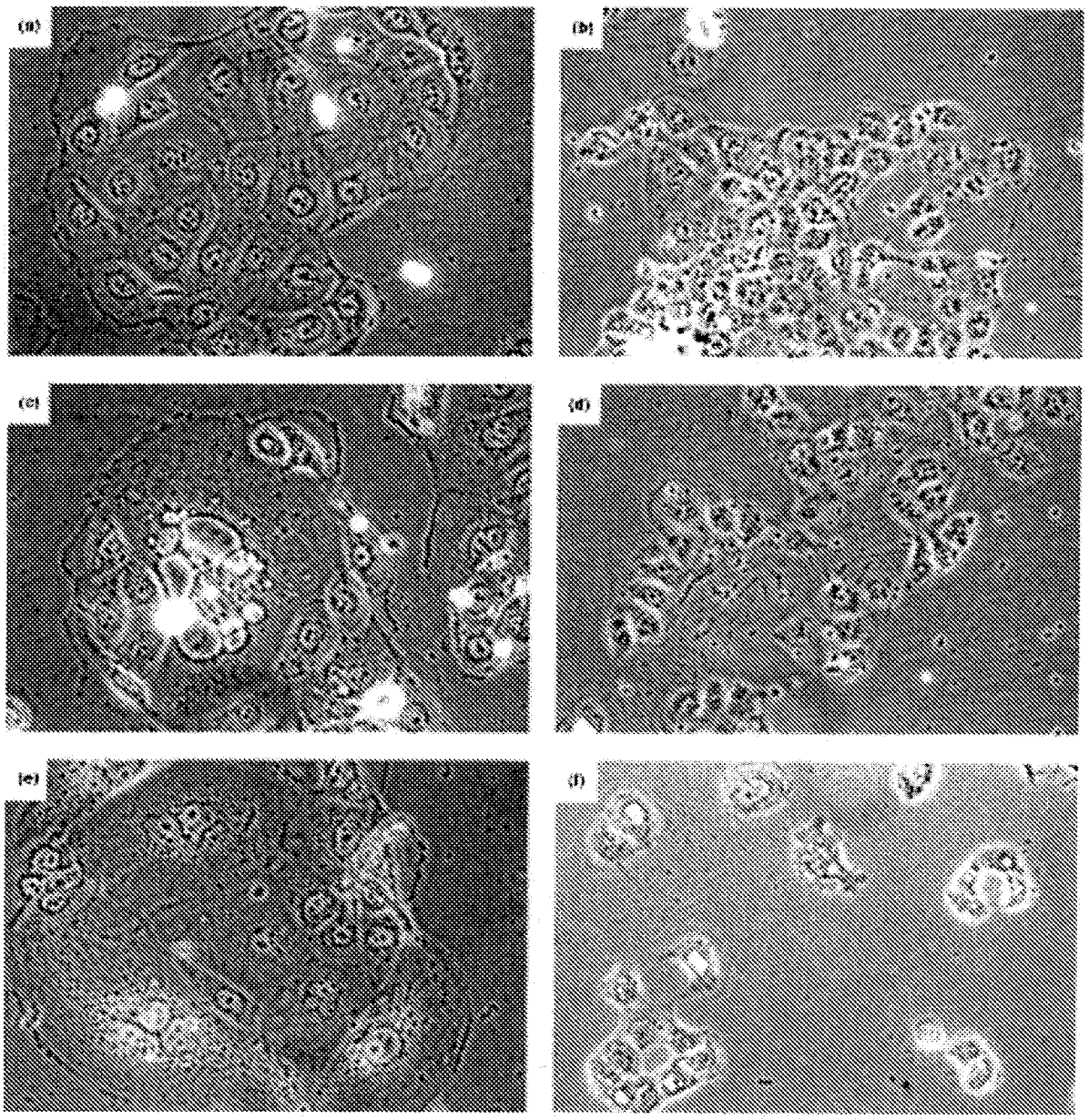

Figure 2. Changes in cell morphology in the presence of RTI. The cellular morphology of the HEC-1 cell line (a,c,e), and MCAS cell line (b,d,f) at the 12th passage in the presence of AZT (a,b), ddI (c,d), AZT-TP (e,f). HEC-1 cells displayed some morphological changes consistent with cellular senescence, including cell enlargement, flattening, containing definite vacuoles (c), and multinucleated cells appeared (e). In MCAS cells, the cytoplasm was irregular (b,d,f) and cytoplastic vacuoles were shown (d,f). Enlarged cells were not observed. a,c,e: × 400 magnifications. b,d,f: ×200 magnifications.

nylon membranes (Hybond N: Amersham, Little Chalfont, Buckinghamshire, U.K.). The membranes were incubated overnight at 37°C with α-^{32}p end labelled $(CCCTAA)_3$ telomeric probe [15], were washed twice at 37°C with 2× standard saline citrate (0.1% SDS), and then subjected to autoradiography at −80°C for 12 h. The mean length of the terminal restriction fragments (TRFs) was estimated from the position of the maximal signal [16].

RNA analysis by RT-PCR

mRNA was prepared with a Quick Prep micro mRNA purification kit (Phalmacia Biotech, Uppsala, Sweden), and the mRNA was quantified by UV spectrophotometry. cDNA was synthesised from 0.5 μg of mRNA in a 10 μL reaction mixture containing MMLV reverse transcriptase buffer, 0.2 mM dNTPs, 20 pmol random hexamer primers, 10 U RNase inhibitor and 200 U MMLV reverse transcriptase (Toyobo, Osaka, Japan). After incubation at 37°C for 60 min, the reaction was heated to 94°C for 2 min, and then reaction volume was brought to 50 μL. A cDNA amount representing 50 ng of mRNA was subjected to PCR in a final volume of 25 μL that included 1 U of Taq polymerase (Toyobo) and 10 pmol oligonucleotide primers for target and control genes. The following oligonucleotide primers were used [17].

Target:
TP53
sense 5-AGGCGCTGCCCCACCA-3
antisense 5-TTCCGTCCCAGTAGATT-3
p21
sense 5-GCCGAAGTCAGTTCCTT-3
antisense 5-TCATGCTGGTCTGCCGC-3
control:
β-tubulin
sense 5-TGCATTGACAACGAGGC-3
antisense 5-CTGTCTTGACATTGTTG-3

PCR conditions were denaturation at 95°C for 30 sec, annealing at 62°C for 1 min and extension at 72°C for 1 min. PCR products were separated by 12% polyacrylamide gel electrophoresis, and bands were visualised by ethidium bromide staining and UV transillumination. The target gene expression levels were expressed as a ratio of the target to control band by a phosphorimaging system. RT-PCR analysis of each sample was done three times to arrive at a mean value for the target/control ratio.

RESULTS

RTI inhibition of proliferation

RTI (AZT, ddI and AZT-TP) was added at various concentrations to MCAS and HEC-1 cells. Cell proliferation after 72 h of incubation was assessed by the MTT assay (Table 1). Both the cell lines demonstrated reduced proliferation with increasing concentrations of RTI. Inhibition of approximately 20% was observed. Concentrations of AZT (100 μM), ddI (10 μM) and AZT-TP (5.0 μM) were selected for subsequent experiments.

Inhibition of telomerase activity and morphological change

AZT and ddI did not alter telomerase activity in MCAS cells, and the activity did not decrease with increased passage number. However, AZT-TP caused a slight decrease in telomerase activity at the 12th passage (Figure 1). In HEC-1 cells, ddI and AZT-TP caused a decrease in telomerase activity in relation to passage number. The time between passages increased, so while cells were passages every 3 to 4 days initially, this was extended to every 6 to 7 days by the 10th passage. Enlarged cells and cells with definite vacuoles increased and the rate of cell proliferation decreased sharply along the repetition of passaging especially in the presence of ddI and AZT-TP (Figure 2).

Relative telomerase activity

Almost no change in activity was seen when MCAS cells were passaged in the absence of RTI. The maximum decrease in activity was 12.6% for AZT, 8.3% for ddI and 32.5% for AZT-TP (Figure 3). In HEC-1 cells the maximum decrease in activity was 32.7% for AZT, 70.3% for ddI and 91.2% for AZT-TP (Figure 3).

Change in telomere length

Changes in telomere length (TRF-terminal restriction fragments) with incubation and passage in the presence of RTI were assessed (Figure 4). In MCAS cells, TRF length showed no clear change with passage in the absence of RTI (mean TRF length: 8.3 to 6.4 kbp), and there was no major change in the presence of AZT (mean TRF length: 6.2 kbp). With ddI there was a slight shortening with cell passage, and the mean TRF length decreased by 27.3% (6.6 kbp before passage to 4.8 kbp after 12 passages). The mean TRF length in the presence of AZT-TP decreased by 34.9% (6.3 kbp before passage to 4.1 kbp after 12 passages).

In HEC-1 cells, TRF length showed no clear change with passage in the absence of RTI (mean TRF length: 5.8 to 4.3 kbp). TRF length was shortened with passage in the presence of each of the RTIs. The mean TRF length in the presence of AZT decreased by 46.6% (5.8 kbp before passage to 3.1 kbp after 12 passages). The mean TRF length in the presence of ddI decreased by 57.9% (5.7 kbp before passage to 2.4 kbp after 12 passages). In the presence of AZT-TP it decreased by 33.3% (5.7 kbp before passage to 3.8 kbp after 12 passages).

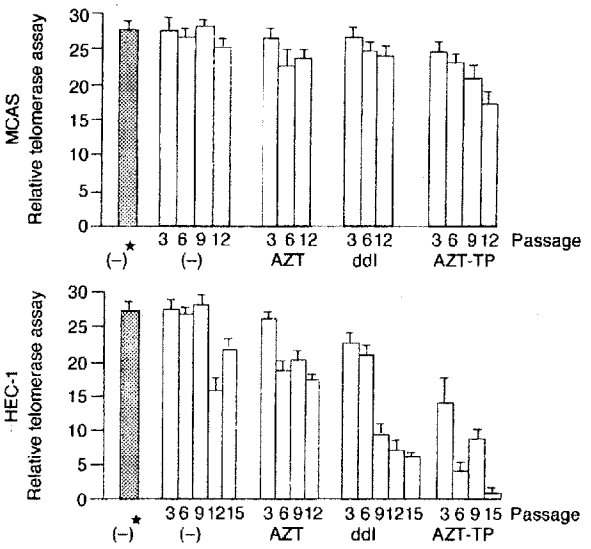

Figure 3. Effect of reverse transcriptase inhibitors on relative telomerase activity. Relative telomerase activity was calculated as the ratio between the sum total of pixel intensity of every 6 bp band and the pixel intensity of internal control band. (−) medium without RTI. *A sample of the cells before passage.

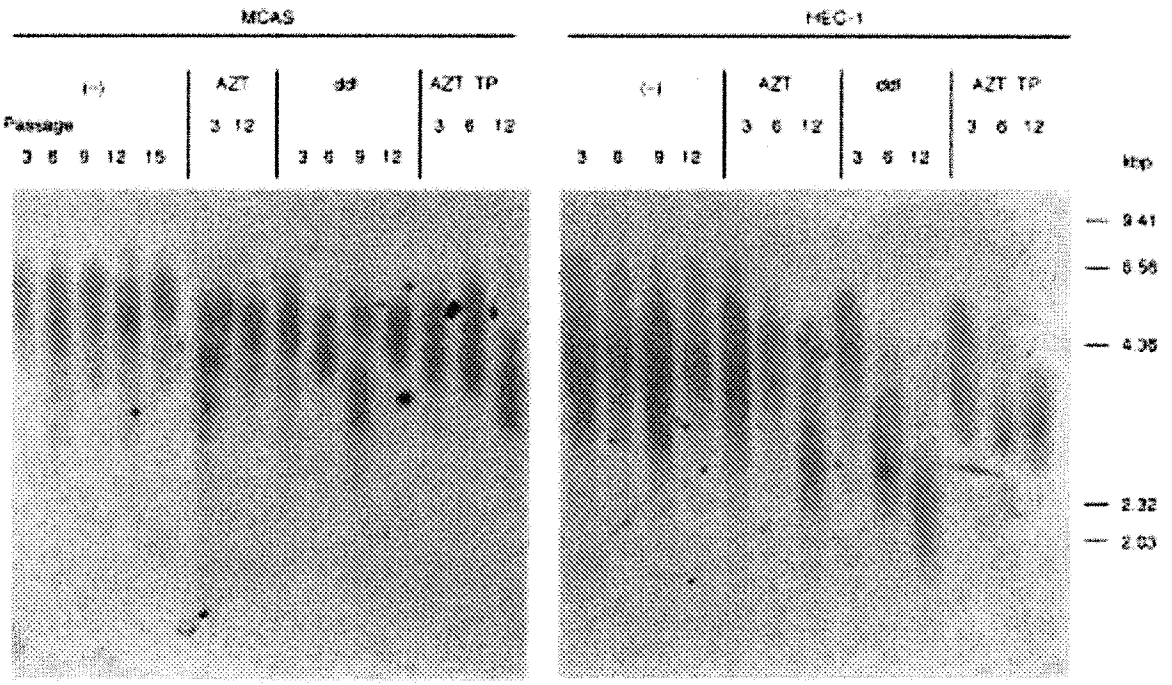

Figure 4. Effect of reverse transcriptase inhibitors on telomere length. The size of terminal restriction fragments was determined by Southern blot hybridisation. Molecular weight standards are shown on the right. (–), medium without RTI.

Effects of RTIs on the action of cisplatin

Cell proliferation was assessed 24 h after the addition of serially diluted cisplatin to cells (12th passage) (Figure 5). Cell proliferation was suppressed in direct relation to the concentration of cisplatin. In MCAS cells, cell proliferation was reduced by approximately 23% at a cisplatin concentration of 1.95 μg/mL in the presence of RTIs. No major differences in effect were seen between the RTIs.

In HEC-1 cells AZT and AZT-TP had similar modest effects on cell proliferation, whilst ddI had a more significant effect. At a cisplatin concentration of 1.95 μg/mL, AZT and AZT-TP caused a 27.3% decrease in proliferation and ddI a 43.8% decrease. At a cisplatin concentration of 15.6 μg/mL, AZT and AZT-TP caused a 32.1% decrease in proliferation and ddI an 81.4% decrease ($P < 0.005$).

Assessment of the TP53 *and* p21 *genes*

Expression of the *TP53* and *p21* genes before and after 12 passages was examined (Figure 6). In MCAS cells, *TP53* expression was minimally affected by AZT, but ddI and AZT-TP caused an increase in expression ($P < 0.005$); the expression of *p21* was essentially unaffected by the RTIs. In HEC-1 cells, the expression of *TP53* increased with ddI ($P < 0.001$) but was unaffected by AZT or AZT-TP. The expression of *p21* increased with ddI ($P < 0.001$) but was not affected by the other two drugs.

DISCUSSION

Several studies have already reported on the effects of inhibitors of telomerase activity. Norton and colleagues [18] reported the specific inhibition of template portions of the human telomerase RNA component (hTR) [19] by various peptide nucleic acids (PNAs) or phosphorothioate (PS) oligomers. PNA, in particular, demonstrated excellent inhibition of telomerase activity [18, 20]. Sun and colleagues [21] reported that telomerase activity could be inhibited by the G-quadruplex-interactive compound as a target of the nucleic acid structure. There have also been studies on the template

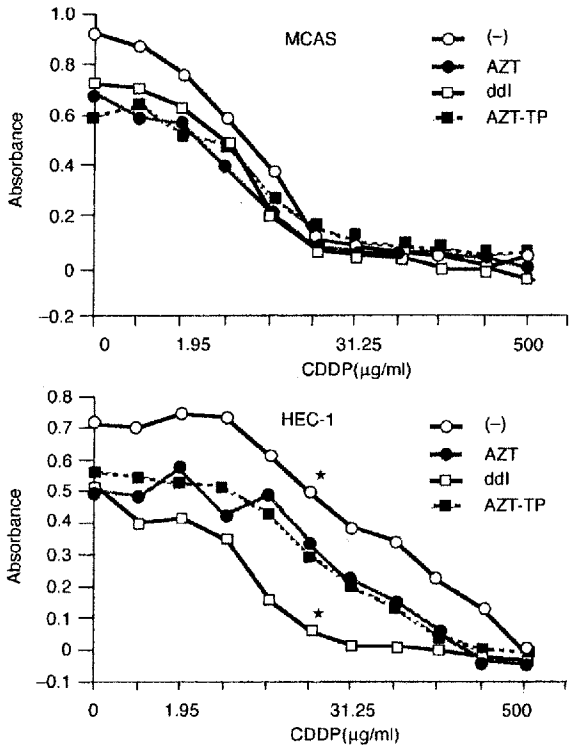

Figure 5. Inhibition of cell proliferation of cisplatin in the presence of RTI. Stepwise dilutions of cisplatin were added to cells at their 12th passage. Cell growth over 24 h was measured by MTT assay. (–), medium without RTI. *$P < 0.005$.

portion using protein phosphate 2A [22] and the hammerhead ribozyme [23]. Strahl and colleagues demonstrated inhibition of telomerase activity in tetrahymena [8] and human T-cell and B-cell lines [10] using a nucleotide analogue which inhibits retroviral reverse transcriptase. They reported good inhibition of telomerase activity with Ara-GTP and ddGTP. Also, AZT significantly reduced telomere length and generated telomere instability. Although AZT-TP has not been shown to inhibit telomerase activity, it is thought to prevent correct binding of the enzyme which forms the telomeric sequence.

In the present study, we examined the effect on telomerase activity of long-term culture with RTI analogues. We also examined the effect of RTI analogues on the susceptibility of cancer cells to cisplatin, a widely used anticancer agent. Strahl and colleagues [8, 10] performed a telomerase activity assay using cells exposed to analogues for the short time required for primer extension and reported that inhibition of telomerase activity by ddI or AZT-TP was slight. It has also been suggested that telomerase is inhibited by AZT, because AZT is converted into AZT-TP and competes with TTP in binding to telomeres, and that ddI is also converted into ddATP intracellularly to inhibit telomerase [24]. In the present study ddI and AZT-TP significantly inhibited telomerase activity in HEC-1 cells, though they had little effect in MCAS cells. Cell proliferation decreased markedly and flatting and enlarged cells increased every time the medium containing ddI was exchanged during culture of HEC-1 cells. It is thought unlikely that these effects were achieved by selective inhibition of telomerase activity and induction of senescence, and it appears more plausible that cell proliferation was decreased by the toxicity of the analogue and telomerase activity decreased as a result. Since AZT inhibited cell proliferation irrespective of the level telomerase activity and this effect became stronger with an increase in concentration [25], AZT may also have shown an effect on telomerase activity if it was used at higher concentrations.

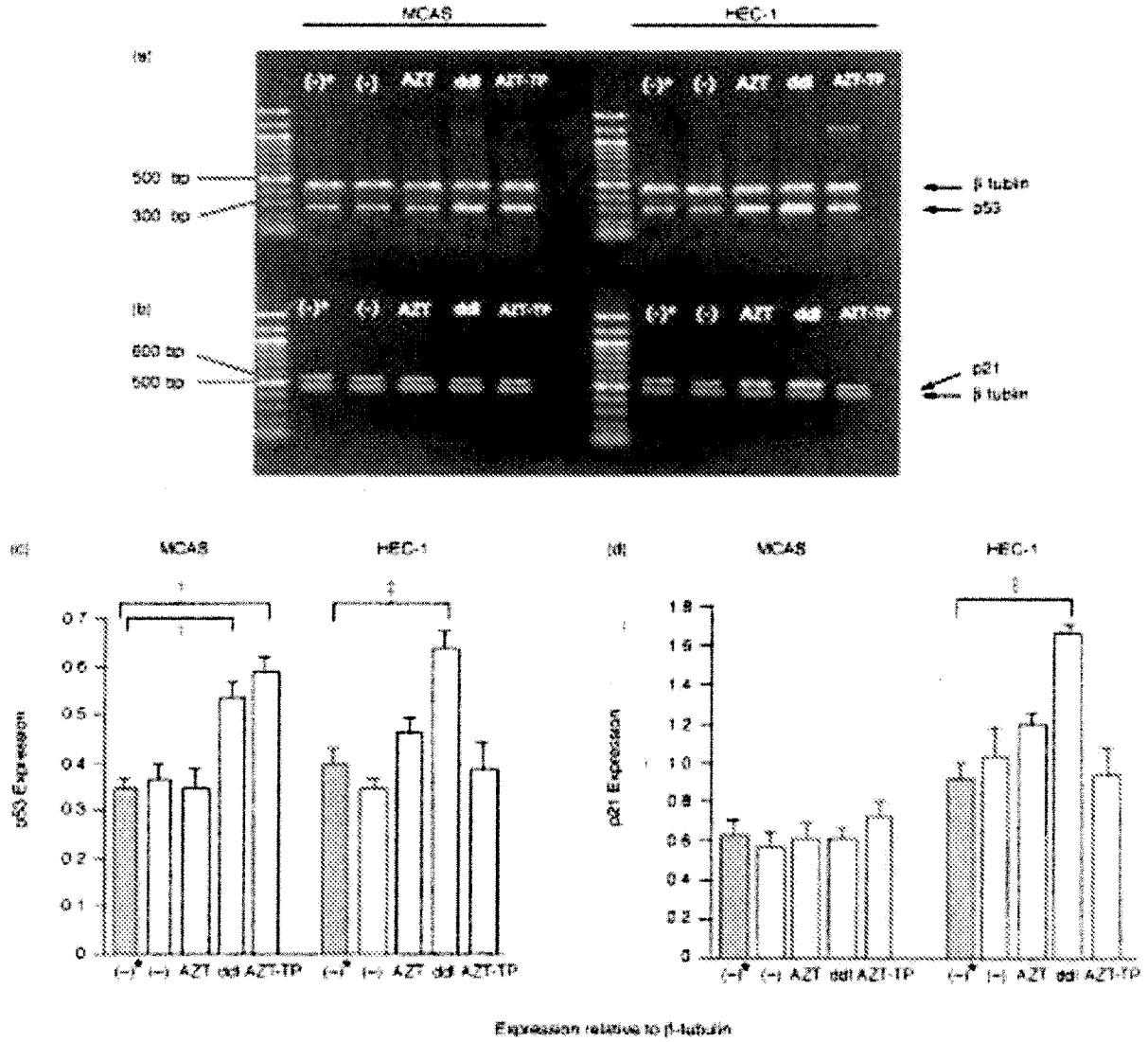

Figure 6. Expression of (a) *TP53* and (b) *p21* in MCAS of HEC1 cells. Gene expression at the 12th passage in the presence of RTI is shown. (–), medium without RTI. (c) *TP53* expression relative to β-tubulin expression. (d) *p21* expression relative to β-tubulin expression. The intensity of each band was measured densitometrically. Quantities are represented as the ratio between target and control, β-tubulin expression. *A sample of the cells before passage. †$P<0.005$, ‡ $P<0.001$.

Telomere shortening analogues such as AZT and Ara-G have caused the most rapid changes in telomere length in tetrahymena and human T and B cells, while ddI and ddG had no effects [8, 10].

AZT is thought to have an important role in the maintenance of telomeres. Many apparently senescent cells appear in long-term cultures in the presence of AZT [9], with aberrant chromosomes that may result from abnormal amplification of telomere like centrometric DNA [11]. Gomez and colleagues [26] cultured HeLa cells that were devoid of telomerase activity in the presence of AZT over a long period. According to their findings, the telomeres were shortened but there were no signs of senescence. In the present study, none of the three agents shortened telomeres in MCAS cells, but ddI and AZT-TP did markedly shorten telomeres in HEC-1 cells. This was thought to be ascribable to the decrease in telomerase activity. It is possible that telomere shortening occurred early as a result of senescent-like phenotype induction by the analogue. Further study is required to characterise the differences seen between the two cell lines.

Cisplatin is widely used in the treatment of gynaecological cancer, particularly ovarian cancer [27, 28]. However, cisplatin resistance is a problem [29, 30]. Burger and colleagues [31] targeted the telometric tandem repeat sequence, a G-rich sequence, by utilising the fact that cisplatin is associated with the G-Pt-G adduct in the formation of intrastrand lesions [32]. These investigators reported that telomerase activity was specifically reduced by inhibition of transcription of the hTR component. Therefore, we examined the effect of cisplatin administration in the presence of an RTI. We found that the antitumour effects of cisplatin were greater in both cell lines in the presence of RTIs. In MCAS cells, the antitumour effects of cisplatin did not differ between the RTIs, but in HEC-1 cells, proliferation was strongly inhibited by ddI. It is interesting that the telomerase activity of AZT-TP exposed cells were different from that of AZT in HEC-1 cells, but the antitumour effect of cisplatin was almost similar. Telomerase activity has been shown to be higher in actively dividing cells [6]. However, AZT-TP lowers telomerase activity and reduces HEC-1 cell proliferation more significantly than AZT. Therefore, the incorporation of cisplatin is reduced, and it is possible that after 24 h of exposure to cisplatin the rate of cell proliferation would be similar to that seen with AZT. The next question is why the antitumour effect of cisplatin in HEC-1 cells increases in the presence of ddI, a drug which reduces both telomerase activity and cell proliferation. Kondo and colleagues [33] transduced an antisense telomerase expression vector and not only found that telomerase activity was inhibited but also that the occurrence of apoptosis induced by cisplatin was enhanced. Since the appearance of morphological change and expression of *p21* was enhanced in HEC-1 cells exposed to ddI, it is suggested that senescene was induced. Although AZT-TP decreased telomerase activity and induced morphological changes to the same extent as ddI, an increase in *p21* expression was not observed in the AZT-TP-exposed cells. ddI may cause different changes to cells, mediated by a different mechanism to that of AZT-TP. Further study is required to understand the mechanism by which RTIs enhance the effect of cisplatin.

To intensify the effect of chemotherapy, dose is increased or multiple drugs are used. However, because of toxicities or other restrictions, it is often difficult to increase the dose. If it was possible to augment the effect of anticancer drugs by auxiliary means, chemotherapy could be more effective even at a low-dose. Since RTI reduces cell proliferation through inhibition of telomerase, it has little effect on normal somatic cells, which have no telomerase activity. Therefore, it may be that RTI could be effectively combined with anticancer drugs. Thus, the effect of ddI on HEC-1 cells observed in this study is notable. It is also necessary to investigate the effects of RTI on stem cells and germ cells, which have telomerase activity. It seems warranted to study RTI further with the intention of achieving its clinical application.

1. Hiyama E, Gollahon L, Kataoka T, Kuroi K, Yokoyama T, Gazdar AF. Telomerase activity in human breast tumours. *J Natl Cancer* 1996, **88**, 116–122.
2. Baccetti S, Counter CM. Telomeres and telomerase in human cancer (review). *Int Natl J Oncol* 1995, 7, 423–432.
3. Breslow RA, Shay JW, Gazdar AF, Srivastava S. Telomerase and early detection of cancer: a National Cancer Institute Workshop. *J Natl Cancer Inst* 1997, **89**, 618–623.
4. Shay JW, Gazdar AF. Telomerase in the early detection of cancer. *J Clin Pathol* 1997, **50**, 106–109.
5. Murakami J, Nagai N, Ohama K. Diagnostic significance of the telomerase activity in ovarian tumours. *Cytometry Res* 1997, **7**, 39–44.
6. Holt SE, Aisner DL, Shay JW, Wright WE. Lack of cell cycle regulation of activity in human cells. *Proc Natl Acad Sci USA* 1997, **94**, 10687–10692.
7. Belair CD, Yeager TR, Lopez PM, Reznikof CA. Telomerase activity: A biomarker of cell proliferation, not malignant transformation. *Proc Nad Acad Sci USA* 1997, **94**, 13677–13682.
8. Strahl C, Blackburn EH. The effects of nucleoside analogues on telomerase and telomeres in Tetrahymena. *Nucleic Acids Research* 1994, **22**, 893–900.
9. Yegorov YE, Chernov DN, Akimov SS, Bolsheva NL, Krayevsky AA, Zelenin AV. Reverse transcriptase inhibitors suppress telomerase function and induce senescence-like processes in cultured mouse fibroblasts. *FEBS Letters* 1996, **389**, 115–118.
10. Strahl C, Blackburn EH. Effect of reverse transcriptase inhibitor on telomere length and telomerase activity in two immortalized human cell line. *Mol and Cell Biol* 1996, **16**, 53–65.
11. Parra I, Flores C, Adrian D, Windle B. AZT induces high frequency, rapid amplification of entrometric DNA. *Cytogenet Cell Genet* 1997, **76**, 128–133.
12. Kim NW, Piatyszek MA, Prowse KR, Harley CB, West MD, Ho PLC. Specific association of human telomerase activity with immortal cells and cancer. *Science* 1994, **266**, 2011–2015.
13. Kim NW, Wu F. Advances in quantification and characterisation of telomerase activity by the telomeric repeat amplification protocol(TRAP). *Nucleic Acids Res* 1997, **25**, 2595–2597.
14. Mosmann T. Rapid calorimetric assay for cellular growth and survival: application to proliferation and cytotoxicity assays. *J Immunol Methods* 1983, **65**, 55–63.
15. Moyzis RX, Buckingham JM, Cram LS, *et al.* A highly conserved repetitive DNA sequence, (TTAGGG)n, present at the telomeres of human chromosomes. *Proc Natl Acad Sci USA* 1988, **85**, 6622–6626.
16. Hiyama K, Ishioka S, Shirotoni Y, *et al.* Alterations in telomeric repeat length in lung cancer are associated with loss of heterozygosity in p53 and Rb. *Oncogene* 1995, **10**, 937–944.
17. Shigemasa K, Hu C, West CM, *et al.* p21: a monitor of p53 dysfunction in ovarian neoplasia. *Int J Gynecol Cancer* 1997, **7**, 296–303.
18. Norton JM, Piatyszek AP, Wright WE, Shay JW, Corey DR. Inhibition of human telomerase activity by peptide nucleic acids. *Nature Biotechnology* 1996, **14**, 615–618.
19. Feng J, Funk WD, Wang SS, *et al.* The RNA component of human telomerase. *Science* 1995, **269**, 1236–1241.
20. Hamilton SE, Pitts AE, Katipally RR, *et al.* Identification of determinants for inhibition binding within the RNA active site of human telomerase using RNA scanning. *Biochemistry* 1997, **36**, 11873–11880.

21. Sun D, Thompson B, Cathers BE, *et al.* Inhibition of human telomerase by a G-quadruplex-interactive compound. *J Med Chem* 1997, **40**, 2113–2116.
22. Li H, Zhao L-L, Funder JW, Liu J-P. Protein phosphatase 2A inhibits nuclear telomerase activity in human breast cancer cells. *J Biol Chem* 1997, **272**, 16729–16732.
23. Kanazawa Y, Ohkawa K, Ueda K, *et al.* Hammer head ribozyme-mediated inhibition of telomerase activity in extracts of human hepatocellular carcinoma cells. *Biochem Biophy Res Comm* 1996, **225**, 570–576.
24. Pai RB, Pai B, Kukhanova M, Dutschman GE, Guo X, Cheng YC. Telomerase from human leukemia cells: properties and its interaction with deoxynucleoside analogues. *Cancer Res* 1998, **58**, 1909–1913.
25. Melana SM, Holland JF, Pogo BG. Inhibition of cell growth and telomerases activity of breast cancer cells *in vitro* by 3′-azido-3′-deoxythymidine. *Clin Cancer Res* 1998, **4**, 693–696.
26. Gomez DE, Tejera AM, Olivero OA. Irreversible telomere shortening by 3′-azido-2′,3′-dideoxythymidine (AZT) treatment. *Biochem Biophys Res Commun* 1998, **246**, 107–110.
27. Bottalico C, Lorusso V, Brandi M, *et al.* Correlation between HPLC-determined lonidamine serum levels and clinical response in patients with advanced ovarian cancer. *Anticancer Res* 1996, **16**, 3865–3869.
28. Soulie R, Bensmaine A, Garrino C, *et al.* Oxaliplatin/cisplatin (L-OHP/CDDP) combination in heavily pretreated ovarian cancer. *Eur J Cancer* 1997, **33**, 1400–1406.
29. Chollet P, Bensmaine MA, Brienza S, *et al.* Single agent activity of oxaliplatin in heavily pretreated advanced epithelial ovarian cancer. *Ann Oncol* 1996, **7**, 1065–1070.
30. Saijo N. Clinical trials of irinotecan hydrochloride (CPT, campto injection, topotecin injection) in Japan. *Ann NY Acad Sci* 1996, **13**, 292–305.
31. Burger AM, Double JA, Newell DR. Inhibition of telomerase activity by cisplatin in human testicular cancer cells. *Eur J Cancer* 1997, **33**, 638–644.
32. Bedford P, Fichtinger-Schepman AMJ, Shellard SA, Walker MC, Masters JRW, Hill BT. Differential repair of platinum-DNA adducts in human bladder and testicular tumour continuous cell lines. *Cancer Res* 1988, **48**, 3019–3024.
33. Kondo Y, Kondo S, Tanaka Y, Haqqi T, Barna BP, Cowell JK. Inhibition of telomerase increases the susceptibility of human malignant glioblastoma cells to cisplatin-induced apoptosis. *Oncogene* 1998, **16**, 2243–2248.

Exhibit 6: Ren et al., "Structure of HIV-2 Reverse Transciptase at 2.35-A Resolution and the Mechanism of Resistance to Non-Nucleoside Inhibitors," *PNAS* 99(22):14410–15 (2002).

Structure of HIV-2 reverse transcriptase at 2.35-Å resolution and the mechanism of resistance to non-nucleoside inhibitors

J. Ren*†, L. E. Bird*†, P. P. Chamberlain*†‡, G. B. Stewart-Jones*, D. I. Stuart*‡, and D. K. Stammers*‡§

*Division of Structural Biology, The Wellcome Trust Centre for Human Genetics, The Henry Wellcome Building for Genomic Medicine, University of Oxford, Roosevelt Drive, Oxford OX3 7BN, United Kingdom; and †Oxford Centre for Molecular Sciences, New Chemistry Building, South Parks Road, Oxford OX1 3QT, United Kingdom

Edited by Stephen C. Harrison, Children's Hospital, Boston, MA, and approved September 4, 2002 (received for review June 19, 2002)

The HIV-2 serotype of HIV is a cause of disease in parts of the West African population, and there is evidence for its spread to Europe and Asia. HIV-2 reverse transcriptase (RT) demonstrates an intrinsic resistance to non-nucleoside RT inhibitors (NNRTIs), one of two classes of anti-AIDS drugs that target the viral RT. We report the crystal structure of HIV-2 RT to 2.35 Å resolution, which reveals molecular details of the resistance to NNRTIs. HIV-2 RT has a similar overall fold to HIV-1 RT but has structural differences within the "NNRTI pocket" at both conserved and nonconserved residues. The structure points to the role of sequence differences that can give rise to unfavorable inhibitor contacts or destabilization of part of the binding pocket at positions 101, 106, 138, 181, 188, and 190. We also present evidence that the conformation of Ile-181 compared with the HIV-1 Tyr-181 could be a significant contributory factor to this inherent drug resistance of HIV-2 to NNRTIs. The availability of a refined structure of HIV-2 RT will provide a stimulus for the structure-based design of novel non-nucleoside inhibitors that could be used against HIV-2 infection.

AIDS | drug resistance | crystallography | polymerase

The reverse transcriptase (RT) of HIV-1 has been one of the main targets for the development of anti-AIDS drugs. Combination therapy involving use of anti-RT drugs together with protease inhibitors has led to diminished mortality rates from AIDS in Western countries. HIV-2 is a distinctive HIV serotype that is less widely disseminated than HIV-1. Individuals infected with HIV-2 can go on to develop AIDS but generally do so after a longer clinical latency period than that for HIV-1 (1). HIV-2 infection is thought to have an overall lower morbidity rate than HIV-1, although certain individuals can be more susceptible (2). HIV-2 is most commonly found in certain areas of West Africa, but there is some evidence of a spread of the virus into other geographical regions such as Western Europe (3) and Asia (4). Although HIV-2 RT shows significant amino acid sequence homology to HIV-1 RT, it has marked differences in inhibition by non-nucleoside reverse transcriptase inhibitors (NNRTIs). Additionally, there are differences in kinetic parameters for both the polymerase and RNaseH activities (5), and HIV-2 RT forms a more stable p68/p55 heterodimer compared with the p66/p51 HIV-1 RT heterodimer (6, 7). NNRTIs are structurally diverse hydrophobic molecules that are largely specific for HIV-1 RT, most compounds being completely inactive against HIV-2 RT (8). NNRTIs inhibit HIV-1 RT by binding to an allosteric site ≈10 Å from the polymerase active site, which results in the distortion of the key catalytic aspartic acid residues (9, 10). Nucleoside analogue inhibitors of RT (NRTIs) such as zidovudine and lamivudine in their 5′-triphosphate forms act as DNA chain terminators and generally have a broad spectrum of antiviral activity that includes HIV-2 as well as HIV-1 (11). Studies of chimeric HIV-1/HIV-2 RTs have indicated some general regions that contribute to the lack of binding of the "first generation" NNRTI nevirapine to HIV-2 RT (12). Some current combination therapies for HIV-1 infection include NNRTI drugs, either nevirapine, delavirdine, or efavirenz. Such regimens would be less effective for treating HIV-2 infection, and thus NNRTI drugs active against this serotype would be desirable. A few examples of inhibition of HIV-2 RT by NNRTIs are known, but such inhibition tends to be orders of magnitude weaker than for HIV-1 RT. Thus, the NNRTI phenylethylthiazolylthiourea (PETT)-2 inhibits HIV-2 RT with an IC_{50} of 2 μM, whereas the corresponding value for HIV-1 RT is 5 nM (13). Kinetic evidence indicates that PETT-2 does not compete with template-primer or dNTP, consistent with it binding to HIV-2 RT at an equivalent to the HIV-1 RT NNRTI site (13).

Although there are numerous crystal structures of HIV-1 RT published, including complexes with inhibitors (14–16), DNA (17, 18), and unliganded structures (9, 19, 20), there have been no crystal structures reported for HIV-2 RT. A number of examples of high level expression and purification of HIV-2 RT have been published (5, 6, 21), yet these preparations apparently have yielded neither crystals nor structures for this enzyme.

We report here the crystal structure of HIV-2 RT, which has been refined to a resolution of 2.35 Å. The availability of this structure will provide a rational framework for the design of non-nucleoside inhibitors active against HIV-2.

Materials and Methods

Protein Purification, Crystallization, and Data Collection. Cloning, expression, purification, and crystallization of HIV-2 RT (from the pROD isolate, but containing a mutation of Arg286Ser) were as described (22). Briefly, crystals were grown by sitting drop vapor diffusion from droplets consisting of equal volumes of 12 mg/ml HIV-2 RT and 40% ammonium sulfate, either unbuffered or with 0.1 M Tris (pH 8.5). Crystals grew in the presence or absence of 0.7 mM PETT-2, 10% glycerol, or up to 20% DMSO, and were equilibrated briefly in combined adjacent droplets not containing crystals, to which further glycerol was added, giving a final concentration of 20% (vol/vol) before being frozen directly in an Oxford Cryosystems Cryostream for data collection at 100 K at synchrotron sources. The beamlines used were as follows: station PX14.2 at SRS Daresbury (Synchrotron Radiation Source Daresbury, Warrington, Cheshire, U.K.; Dataset 1); station ID14-EH2 at ESRF (European Synchrotron Radiation Facility, Grenoble, France; Dataset 2). In the latter case, data from two separate crystals were merged. Data frames of 1° were recorded on ADSC-q4 (Area Detector Systems

This paper was submitted directly (Track II) to the PNAS office.

Abbreviations: RT, reverse transcriptase; NNRTI, non-nucleoside RT inhibitor; PETT, phenylethylthiazolylthiourea.

Data deposition: The atomic coordinates and structure factors for the 2.35-Å resolution HIV-2 RT structure have been deposited in the Protein Data Bank, www.rcsb.org (PDB ID code 1MU2).

†J.R., L.E.B., and P.P.C. contributed equally to this work.

§To whom correspondence should be addressed. E-mail: daves@strubi.ox.ac.uk.

www.pnas.org/cgi/doi/10.1073/pnas.222366699

Table 1. Statistics for crystallographic structure determinations

Data set	1	2
Data collection site	SRS PX14.2	ESRF ID14-EH2
Wavelength, Å	0.979	0.933
Unit cell (*a*, *b*, *c* in Å)	151.9, 111.9, 82.5	149.8, 107.8, 82.2
Resolution range, Å	25.0–3.30	30.0–2.35
Observations	112,302	631,721
Unique reflections	21,667	56,142
Completeness, %	99.5	100
$I/\sigma I$	5.2	16.0
R_{merge}*	0.239	0.128
Outer resolution shell		
Resolution range, Å	3.42–3.30	2.43–2.35
Unique reflections	2,072	5,520
Completeness, %	97.9	100
$I/\sigma I$	1.3	1.1
Refinement statistics:		
Resolution range, Å		30.0–2.35
No. of reflections (working/test)		53236/2838
R factor† ($R_{working}/R_{free}$)		0.189 (0.194/0.241)
No. of atoms (protein/water/others)		7,744/284/160
rms bond length deviation, Å		0.0081
rms bond angle deviation, °		1.39
Mean *B* factor, Å²‡		50/58/48/107
rms backbone *B*-factor deviation§		4.5

*$R_{merge} = \Sigma|I - \langle I\rangle|/\Sigma\langle I\rangle$.
†*R* factor $= \Sigma||F_o| - |F_c||/\Sigma|F_o|$.
‡Mean *B* factor for main-chain, side-chain, water, and other molecules (sulfate and glycerol), respectively.
§rms deviation between *B*-factors for bonded main-chain atoms.

Corporation, San Diego) charge-coupled device (CCD) detectors. HIV-2 RT crystals belong to the orthorhombic space group $P2_12_12_1$, with a single heterodimer in the asymmetric unit, and showed variations in unit cell dimensions (Table 1). Data were processed with DENZO and SCALEPACK (23).

Structure Solution and Refinement. The HIV-2 RT structure was solved by molecular replacement with the program CNS (24) using coordinates for the unliganded HIV-1 RT heterodimer 1hmv (19). The structure was refined by using CNS, with positional, simulated annealing and individual *B*-factor refinement with bulk solvent correction and anisotropic *B*-factor scaling. Model building was carried out by using O. Coordinates for HIV-1 and HIV-2 RT were overlapped using SHP (25). Statistics for the refined structures are shown in Table 1.

Results and Discussion

Structure Determination of HIV-2 RT. Of a range of HIV-1 RT coordinate sets tested as search molecules for the molecular replacement, the unliganded structure (19) was successful in producing a solution using HIV-2 RT data to 3.3-Å resolution (Dataset 1, see Table 1). The limited resolution of these data allowed partial refinement of the structure (R_{work} of 0.36). Subsequent growth of better quality crystals of HIV-2 RT led to a higher resolution dataset to 2.7 Å, against which the HIV-2 RT coordinates from Dataset 1 were refined (R_{work} of 0.187, data not shown). Finally, larger crystals were obtained, which allowed the collection of high-resolution data (2.35 Å, Dataset 2), and the model was refined to an *R* factor of 0.189 (R_{work}/R_{free} of 0.194/0.241) with the retention of good stereochemistry (Table 1). Electron density was of excellent quality (Fig. 1*A*) and clear for the majority of the polypeptide chain except for breaks at residues 1–2, 68–71, 357–358, and 556–559 in the p68 subunit and 1–5, 92–94, 212–228, and 432 onwards in p55. Dataset 1 gave no convincing electron density for PETT-2 despite the inclusion of this inhibitor in the cocrystallization, and thus HIV-2 RT preferentially crystallizes as the unliganded form under the conditions used. Although the HIV-2 RT crystals have the same space group and similar unit cell dimensions to our HIV-1 RT crystals (26, 27), the molecular packing in the crystals is different, resulting in the central RNA/DNA binding cavity being open to solvent for HIV-2 RT while it is blocked in the HIV-1 RT crystals by the p51 thumb domain from a symmetry-related molecule. Neither the presence of the Arg286Ser mutation (in either p68 or p55) nor the truncated C-terminal region of p55 appear to be near crystal contacts and thus do not apparently directly contribute to the formation of these high-resolution crystals of HIV-2 RT.

Overall Fold of HIV-2 RT and Comparison with HIV-1 RT. The subunit and domain organization of the HIV-2 RT p68/p55 heterodimer is shown in Fig. 1 *B* and *C*. The domain structure of HIV-2 RT p68/p55 corresponds to that of the p66/p51 HIV-1 RT heterodimer (14, 15, 18, 19). There are five domains in the larger subunit, the first three (termed fingers, palm, and thumb) are arranged as in a right hand and are followed by the connection and C-terminal RNaseH domains (14). The smaller subunit lacks the RNaseH domain, and the four remaining domains are disposed differently and more tightly packed than for the p68 subunit. In our model, the p55 subunit ends at residue 431, which agrees with mass spectrometry, suggesting that, as well as truncation of the C-terminal region, there are five residues absent from the N terminus (22). The thumb domain of the p68 subunit adopts a folded down conformation (Fig. 1 *B* and *C*) similar to that seen in crystals grown of the unliganded HIV-1 RT (19, 20), resulting in a partial occlusion of the cleft, which explains why the initial molecular replacement models of HIV-1 RT containing a more extended thumb domain conformation did not give the correct solution. The thumb domain of the p68 of HIV-2 RT is rotated by 8°, 37°, and 48° relative to unliganded (19), DNA/dNTP-bound (17) and nevirapine-bound (15) HIV-1 RTs, respectively, after the overlap of the whole molecules. Detailed comparison confirms that the greatest similarity of HIV-2 RT to an HIV-1 RT is indeed with the unliganded structure (19) where 720 residues can be superimposed with an rms deviation in Cα positions of 1.6 Å.

Comparison of the NNRTI Site in HIV-1 RT with the Equivalent Region of HIV-2 RT. The NNRTI site in HIV-1 RT is positioned within the palm domain of the p66 subunit, and a comparison of this with the structurally equivalent region of HIV-2 RT (both as unliganded states) is shown in Fig. 2*A*. For HIV-1 RT, the presence of a bound NNRTI leads to some conformational rearrangements; for example, the side chains of two residues of the pocket, Tyr-181 and Tyr-188, rotate upwards through ≈120°. For HIV-2 RT, it can be seen that, despite amino acid sequence differences, the overall structure of this region is maintained, and the rms deviations for α-carbons for the overlap of 110 HIV-1 and HIV-2 residues surrounding the NNRTI site is 1.1 Å. Residues that are involved in NNRTI contacts in HIV-1 RT include 95, 100–103, 106, 138 (P51), 179, 181, 188, 190, 224–225, 227, 229, 234–236, and 318. There are numerous changes in the nature of the side chains of these regions: Lys101Ala, Val106Ile, Val179Ile, Tyr181Ile, Tyr188Leu, Gly190Ala, Glu224Asp, His235Trp, and Glu138Ala (p55) (HIV-1 relative to HIV-2). These amino acid substitutions not only lead to significant changes in side-chain bulk but also in electrostatic properties; thus, in two cases there is a change of a positive to neutral charge and in one a change from negative to neutral charge (28). The sequence differences at the two key tyrosine residues 181 and 188 of HIV-1 RT do not

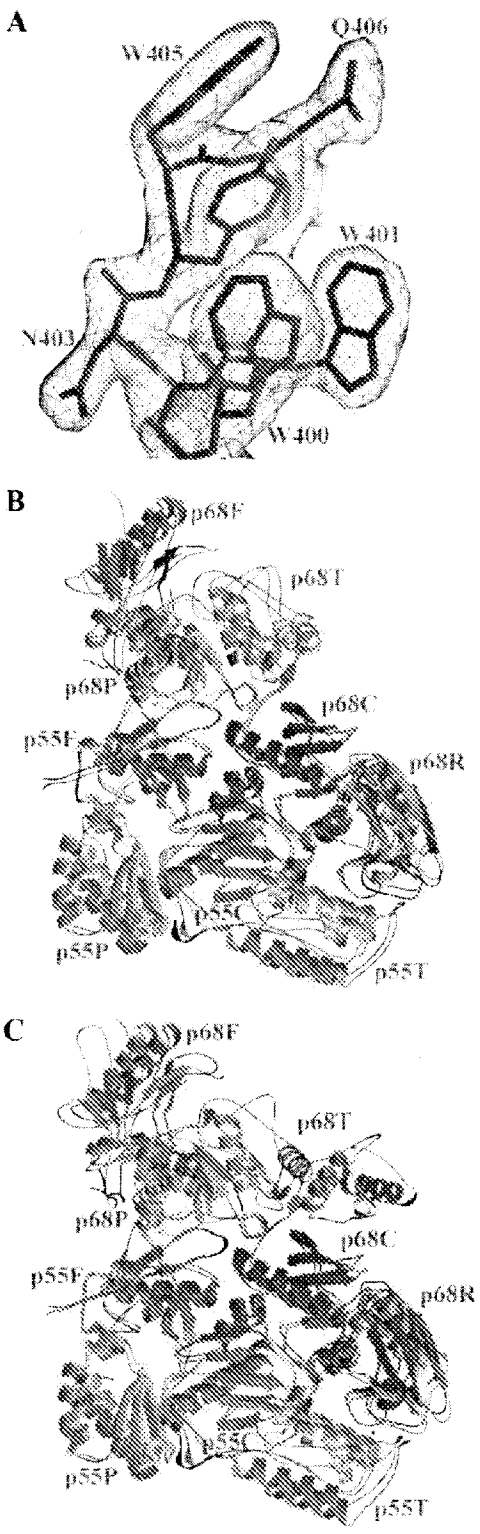

Fig. 1. (*A*) $2|F_o| - |F_c|$ electron density map contoured at 1 σ showing residues from 400 to 406 in p68 of HIV-2 RT. (*B*) Ribbon diagram showing the overall fold of HIV-2 RT overlapped with unliganded HIV-1 RT (1hmv); the HIV-1 RT is shown in gray, and the domains of HIV-2 RT are colored as follows: fingers, blue; palm, green; thumb, orange; connection, red; and RNase H, purple. (*C*) Ribbon diagram showing the overall fold of HIV-2 RT overlapped with the HIV-1 RT/nevirapine complex (1rtv); the color scheme is as in *B*.

lead to large shifts in main-chain positions (deviation in α-carbon positions of 0.5 and 0.4 Å, respectively). Indeed, some conserved residues show larger differences; for example, the Cα of Leu-100 moves by 1.0 Å, with side-chain CG atoms displaced by 2.5 Å (Fig. 2*A*). For the conserved Trp-229 residue, the Cα is displaced by 1.3 Å from its position in HIV-1 RT. The structural differences in this region appear somewhat larger than earlier suggestions and include main-chain movements (28).

At residue 235, the main chain forms part of the NNRTI site, and there is a change from His (HIV-1 RT) to Trp (HIV-2 RT), resulting in a widening of this region of the pocket in HIV-2 RT, which is in contrast to an earlier suggestion that the marked difference in the binding potency for PETT-1 and PETT-2 compounds (which differ only by a chlorine or nitrile substituent on a pyridine ring) to HIV-2 RT could partly be explained by a narrowing of the NNRTI pocket at this point (13). It is thus possible that PETT-2 binds to HIV-2 RT in a somewhat different mode to that observed for HIV-1 RT.

Structural Basis for Resistance of HIV-2 RT to NNRTIs: Evidence from the p68 Subunit. The determination of the structure of HIV-2 RT allows us to attempt to rationalize its inherent drug resistance to the NNRTIs. First, it should be noted that, although the structure of the binding site is not grossly dissimilar between HIV-1 and HIV-2 RTs, there are alterations in the positions of some conserved residues (e.g., Leu-100) that could in turn perturb potential NNRTI binding. There are also significant side-chain differences between HIV-2 and HIV-1 RT. Although Tyr181Ile and Tyr188Leu retain similar locations in the two structures, the loss of both aromatic side chains results in the abolition of ring stacking interactions with many inhibitors. Such interactions are a major contribution to the binding energy of first generation NNRTIs such as nevirapine to HIV-1 RT (12, 29–31). Inhibition data for chimeric HIV-1/HIV-2 RTs (12) indicate that additional amino acids in the region of 179–189 also contribute to NNRTI binding. However, even these residues do not fully account for all of the difference in affinity for nevirapine. In particular, we have to consider those residues in the 100–106 region, which also interact with NNRTIs. The change of Val106Ile mimics a mutation observed in HIV-1 RT where it confers drug resistance to UC-781 (32). The result of this change in HIV-2 RT is that the isoleucine side chain extends a further 2.8 Å into the pocket, potentially blocking some NNRTIs. The Lys101Glu mutation in HIV-1 RT gives resistance to NNRTIs such as GW420867X (33). In HIV-2 RT, this residue is an alanine, which shows the same trend in size and electrostatic properties as seen for the drug resistance mutation in HIV-1. Residue 101 is positioned at the edge of the NNRTI pocket in HIV-1 RT and can hydrogen bond to Glu-138 in the adjacent p51 subunit, effectively sealing off one side of the pocket from solvent. Mutation of Glu138Arg or Glu138Lys (in p51 of HIV-1 RT) gives resistance to certain NNRTIs, including PETT compounds (34). Residue 138 in HIV-2 RT is alanine, a change to a less bulky uncharged side chain compared with HIV-1 RT. The changes to alanine residues at both positions 101 and 138 would result in greater access for solvent, presumably destabilizing the pocket and weakening inhibitor binding. A further consequence of these changes is the creation of a cavity that in our HIV-2 RT structure is occupied by a glycerol molecule and a sulfate ion (Fig. 2*C*). A further change in a residue flanking the NNRTI pocket occurs at position 108, which is changed from valine to isoleucine in HIV-2 RT, a known drug resistance mutation in HIV-1 RT (35). Although not in direct contact with NNRTIs, this 108 mutation is thought to exert an effect indirectly via residue 188 which is itself different in HIV-2 RT. Finally, Gly-190 can form a close contact with some NNRTIs such as nevirapine (14, 15), and, although the Gly190Ala change is not

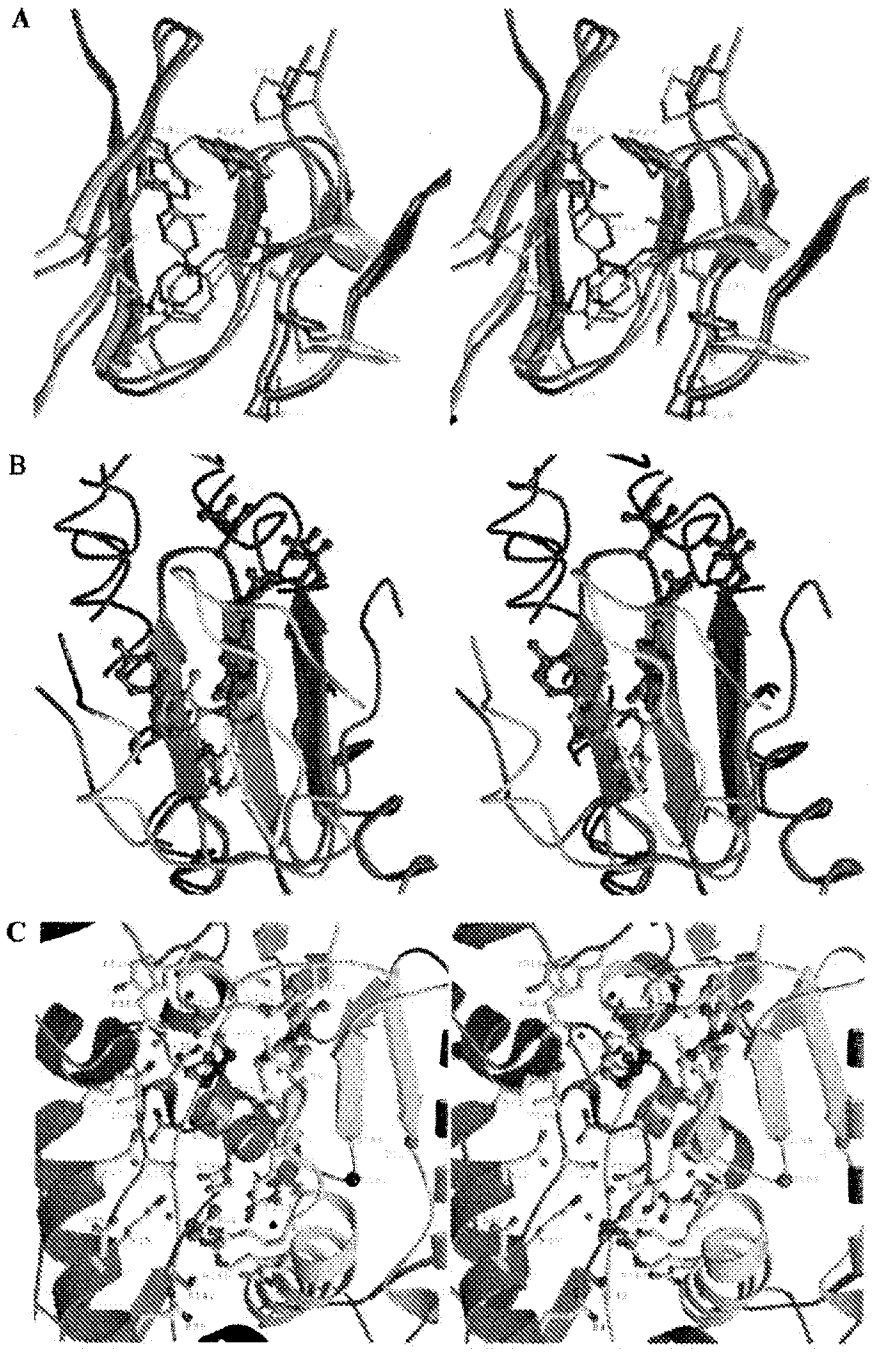

Fig. 2. (*A*) Stereo diagram comparing the NNRTI site of an unliganded HIV-1 RT and the corresponding region of HIV-2 RT. The HIV-1 RT is colored in gray, and the main chain and side chains of HIV-2 RT are shown in green and orange, respectively. (*B*) Stereo diagram showing part of the HIV-2 RT p55 subunit containing the Ile-181 and Leu-188 side chains (blue and green) overlapped with the corresponding region of the p66 subunit in the nevirapine-bound HIV-1 RT (orange and red). Nevirapine is drawn as ball-and-sticks and colored by atoms. (*C*) Stereo diagram showing a cavity located at the junction of the p68 palm, p68 connection, and p55 fingers domains (ribbon and coils colored in green, red, and blue, respectively). Side chains of the residues lining the cavity, a bound glycerol and a sulfate are shown in ball-and-stick representation, and are colored by atoms, with carbon atoms in cyan for the side chains and black for the glycerol. Water molecules in the cavity are shown as small red spheres. Larger red spheres label the Cα position of the three catalytic Asp residues at the polymerase active site. Nevirapine colored in gray is shown to mark the NNRTI site in HIV-1 RT. The dashed yellow sticks indicate the four H-bonds from the glycerol to the carbonyl oxygen of Gly-99, the main-chain nitrogen of Ala-101, and a water molecule.

a known resistance mutation in HIV-1 RT, it would cause a steric clash with certain NNRTIs.

In addition to simply mapping the HIV-2 mutations into the NNRTI binding pocket, we must also address the question of whether conformational changes required for the formation of an NNRTI binding site would be structurally feasible in HIV-2

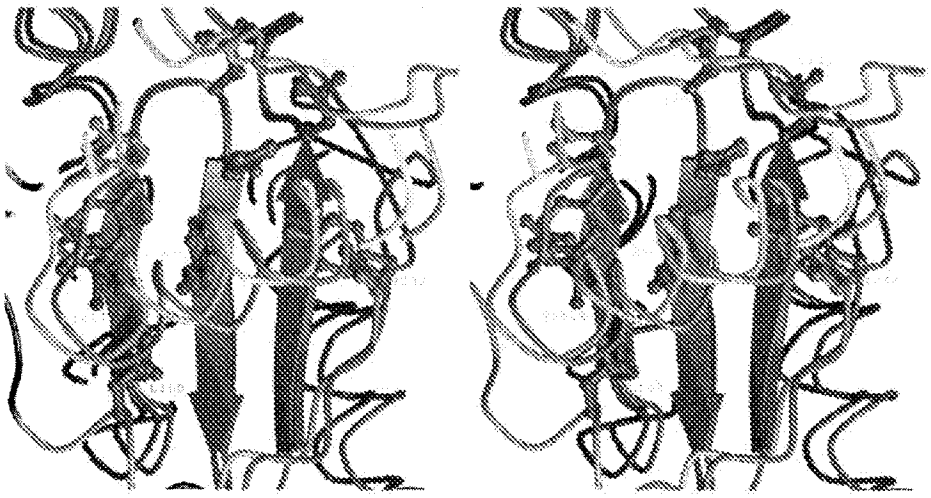

Fig. 3. Comparison of the structure around residues 181 and 188 of the p55 subunit in HIV-2 RT with that of p51 subunit in HIV-1 RT. The main chains are shown as ribbons and coils, and side chains as ball-and-stick representations, with HIV-1 RT colored orange and red, and HIV-2 RT blue and green.

RT. We have previously shown that the structural mechanism for the inhibition of HIV-1 RT by NNRTIs is via a distortion of the active site aspartates (9). This rearrangement appears directly linked to the formation of the NNRTI pocket in which Tyr-181 and Tyr-188 undergo a transition from a "down" to an "up" position. The presence of the same architecture for the polymerase active sites of HIV-1 and HIV-2 RTs means that the β-sheet (β4, β7, and β8) containing the key catalytic aspartate residues has no apparent barrier to the movement seen in HIV-1 RT resulting from the binding of an NNRTI in the adjacent pocket. We show from the results reported here that, for the unliganded state, the overall structure for the NNRTI binding region is similar but not identical between HIV-1 and HIV-2 RT.

Structural Basis for Resistance of HIV-2 RT to NNRTIs: Evidence from the Inactive p55 Subunit. We are fortunate that some features of the p66 NNRTI binding site can, for HIV-1 RT, be inferred in the absence of ligands by examining the corresponding region in the inactive p51 subunit of HIV-1 RT. Thus, we previously noted that this region adopts a very similar conformation to the pocket with an NNRTI bound in the p66 subunit, with both Tyr-181 and Tyr-188 in the up position characteristic of the NNRTI bound state (9). Because both of these residues in HIV-2 RT are much more compact, the question arises of how an energetically unfavorable void is overcome in the p55 subunits. In fact, the stabilization is achieved through some rather modest rearrangements, the two major changes being in the tyrosine residues conserved between HIV-1 and HIV-2 RTs (Tyr-183 and Tyr-232), which swing around to occupy the cavity formed in the vicinity of Ile-181 and Leu-188 (Fig. 3). Residue 183 may be in a somewhat strained conformation because there is also evidence in the electron density for a second minor conformation. The conformation of 181 and 188 themselves also differ between the p68 and p55 subunits; Leu-188 adopts an up position and has a similar χ1 value to Tyr-188 of HIV-1 RT (-33 and $-68°$, respectively). Despite this similarity in χ1 value, the leucine side chain projects into the space that would be occupied by an NNRTI due to its branched aliphatic stereochemistry. Ile-181 is not in a fully up position ($\chi1 = 100$ and 173°), and together with its branched aliphatic side chain, means it projects more into the volume of the binding site, occupied by NNRTIs in HIV-1 RT (Fig. 2*B*). It would thus seem unlikely that first generation NNRTIs could be located in the pocket in an analogous way to that in HIV-1 RT, and this appears to be a significant contributing factor to the lack of potency for this class of NNRTI binding to HIV-2 RT. The second generation NNRTI efavirenz has some interaction with Tyr-188 yet has minimal contact with Tyr-181 (36, 37), in contrast to nevirapine (14, 15), and these differences in interactions could explain in part why the mutant Leu188Tyr HIV-2 RT has significant sensitivity to efavirenz but not to nevirapine (38). By contrast, delavirdine, which is classed as a first generation NNRTI but has no contact with Tyr-181 in HIV-1 RT (39), can strongly inhibit Leu188Tyr HIV-2 RT (38). Intriguingly PETT-2, a first generation NNRTI with close ring stacking interactions with Tyr-181 in HIV-1 RT (13), retains significant inhibitory potency against wild-type HIV-2 RT, perhaps indicating a different binding mode in HIV-2 RT.

Design of Non-Nucleoside Drugs Active Against HIV-2 RT. We have seen that the structure of the NNRTI pocket in HIV-2 RT is more constricted than in HIV-1 RT. However, there is some residual volume that might accommodate potential inhibitors, which would be likely to be significantly different to those tailored for HIV-1 RT. The less bulky side chains at positions 138(p55) and 101 in HIV-2 RT create a potential binding site that is occupied in our structure by a glycerol molecule (Fig. 2*C*). We suggest that other drug-like molecules could be designed to fit this site. Although occupation of this pocket would not distort the catalytic aspartates, it might inhibit relative domain movements because it is positioned at the boundary of the p68 palm, p68 connection, and p55 fingers domains. Alternatively, an inhibitor might be designed that spans the 5 Å from this novel site to the NNRTI pocket.

The availability of a high-resolution HIV-2 RT structure determined to 2.35 Å has allowed us to dissect out factors giving rise to the inherent NNRTI resistance of this HIV serotype. Although the changes in the chemical nature and conformation at residues Ile-181 and Leu-188 probably contribute most to this resistance, differences such as at 101, 106, 108, 138, and 190 also appear significant. The challenge now will be to use structural information to allow the design of novel inhibitors that target HIV-2 RT, which might not only lead to more effective therapies against this HIV serotype but also could help in the development of non-nucleoside inhibitors active against reverse transcriptases from a broader range of human retroviral pathogens.

We thank the staff of the Daresbury Synchrotron Radiation Source (Warrington, Cheshire, U.K.) and the European Synchrotron Radiation Facility (Grenoble, France). We thank the United Kingdom Medical Research Council for long-term funding of the RT project with grants to D.K.S. and D.I.S. Support from the European Union through Grant QLKT-2000-0029 (to D.K.S.) is also acknowledged.

1. Whittle, H., Morris, J., Todd, J., Corrah, T., Sabally, S., Bangali, J., Ngom, P. T., Rolfe, M. & Wilkins, A. (1994) *AIDS* **8,** 1617–1620.
2. Lucas, S. B., Hounnou, A., Peacock, C., Beaumel, A., Djomand, G., N'Gbichi, J. M., Yeboue, K., Honde, M., Diomande, M., Giordano, C., *et al.* (1993) *AIDS* **7,** 1569–1579.
3. Cilla, G., Rodes, B., Perez-Trallero, E., Arrizabalaga, J. & Soriano, V. (2001) *AIDS Res. Hum. Retroviruses* **17,** 417–422.
4. Kim, S. S., Kim, E. Y., Park, K. Y., Suh, S. D., Park, H. K., Shin, Y. O., Bae, M. & Lee, J. S. (2000) *Acta Virol.* **44,** 15–22.
5. Hizi, A., Tal, R., Shaharabany, M. & Loya, S. (1991) *J. Biol. Chem.* **266,** 6230–6239.
6. Fan, N., Rank, K. B., Poppe, S. M., Tarpley, W. G. & Sharma, S. K. (1996) *Biochemistry* **35,** 1911–1917.
7. Divita, G., Rittinger, K., Restle, T., Immendorfer, U. & Goody, R. S. (1995) *Biochemistry* **34,** 16337–16346.
8. De Clercq, E. (1993) *Med. Res. Rev.* **13,** 229–258.
9. Esnouf, R., Ren, J., Ross, C., Jones, Y., Stammers, D. & Stuart, D. (1995) *Nat. Struct. Biol.* **2,** 303–308.
10. Spence, R. A., Kati, W. M., Anderson, K. S. & Johnson, K. A. (1995) *Science* **267,** 988–993.
11. De Clercq, E. (1994) *Biochem. Pharmacol.* **47,** 155–169.
12. Shih, C. K., Rose, J. M., Hansen, G. L., Wu, J. C., Bacolla, A. & Griffin, J. A. (1991) *Proc. Natl. Acad. Sci. USA* **88,** 9878–9882.
13. Ren, J., Diprose, J., Warren, J., Esnouf, R. M., Bird, L. E., Ikemizu, S., Slater, M., Milton, J., Balzarini, J., Stuart, D. I. & Stammers, D. K. (2000) *J. Biol. Chem.* **275,** 5633–5639.
14. Kohlstaedt, L. A., Wang, J., Friedman, J. M., Rice, P. A. & Steitz, T. A. (1992) *Science* **256,** 1783–1790.
15. Ren, J., Esnouf, R., Garman, E., Somers, D., Ross, C., Kirby, I., Keeling, J., Darby, G., Jones, Y., Stuart, D. & Stammers, D. (1995) *Nat. Struct. Biol.* **2,** 293–302.
16. Ding, J., Das, K., Tantillo, C., Zhang, W., Clark, A. D. J., Jessen, S., Lu, X., Hsiou, Y., Jacobo-Molina, A., Andries, K., *et al.* (1995) *Structure (London)* **3,** 365–379.
17. Huang, H., Chopra, R., Verdine, G. L. & Harrison, S. C. (1998) *Science* **282,** 1669–1675.
18. Jacobo-Molina, A., Ding, J. P., Nanni, R. G., Clark, A. D. J., Lu, X., Tantillo, C., Williams, R. L., Kamer, G., Ferris, A. L., Clark, P., Hizi, A., Hughes, S. H. & Arnold, E. (1993) *Proc. Natl. Acad. Sci. USA* **90,** 6320–6324.
19. Rodgers, D. W., Gamblin, S. J., Harris, B. A., Ray, S., Culp, J. S., Hellmig, B., Woolf, D. J., Debouck, C. & Harrison, S. C. (1995) *Proc. Natl. Acad. Sci. USA* **92,** 1222–1226.
20. Hsiou, Y., Ding, J., Das, K., Clark, A. D., Jr., Hughes, S. H. & Arnold, E. (1996) *Structure (London)* **4,** 853–860.
21. Muller, B., Restle, T., Kuhnel, H. & Goody, R. S. (1991) *J. Biol. Chem* **266,** 14709–14713.
22. Bird, L. E., Chamberlain, P. C., Stewart-Jones, G., Ren, J., Stuart, D. I. & Stammers, D. K. (2002) *Protein Expression Purif.*, in press.
23. Otwinowski, Z. & Minor, W. (1996) *Methods Enzymol.* **276,** 307–326.
24. Brunger, A. T., Adams, P. D., Clore, G. M., Delano, W. L., Gros, P., Grosse, K. R. W., Jiang, J. S., Kuszewski, J., Nilges, M., Pannu, N. S., *et al.* (1998) *Acta Crystallogr. D* **54,** 905–921.
25. Stuart, D. I., Levine, M., Muirhead, H. & Stammers, D. K. (1979) *J. Mol. Biol.* **134,** 109–142.
26. Stammers, D. K., Somers, D. O. N., Ross, C. K., Kirby, I., Ray, P. H., Wilson, J. E., Norman, M., Ren, J. S., Esnouf, R. M., Garman, E. F., *et al.* (1994) *J. Mol. Biol.* **242,** 586–588.
27. Esnouf, R. M., Ren, J., Garman, E. F., Somers, D. O. N., Ross, C. K., Jones, E. Y., Stammers, D. K. & Stuart, D. I. (1998) *Acta Crystallogr. D* **54,** 938–954.
28. Tantillo, C., Ding, J., Jacobo-Molina, A., Nanni, R. G., Boyer, P. L., Hughes, S. H., Pauwels, R., Andries, K., Janssen, P. A. J. & Arnold, E. (1994) *J. Mol. Biol.* **243,** 369–387.
29. Hsiou, Y., Das, K., Ding, J., Clark, A. D., Kleim, J.-P., Rosner, M., Winkler, I., Riess, G., Hughes, S. H. & Arnold, E. (1998) *J. Mol. Biol.* **284,** 313–323.
30. Das, K., Ding, J., Hsiou, Y., Clark, A. D., Moereels, H., Koymans, L., Andries, K., Pauwels, R., Janssen, P. A., Boyer, P. L., *et al.* (1996) *J. Mol. Biol.* **264,** 1085–1100.
31. Ren, J., Nichols, C., Bird, L., Chamberlain, P., Weaver, K., Short, S., Stuart, D. I. & Stammers, D. K. (2001) *J. Mol. Biol.* **312,** 795–805.
32. Buckheit, R. W., Jr., Hollingshead, M., Stinson, S., Fliakas-Boltz, V., Pallansch, L. A., Roberson, J., Decker, W., Elder, C., Borgel, S., Bonomi, C., *et al.* (1997) *AIDS Res. Hum. Retroviruses* **13,** 789–796.
33. Balzarini, J., De Clercq, E., Carbonez, A., Burt, V. & Kleim, J. P. (2000) *AIDS Res. Hum. Retroviruses* **16,** 517–528.
34. Zhang, H., Vrang, L., Backbro, K., Lind, P., Sahlberg, C., Unge, T. & Oberg, B. (1995) *Antiviral Res.* **28,** 331–342.
35. Schinazi, R. F., Larder, B. A. & Mellors, J. W. (2000) *Int. Antiviral News* **8,** 65–91.
36. Ren, J., Milton, J., Weaver, K. L., Short, S. A., Stuart, D. I. & Stammers, D. K. (2000) *Structure Fold. Des.* **8,** 1089–1094.
37. Young, S. D., Britcher, S. F., Tran, L. O., Payne, L. S., Lumma, W. C., Lyle, T. A., Huff, J. R., Anderson, P. S., Olsen, D. B., Carroll, S. S., *et al.* (1995) *Antimicrob. Agents Chemother.* **39,** 2602–2605.
38. Isaka, Y., Miki, S., Kawauchi, S., Suyama, A., Sugimoto, H., Adachi, A., Miura, T., Hayami, M., Yoshie, O., Fujiwara, T. & Sato, A. (2001) *Arch. Virol.* **146,** 743–755.
39. Esnouf, R. M., Ren, J., Hopkins, A. L., Ross, C. K., Jones, E. Y., Stammers, D. K. & Stuart, D. I. (1997) *Proc. Natl. Acad. Sci. USA* **94,** 3984–3989.

Exhibit 7: Joly and Yeni, "Non-Nucleoside Reverse Transcriptase Inhibitors," *AIDS Rev* 1:37–44 (1999).

AIDS Rev 1999; 1: 37-44

Non Nucleoside Reverse Transcriptase Inhibitors

Véronique Joly and Patrick Yeni

Médecine Interne, Hôpital Bichat-Claude Bernard, Paris, France

Abstract

The non nucleoside reverse transcriptase inhibitors (NNRTIs) directly inhibit the HIV-1 reverse transcriptase (RT) by binding in a reversible and non competitive manner to the enzyme. The currently available NNRTIs are nevirapine, delavirdine, and efavirenz; other compounds are under evaluation. NNRTIs are extensively metabolized in the liver through cytochrome P450, leading to pharmacokinetic interactions with compounds utilizing the same metabolic pathway, particularly PIs, whose plasma levels are altered in the presence of NNRTIs. NNRTIs are drugs with a low genetic barrier, i.e. a single mutation in RT gene induces a high-level of phenotypic resistance, preventing the use of NNRTIs as monotherapy. In naïve patients, several trials have shown the value of NNRTIs in combination with nucleosides and/or PIs. Small pilot studies have shown that NNRTIs may be useful as second-line therapy. However, due to the rapid emergence of resistant virus to these compounds in case of uncomplete viral suppression, NNRTIs should not be added to current failing antiretroviral regimen. The most common side-effect reported with nevirapine and delavirdine is rash. The incidence of rash is rather similar under these two compounds, but severe rash is less frequent with delavirdine. The most common adverse reactions reported with efavirenz are central nervous system complaints such as dizziness. Rash is reported less frequently than with nevirapine or delavirdine, and is usually mild. NNRTIs resistance mutations are located in the aminoacid residues aligning the NNRTI-binding "pocket" site. High-level resistance is often associated with a single point mutation which develops within this site (especially codon groups 100–108 and 181–190). Patients failing on one NNRTI are very likely to possess multiple NNRTI resistance mutations. NNRTIs should always be used as part of a potent antiretroviral therapy to insure suppression of viral replication, thus circumventing the rapid selection of cross-resistant variants.

Key words

Reverse transcriptase inhibitors. Nevirapine. Delavirdine. Efavirenz. Drug resistance.

Correspondence to:
Patrick Yeni
Médecine Interne, Hôpital Bichat
46 rue Henri Huchard
75877 Paris
France

Introduction

The non nucleoside reverse transcriptase inhibitors (NNRTIs) are structurally and chemically dissimilar compounds that are highly potent inhibitors of HIV-1 reverse transcriptase (RT). Unlike nucleoside analogs, the NNRTIs are not incorporated

in the growing strand of HIV DNA, but directly inhibit the HIV-1 RT by binding in a reversible and non competitive manner to the enzyme. The binding site is a hydrophobic pocket close to the polymerase catalytic site in the p66 subunit of RT, leading to a significant slowing rate of polymerization catalyzed by the enzyme. Because NNRTIs interact with a specific binding site on the enzyme, any slight variation brought about by a single point mutation can have a significant impact on the sensitivity of virus to members of this group and high-level resistance can develop quickly[1]. Other retroviral RT, such as HIV-2, hepatitis virus, herpes virus and mammalian enzyme systems are unaffected by these compounds.

The currently available NNRTIs are nevirapine, delavirdine and efavirenz, and were approved by the US FDA in June 1996, April 1997 and September 1998, respectively. Their antiviral properties are summarized in Table 1. Other compounds are under evaluation, such as MKC 442 (Triangle Pharmaceuticals), S1153 (Lexigen Pharmaceuticals) and HBY 097 (Hoechst Bayer).

Pharmacologic properties

The compounds are active in their native state, requiring no activation, particularly no phosphorylation. Table 2 reports selected pharmacological characteristics of currently availale NNRTIs. A major characteristic of nevirapine pharmacokinetics is a metabolic autoinduction of cytochrome P450 enzymes, resulting in a 1.5 to 2 - fold increase in systemic clearance during the first 2-4 weeks of dosing[2]. Thus, it is recommended to initiate therapy with half of the standard 400 mg/day dose for the first 14 days. After this period, the recommended dosing of nevirapine is 200 mg BID, but the long half-life of the drug (25–30 h) suggests that it could be administered once daily. Dusek *et al*[3] conducted a retrospective, cross-sectional analysis of data from 5 clinical trials. In patients treated with nevirapine 400 mg OD, alone or in combination with a nucleoside, serum levels were consistently 250-fold above the IC_{90}, suggesting that this drug could probably be used on this once daily basis. Nevirapine levels in the cerebrospinal fluid reach 45% of plasma concentrations.

The recommended dosing of delavirdine is 400 mg TID, but preliminary results suggest that 600 mg BID should be appropriate[4].

NNRTIs are extensively metabolized in the liver through cytochrome P450, leading to pharmacokinetic interactions. Contrarily to nevirapine and efavirenz, which are both inducers of cytochrome P450 activity, delavirdine is an inhibitor of the cytochrome P450. Thus, compared to nevirapine and efavirenz, delavirdine has opposite interactions with compounds utilizing the same metabolic pathway, particularly protease inhibitors (PIs), whose plasma levels are increased in the presence of delavirdine[5,6]. The effects of delavirdine, nevirapine and efavirenz on the pharmacokinetics of available PIs are summarized in Table 3. Plasma levels of these 3 NNRTIs are not significantly altered by these PIs, except delavirdine whose AUC is decreased by 40% in the presence of nelfinavir, and efavirenz whose plasma AUC is increased by 21% in the presence of ritonavir.

Therapeutic efficacy

Phase I trials of monotherapy with nevirapine[7] or delavirdine[8] have shown that their *in vivo* antiviral effect was transient, viral load and CD4 cell counts returning to baseline by week 12. The loss in antiviral efficacy was associated with the emergence of resistant virus[7,9,10]. It appeared very soon that NNRTIs were drugs with a low genetic barrier, i.e. a single mutation in RT gene induced a high-level of

Table 1. *Summary of antiviral properties of currently available NNRTIs.*

Compound	IC50 RT	IC50 HIV-1	CC50	Selectivity index
Nevirapine	84 nM	48 nM	> 50 µM	> 1,000
Delavirdine	260 nM	10 nM	> 100 µM	> 10,000
Efavirenz	3 nM	1 nM	80 µM	> 80,000

IC : inhibitory concentration, CC : cytotoxic concentration

Table 2. *Pharmacological properties of currently available NNRTIs.*

	Nevirapine	Delavirdine	Efavirenz
Daily dose	400 mg	1200 mg	600 mg
Dosing	OD or BID	TID (BID under evaluation)	OD (or BID)
Steady-state trough	15.8 µM	16 µM	7 µM
T1/2	25 – 30 h	7 – 21 h	40 – 55 h
Bioavailability	> 90%	> 50%	> 60%
Protein binding	60%	98%	99.8%
Metabolism	P450 inducer	P450 inhibitor	P450 inducer

Table 3. *Percentage of alteration in area under the curve of plasma levels of each available protease inhibitor in the presence of NNRTIs.*

INTERACTING NNRTI	AFFECTED DRUG			
	INDINAVIR	RITONAVIR	SAQUINAVIR	NELFINAVIR
DELAVIRDINE	+ 100%[5]	+ 60%[54]	+ 500%[5]	+ 113%, - 50% for metabolite[6]
NEVIRAPINE	- 28%[55]	No effect[55]	+ 25%[56,57]	-46 to + 8%[58,59]
EFAVIRENZ	- 30%[45]	+ 18%[60]	- 60%[45]	+ 20%, - 37% for metabolite[60]

phenotypic resistance to the drug. This prevented the use of NNRTIs as monotherapy.

Further trials evaluated nevirapine or delavirdine in combination with one or two nucleosides. Each of these drugs, as part of a dual therapy, also appeared to have a transient effect on biological markers of HIV disease, due to the incomplete suppression of HIV replication, favoring once again the emergence of resistant virus to NNRTIs[11-13]. The combination of nevirapine or delavirdine with two nucleosides exhibited an antiviral effect that was clearly dependent on the therapeutic history of patients. In protocol ACTG 193A, designed for a pretreated and advanced patient population (CD4 cells < 50/µL), there was a trend for improved survival in the AZT/ddI/nevirapine arm compared with the zidovudine/ddI arm, but the difference did not reach statistical significance[14]. In another trial designed for nucleoside heavily pretreated patients, ACTG 241 trial, AZT/ddI/nevirapine was slightly more effective than AZT/ddI to increase CD4 cell count (18% higher mean) and to decrease plasma HIV RNA (0.25 $\log_{10}$ lower mean)[15]. By contrast, the INCAS trial comparing the combination of nevirapine/ddI/AZT *versus* two double combinations (AZT/nevirapine and AZT/ddI) in 151 antiretroviral naïve patients, showed the superiority of the triple drug arm[16]. At week 8, plasma HIV RNA levels had decreased by 2.18, 1.55 and 0.90 log in the triple drug arm, AZT/ddI and AZT/nevirapine groups, respectively. The proportions of patients with plasma HIV RNA levels below 20 copies/mL at week 52 was 51%, 12% and 0% in the triple drug arm, AZT/ddI and AZT/nevirapine groups, respectively. In a small subset of patients, the surrogate marker responses were found to be correlated to patient's compliance. Ward *et al*[17] reported the efficacy of a triple combination therapy of nevirapine with 2 nucleosides in clinical practice. This combination, given as first-line therapy in patients with a CD4 cell count > 300/µL and HIV-RNA below 15,000 copies/mL, or in patients with undetectable viral load under 2 nucleosides, allowed to obtain HIV-RNA below 400 copies/mL for at least the first twelve months of therapy in 24 out of 28 patients (86%).

Patients treated with AZT/ddI/delavirdine demonstrated more sustained improvements in CD4 counts, HIV-RNA and virus titers in plasma than patients treated with AZT/ddI, or AZT/delavirdine. The magnitude of the response correlated with the intensity of prior nucleoside analog treatment and the lack of genotypic resistance to AZT, evaluated by mutation at codon 215 in the RT genotype[8]. In naïve patients with baseline mean CD4 of 359/mm^3 and HIV RNA of 4.41 $\log_{10}$ copies/mL, the AZT/3TC/delavirdine triple therapy was more effective than DLV/AZT or AZT/3TC. At week 52, 59% of patients on the triple drug arm were below level of detection of 40 copies/mL, compared to 9% and 1% in the AZT/3TC and AZT/delaviridine arms, respectively[18].

The addition of 600 mg efavirenz to an ongoing regimen of AZT with 3TC induced HIV-1 suppression, defined as less than 400 copies/mL, in 69% of patients after 4 weeks of therapy but in only 29% of patients at week 16[19]. Thus, the antiviral effect was not sustained, although baseline plasma viral load was relatively low (8500 copies/mL). These results show that, like for other NNRTIs, addition of efavirenz as functional monotherapy to the regime of patients with active replication is not appropriate. In another study evaluating efavirenz efficacy in nucleoside experienced subjects (ACTG 364), virological response to triple drug therapy with 2 nucleosides and efavirenz was observed in a higher proportion of patients, since 71% of subjects had less than 500 copies/mL at week 16[20]. In this study, dual nucleoside therapy included at least one new component. A phase III, open-label, randomized trial showed that triple drug therapy with AZT/3TC/efavirenz combination in 3TC naïve patients (baseline viral load: 60,250 copies/mL) exerted a potent antiviral effect and was at least as effective as a conventional triple drug therapy with 2 nucleosides and a PI. In fact, at week 36, HIV-RNA level below 50 copies/mL, was observed in 88% and 82% of patients treated with AZT/3TC/efavirenz and AZT/3TC/indinavir, respectively[21].

Combinations of NNRTIs with PIs have been evaluated in patients naïve for PIs, nucleoside experienced or not, and in patients failing combination therapy with PIs, but naïve for NNRTIs. The first group of PIs naïve subjects allows the evaluation of the real benefit of the combination PI/NNRTI. Harris *et al*[22] reported the effects of nevirapine, indinavir and 3TC in combination in severely immunosuppressed patients (CD4 count < 50/mm^3), with previous exposure to nucleosides including 3TC. Median plasma HIV RNA was 5.16 $\log_{10}$ copies/mL at baseline and decreased by a median of 3.12 log copies/mlL at week 24. Median CD4 cell count was 30/mm^3, increasing by a median of 95/mm^3 at week

24. Viral load was below 500 copies/mL and below 20 copies/mL in 73% and 40% of patients remaining under therapy, respectively. This substantial virologic and immunologic effect was observed although indinavir plasma levels were lower than expected due the kinetic interaction between nevirapine and indinavir. The triple drug therapy nevirapine/nelfinavir/d4T in NNRTIs and PIs naïve patients with a CD4 count of 372 cells/µL and HIV-RNA plasma level of 4,5 $\log_{10}$ copies/mL decreased the plasma viral load below 400 copies/mL in 82% of subjects for at least 45 weeks[23]. Efavirenz 600 mg OD in combination with indinavir 1000 mg TID was evaluated in the third arm of the large open-label randomized trial cited above[21]. At week 36, 67% of patients had a plasma viral load below 500 copies/mL. Efavirenz in combination with nelfinavir 750 mg TID was evaluated in 62 patients (baseline HIV-RNA 4,59 log copies/mL). This combination decreased HIV-RNA below 50 copies/mL in 60% of patients at week 24[24].

In nucleoside experienced patients, the combination of efavirenz plus indinavir and 1 or 2 nucleosides (new or maintained) demonstrated superior efficacy to indinavir plus 1 or 2 nucleosides as defined by the percentage of subjects with less than 400 HIV-RNA copies/mL (85% versus 65%) and less than 50 copies/mL (74% versus 45%)[25]. In the ACTG 364 trial mentioned above, evaluating the efficacy of nelfinavir and/or efavirenz in nucleoside experienced patients, the 4 drug combination of efavirenz, nelfinavir and 2 nucleosides suppressed plasma viral load below 50 copies/mL in 75% of patients and was more efficient than the triple drug arm combining nelfinavir with 2 nucleosides in a pairwise comparison[20].

NNRTIs have also shown activity in patients failing triple drug therapy with PIs. The effect of combination therapy with delavirdine was studied in 25 patients who had extensive previous antiviral experience with nucleosides and PIs[26]. Patients received indinavir plus nelfinavir and delavirdine. Results showed a 1,9 $\log_{10}$ mean reduction in viral load and a 55 cell/µL increase in CD4 cell count after 6 months of therapy. In a group of 47 patients failing combination therapy with indinavir and nucleosides, the addition of delavirdine to current therapy and a switch from AZT to d4T in about half of the patients produced a decrease in HIV-RNA of 1.1 $\log_{10}$ copies/mL over 6 months. In 33% of subjects, viral burden declined below 400 copies/mL after 6 months[27]. The beneficial effect of delavirdine may be due to both positive pharmacokinetic interactions between delavirdine and indinavir and intrinsic antiviral activity of delavirdine.

Very few data are available on the efficacy of second-line therapy including a NNRTI and nucleosides (or nucleotides) without PI in patients failing combination therapy with PI. Pell *et al*[28] showed that 13 out of 24 patients (54%) who had detectable virus levels on a protease-containing regimen and were switched to d4T/ddI/nevirapine fell below 400 copies/mL at 26 weeks.

To summarize, small pilot studies have shown that NNRTIs may be useful as second-line therapy. However, due to the rapid emergence of resistant virus to these compounds in case of uncomplete viral suppression, NNRTIs should not be added to current failing antiretroviral regimen as assessed by a rebound in viral load. Drugs to which the patient is still naïve should be associated to NNRTI, knowing however, that cross-resistance is observed in each class of antiretroviral agents and contributes to decrease the efficacy of salvage therapy each time the combination shares common drug classes with first-line therapy.

NNRTIs may be well suited in prevention of vertical transmission because of their safety profile. Nevirapine has been tested in these settings. Administration of 200 mg to pregnant women during labor and 2 mg/kg to infants at 48–72 hours of life was safe and maintained serum level > 100 ng/mL (10-fold the IC50 of wild type virus)[29]. PACTG 316 is a randomized double blind phase trial to determine if such protocol of nevirapine administration can reduce mother to infant HIV transmission[30].

Tolerance

The major toxicity associated with nevirapine is a maculopapular rash which may be accompanied by fever and has a characteristic onset within the first 6 weeks of treatment. Nevirapine-related rash is reported in 17% of patients with 6% reaching grade 3/4 on the ACTG toxicity scale[31]. Several cases of Stevens-Johnson syndrome have been reported and at least 3 deaths have occurred. In 2800 patients treated with nevirapine, the incidence of this risk has been evaluated to be 0.3%[31,32]. There is a trend for higher incidence of rash in patients with lower CD4 cell counts. If a rash develops, the dosage of nevirapine should not be escalated until it abates. If the rash is extensive, moist, or involves the mucous membranes, or is associated with fever, nevirapine should be permanently discontinued. Hepatitis has also rarely been associated with nevirapine use. The 600 mg/day dosing regimen was discontinued in trials due to an unacceptable level of toxicity compared to the 400 mg/day regimen[9].

The major toxicity associated with delavirdine is a diffuse, pruritic maculopapular rash occurring within the first month of therapy. Delavirdine-related rash has been reported in 18% of patients[12,18]. The incidence of rash is higher in patients with a CD4+ count of less than 50 cells/µL. The incidence of rash is rather similar under delavirdine or nevirapine therapy. However, severe rash is less frequent with delavirdine (3.8% of the rashes), leading less often to hospitalization or to discontinuation of NNRTI. Only 3 cases of Stevens-Johnson syndrome have been reported by December 1st, 1998. In 85% of the cases, patients receiving delavirdine can be treated through the rash. Elevated hepatic transaminases have been observed with delavirdine.

The most common adverse reactions reported with efavirenz are central nervous system complaints such as dizziness, mild or moderate in severity, which often resolves after a few weeks.

Rash is reported less frequently than with nevirapine or delavirdine, and is usually mild.

Whether patients developing rash with one NNRTI can use other NNRTIs without increased risk of rash is unknown.

Resistance

NNRTIs are notorious for rapidly trigerring the emergence of drug-resistant HIV-1 variants. NNRTI resistance mutations are located in the aminoacid residues aligning the NNRTI-binding "pocket" site. High-level resistance is often associated with a single point mutation which develops within this site (especially codon groups 100–108 and 181–190).

Resistance to nevirapine has been associated with mutations at codon 98, 100, 103, 106, 108, 181, 188 and 190 of reverse transcriptase[34]. During monotherapy, the most frequently isolated nevirapine-resistant mutants contain the Y181C substitution, which results in a more than 100-fold reduction in viral susceptibility[35]. The Y181C mutation, that resensitizes to AZT virus containing the codon 215 mutation is infrequently selected by coadministration of nevirapine and AZT. By contrast, selection of K103N, Y188C, G190A is favored. Y188C mutation confers more than 7,5 fold resistance to nevirapine. A study analyzing 167 viral isolates from 38 patients treated with nevirapine, alone or in combination with AZT, found that isolates with greater than 100-fold reductions in nevirapine susceptibility uniformely emerged within 8 weeks of therapy in all patients[34]. Y181C mutants are highly resistant to delavirdine, but remain sensitive to efavirenz.

Phenotypic analyses of isolates from patients treated with delavirdine as monotherapy showed a 50–500 fold reduction in sensitivity in 14 of 15 patients by week 8 of therapy[36]. *In vitro* analysis of patients' isolates from clinical trials with delavirdine monotherapy or combination therapy has shown that the predominant RT substitution was K103N. Y181C or P236L were seen, at a lower frequency, as single or dual mutations with K103N. The presence of K103N and Y181C mutations results in 500-fold decreased viral susceptibility to delavirdine as measured by IC50 values. P236L confers 70-fold resistance to delavirdine *in vitro*[37], while increasing 10-fold susceptibility to nevirapine[38].

In vivo, the most frequently observed mutation associated with viral load rebound in patients receiving efavirenz is K103N, which has been found to confer an approximately 19-fold reduction in susceptibility[39]. Viruses with K103N mutation are cross resistant to efavirenz, delavirdine and nevirapine. *In vitro* results showed that a Y181C construct highly resistant to nevirapine and delavirdine maintained sensitivity towards efavirenz. Viruses with Y188C or G190SA mutations have a 4-fold decrease in susceptibility to efavirenz, but viruses with the Y188L or G190S mutations, that require two or more nucleotide substitutions, were found to be 100 to 200 fold resistant to efavirenz. The combination of at least 2 mutations leads to a high-level efavirenz resistant virus[40]. Thus, efavirenz may require more than one aminoacid substitution in order for the IC_{50} of the drug to be significantly increased, but patients failing on any of the other NNRTIs are very likely to possess multiple NNRTI resistance mutations, arguing against the use of efavirenz in patients failing with nevirapine or delavirdine.

NNRTIs under development

A large number of NNRTIs are currently under development. It is unclear as yet whether these drugs will offer significant advantages over the three currently available NNRTIs. Carboxanilide analogues are NNRTIs with very long half-lives, requiring i.v. formulation. Calanolide A analogues are in early Phase I trial. PNU 242721 (thiopyrimidine) has a low protein binding and allows BID or OD dosing. HBY 097, a quinoxaline derivative[41], has a half-life between 10 and 12 hours. The most common adverse events are gastrointestinal complaints and rash[42]. This compound is now in Phase II trial. S 1153 has a 10-fold greater *in vitro* potency than either delavirdine or nevirapine. In a phase I dose-escalation study, 25 subjects were treated with S-1153 for 28 days; 10 out of these were taking concomitant nucleosides. The average viral load decrease was 1.74 log and 12 patients had a drop in viral load below 400 copies/mL. No rashes were observed over the study period. Target blood levels of S-1153 were maintained with TID or BID dosing[43]. MKC 442 is in Phase II/III pivotal clinical trials. In Phase I trials, it has been shown that MKC-442 monotherapy (350 mg BID) induced a maximal decrease of 1 log in HIV-RNA which rebounded after one month of treatment[44].

NNRTIS in therapeutic strategies

Over the last decade, the treatment of HIV infection has changed radically. A more individualized approach to HIV therapy has emerged, associated with the approval of a range of potent antiretroviral agents, demonstration of the benefits of combination therapy and access to rapid and powerful assays for quantifying levels of HIV-RNA in the plasma of HIV-infected individuals. In order to assist physicians, comprehensive treatment guidelines have been published[45]. The optimal treatment response is a reduction in viral load to below the level of detection of a sensitive HIV-RNA assay.

Initial therapy

Combinations consisting of two nucleoside analogues plus a potent PI are suggested as optimum initial therapy. An alternative is two nucleoside analogues plus an NNRTI. This option permits deferral of the use of PI, thus delaying the risk of toxicity related to this class of compounds and sparing their full potency when used as salvage therapy in case of virological failure. NNRTIs should be used only in regimens designed to be maximally suppressive due to the rapid emergence of NNRTI resistant virus in case of incomplete viral suppression. Thus, the

combination of two nucleoside analogues and one NNRTI is not recommended for patients with advanced disease (low CD4 cell counts and/or high viral plasma load). This regimen needs a strict adherence to treatment. The compounds with a long half-life (nevirapine, efavirenz) allowing a once daily dosing should improve adherence to therapy and will be more compatible with active lifestyle.

Regimens combining a PI with a NNRTI, with or without a nucleoside, hold promise based on durable responses reported for the combination of indinavir and efavirenz[21,46] or nevirapine and indinavir[22]. When doing so, one must be cautious because the pharmacokinetic interactions between these agents are particular to each combination. In addition, one major concern with employing representatives of each of the three available drug classes in an initial regimen, is the potential for multidrug-class resistance when the initial regimen fails.

Second-line therapy

In case of treatment failure with viral load rebound, addition of a single new drug to the current therapy is to be strongly discouraged since this is equivalent to sequential monotherapy and will lead to more rapid emergence of drug-resistant virus, particularly in the case of NNRTIs. Efforts should be made to change the entire regimen, using drugs with least potential for cross-resistance with current drugs. In patients who failed when treated with a PI containing regimen, use of an NNRTI with new nucleoside(s) and new PI(s) is an appropriate therapeutic option. The value of combination therapy including an NNRTI and nucleoside(s) without PI remains to be determined in this population of patients. In patients who fail when treated with a NNRTI containing regimen, switching for a new regimen containing another NNRTI is, at the present time, not appropriate due to the large degree of cross-resistance between the currently available NNRTIs. Introduction of genotypic and/or phenotypic testing in routine clinical practice as well as availability of new NNRTIs could modify this recommendation.

Another unanswered question is the value of NNRTIs in patients who successfully respond to PI in combination with nucleosides. There is increasing recognition of complications from long-term exposure to PI-containing antiretroviral therapies, including hyperglycemia, hyperlipidemia, lipodystrophy and visceral fat accumulation[47-49]. Although the precise pathogenic mechanisms remain to be elucidated, a number of studies suggest that these abnormalities are mainly related to the use of PIs[48-52]. Switching PI for NNRTI as part of a triple-drug combination in patients with undetectable viral load should be evaluated. Apart from potentially reducing drug toxicity, this therapeutic strategy would offer to NNRTIs the best conditions for a potent and sustained antiviral efficacy due to the lack of viral replication at time of drug initiation, thus minimizing the risk of viral resistance.

Special considerations

- *HIV infection in pregnancy*

NNRTIs may be well suited in prevention of vertical transmission because of their safety profile. Nevirapine has been tested in this setting and larger studies are going on.

- *Post exposure prophylaxis*

Experimental data indicate that NNRTIs may have clinical potential for this indication[53]. If the decision is made to initiate prophylaxis, a potent combination therapy should be used. NNRTIs could be used, in combination, when a PI and/or nucleosides resistant virus is suspected.

In conclusion, NNRTIs are highly potent antiretroviral agents that can be combined with nucleosides and/or PIs without added toxicity. Their Achille heel is their potential for the rapid selection of cross-resistant variants to all compounds of this class. To circumvent this problem, NNRTIs should always be used in combination with other antiretrovirals to insure suppression of viral replication.

References

1. De Clercq E. Non-nucleoside reverse transcriptase inhibitors for the treatment of human immunodeficiency virus type 1 (HIV-1) infections: strategies to overcome drug resistance development. Medicinal Research Reviews 1996; 16: 125-57.
2. Murphy R and Montaner J. Nevirapine: A review of its development, pharmacological profile and potential for clinical use. Exp Opin Invest Drugs 1996; 5: 1183-99.
3. Dusek A, Hall D, Lamson M, *et al.* Once daily dosing of nevirapine: a retrospective, cross-study analysis. 12th World AIDS Conference, Geneva, 1998. Abstract 12360.
4. Wathen L, Freimuth W, Cox S, *et al.* Antiviral efficacy of twice daily rescriptor® (Delavirdine Mesylate) plus nelfinavir, didanosine and stavudine in an openlabel randomized study of triple and quadruple treatment regimens in HIV-1 infected individuals. 4th International Congress on Drug Therapy in HIV Infection, Glasgow, UK , 1998. Abstract P78.
5. Cox S, Ferry J, Batts D, *et al.* Delavirdine and marketed protease inhibitors: pharmacokinetic interaction studies in healthy volunteers. 4th Conference on Retroviruses and Opportunistic Infections. Washington, DC, 1997. Abstract 372.
6. Cox S, Schneck D, Herman B, *et al.* Delavirdine and nelfinavir: a pharmacokinetic drug-drug interaction in healthy volunteers. 5th Conference on Retroviruses and Opportunistic Infections, Chicago, 1998, Abstract 345.
7. Cheeseman S, Havlir D, McLaughlin M, *et al.* Phase I/II evaluation of nevirapine alone and in combination with zidovudine for infection with human immunodeficiency Virus. J Acquir Immune Defic Syndr 1995; 8: 141-51.
8. Davey R, Chaitt D, Reed G, *et al.* Randomized, controlled phase I/II trial of combination therapy with delavirdine (U-90152S) and conventional nucleosides in human immunodeficiency virus type 1-infected patients. Antimicrob Agents Chemother 1996; 40: 1657-64.
9. Havlir D, Cheeseman S, Mc Laughin M, *et al.* High-dose nevirapine: safety, pharmacokinetics, and antiviral effect in patients with human immunodeficiency virus infection. J Infect Dis 1995; 171: 537-45.
10. De Jong M, Vella S, Carr A, *et al.* High-dose nevirapine in previously untreated human immunodeficiency virus type-1-infected persons does not result in sustained suppression of viral replication. J Infect Dis 1997; 175: 966-70.
11. Carr A, Vella S, de Jong M, *et al.* A controlled trial of nevirapine plus zidovudine versus zidovudine alone in p24 antigenaemic HIV-infected patients. AIDS 1996; 10: 635-41.
12. Joly V on Behalf the M/3331/013B Study Group. Tolerance and efficacy of delavirdine mesylate (DLV) and zidovudine (ZDV)

therapy in the treatment of HIV Infected patients (Study M/3331/013B). 4th International Congress on Drug Therapy in HIV Infection, Glasgow, UK , 1998. Abstract P92.
13. Freimuth W, Chuang-Stein C, Greenwald C, *et al.* Delavirdine (DLV) combined with zidovudine (ZDV) or didanosine (ddI) produces sustained reduction in viral burden and increases in CD4 count in early and advanced HIV-1 infection. XI International Conference on AIDS, Vancouver, July 1996, Abstract MoB 295.
14. Henry K, Tiemy C, Kahn J, *et al.* A randomized, double-blind, placebo-controlled study comparing combination nucleoside and triple therapy for the treatment of advanced HIV disease. 4th Conference on Retroviruses and Opportunistic Infections. Washington, 1997. Abstract I.B6.
15. D'Aquila R, Hughes M, Johnson V, *et al.* Nevirapine, zidovudine and didanosine compared with zidovudine and didanosine in patients with HIV-1 infection. A randomized, double-blind, placebo-controlled trial. Ann Intern Med 1996; 124: 1019-30.
16. Montaner J, Reiss P, Cooper D, *et al.* A randomized, double-blind trial comparing combinations of nevirapine, didanosine and zidovudine for HIV-infected patients. The INCAS Trial. JAMA 1998; 279: 930-7.
17. Ward D, Elion R, Owen C. Triple combination therapy with nevirapine in a clinical practice. 12th World AIDS Conference, Geneva, 1998. Abstract 22378.
18. Sargent S, Green S, Para M, *et al.* Sustained plasma viral burden reductions and CD4 increases in HIV-1 infected patients with rescriptor plus retrovir plus epivir. 5th Conference on Retroviruses and Opportunistic Infections, Chicago, 1998. Abstract 699.
19. Mayers D, Jemesk J, Eyster E, *et al.* A double-blind, placebo-controlled study to assess the safety, tolerability and antiretroviral activity of efavirenz in combination with open-label zidovudine and lamivudine in HIV-1 Infected Patients [DMP 266-004]. 12th World AIDS Conference, Geneva, June 28 – July 3, 1998, Abstract 22340.
20. Albrecht M, Katzenstein D, Bosch R, *et al.* ACTG 364: Virologic efficacy of nelfinaria and/or efavirenz in combination with new nucleoside analogs in nucleoside experienced subjects. 12th World AIDS Conference, Geneva, 1998. Abstract 12203.
21. Morales-Ramirez J, Tashima K, Hardy D, *et al.* A phase III, multicenter, randomized, open-label study to compare the antiretroviral activity and tolerability of efavirenz (EFV) + indinavir (IDV), versus EFV + zidovudine (ZDV) + lamivudine (3TC), versus IDV + ZDV + 3TC at 36 weeks (DMP 266-006). 38th Interscience Conference on Antimicrobial Agents and Chemotherapy, San Diego, 1998. Abstract I–103.
22. Harris M, Durakovic C, Rae S, *et al.* A pilot study of nevirapine, indinavir and lamivudine among patients with advanced human immunodeficiency virus disease who have had failure of combination nucleoside therapy. J Infect Dis 1998; 177: 1514-20.
23. Skowron G, Leoung G, Berman B, *et al.* Stavudine (d4T), nelfinavir (NFV) and nevirapine (NVP): suppression of HIV-1 RNA to fewer than 50 copies/mL during 5 months of therapy. 12th World AIDS Conference, Geneva, 1998. Abstract 12275.
24. Jemsek J, Kagan S, Martin G, *et al.* A phase II, open-label, multicenter study to characterize the effectiveness, safety and pharmacokinetics of nelfinavir in combination with DMP 266 in antiretroviral therapy naïve or nucleoside analogue experienced HIV-infected patients (DMP 266-024). 38th Interscience Conference on Antimicrobial Agents and Chemotherapy, San Diego, 1998. Abstract I -102.
25. Haas D, Fessel W, Delaphena R, *et al.* A phase III, double-blind, placebo-controlled, multicenter study to determine the effectiveness and tolerability of the combination of efavirenz and indinavir *versus* indinavir in HIV-1 infected patients receiving nucleoside analogue therapy at 36 weeks. 38th Interscience Conference on Antimicrobial Agents and Chemotherapy, San Diego, September 24 – September 27, 1998. Abstract I – 244.
26. Lyle G. Effect of nelfinavir/indinavir/delavirdine in HIV+ patients with extensive antiviral experience. 12th World AIDS Conference, Geneva, 1998. Abstract 12329.
27. Bellman P. Clinical experience with adding delavirdine to combination therapy in patients in whom multiple antiretroviral treatment including protease inhibitors has failed. AIDS 1998; 12: 1333-40.
28. Pell C, Bodsworth N, Donovan B, *et al.* Efficacy of the combination stavudine, didanosine and nevirapine as initial antiretroviral therapy and following treatment with HIV-1 protease inhibitors – 26 Week Data. 12th World AIDS Conference, Geneva, 1998. Abstract 22357.
29. Mirochnik M, Sullivan J, Gagnier P, *et al.* and the ACTG protocol 250 team. safety and pharmacokinetics of nevirapine in neonates born to HIV-1 infected women. 4th Conference on Retroviruses and Opportunistic Infections, Washington, 1997. Abstract 723.
30. Dorenbum-Kracer A, Sullivan J, Gelber R, *et al.* Antiretroviral use in pregnancy in PACTG 316; a phase III randomized, blinded study of single-dose intrapartum/neonatal nevirapine to reduce mother to infant HIV transmission. 12th World AIDS Conference, Geneva, 1998. Abstract 23281.
31. Kohlbrenner V, Dransfield K, Cotton D, *et al.* Cutaneous eruptions associated with nevirapine therapy in HIV-1 infected individuals. XI International Conference on AIDS, Vancouver, 1996. Abstract MoB 1202
32. Warren K, Boxwell D, Kim N, *et al.* Nevirapine-associated Stevens-Johnson syndrome. Lancet 1998; 351: 567.
33. Barner A, Myers M. Nevirapine and rashes. Lancet 1998, 351: 1133.
34. Richman D, Havlir D, Corbeil J, *et al.* Nevirapine resistance mutations of human immunodeficiency virus type 1 selected during therapy J Virol 1994; 68: 1660-6.
35. Richman D, Shih C-K, Lowy I, *et al.* Human immunodeficiency virus type 1 mutants resistant to nonucleoside inhibitors of reverse transcriptase arise in tissue culture. Proc Natl Acad Sci USA 1991; 88: 11241-5.
36. Demeter L, Shafer R, Para M, *et al.* Delavirdine (DLV) susceptibility of HIV-1 isolates obtained from patients receiving DLV monotherapy. 3rd Conference on Retroviruses and Opportunistic Infections, 1996, Washington, Abstract 323.
37. Dueweke T, Pushkarskays T, Poppe S, *et al.* A mutation in reverse transcriptase of bis(heteroaryl)piperazine-resistant human immunodeficiency virus type 1 that confers increased sensitivity to other nonucleoside inhibitors. Proc Natl Acad Sci USA 1993; 90: 4713-7.
38. Demeter L, Meehan P, Morse G, *et al.* HIV-1 drug susceptibilities and reverse transcriptase mutations in patients receiving combination Therapy with didanosine and delavirdine. J AIDS 1997; 14: 136-44.
39. Bacheler L, Weislow O, Snyder S, *et al.* And the Sustive Study Group. Virological Resistance to Efavirenz. 12th World AIDS Conference, Geneva, 1998. Abstract 41213.
40. Young S, Britcher S, Tran L, *et al.* L-743,726 (DMP 266): A novel, highly potent non-nucleoside inhibitor of the human immunodeficiency virus type 1 reverse transcriptase. Antimicrob Agents Chemother 1995; 39: 2606-5.
41. Kleim J, Bender R, Kirsch R, *et al.* Preclinical evaluation of HBY 097, a new non-nucleoside reverse transcriptase inhibitor of human immunodeficiency virus type 1 replication. Antimicrob Agents Chemother 1995; 39: 2253-7.
42. Rubsamen-Waigmann H, Huguenel E, Paessens A, *et al.* Second-generation non-nucleosidic reverse transcriptase inhibitor HBY 097 and HIV-1 viral load. Lancet 1997; 349: 1517.
43. Dezube D, Jacobs M, Leoung G, *et al.* A second generation non-nucleoside reverse transcriptase inhibitor (S-1153) for the Treatment of HIV infection: A phase I study. 12th World AIDS Conference, Geneva, 1998. Abstract 12214.
44. Moxham C, Borroto-Esoda K, Noël D, *et al.* Preliminary efficacy and safety of repeated multiple doses of MKC-442 in HIV-infected volunteers. 4th Conference on Retroviruses and Opportunistic Infections, Washington, 1997. Abstract LB1.
45. Carpenter C, Fischl M, Hammer S, *et al.* Antiretroviral therapy for HIV infection in 1998. Updated Recommendations of the International AIDS Society – USA panel. JAMA 1998; 280: 78–86.
46. Havlir D, Hicks C, Kahn J, *et al.* Durability of antiviral activity of Efavirenz in combination with indinavir [DMP 266-003, Cohort IV]. 38th Interscience Conference on Antimicrobial Agents and Chemotherapy, San Diego, 1998. Abstract I – 104.
47. Lipsky J. Abnormal fat accumulation in patients with HIV-1 infection. Lancet 1998; 351: 867-70.

48. Miller K, Jones E, Yanovski JA, *et al.* Visceral abdominal-fat accumulation associated with use of indinavir. Lancet 1998; 351: 871-5.
49. Carr A, Samaras K, Burton S, *et al.* A syndrome of peripheral lipodystrophy, hyperlipidemia and insulin resistance due to HIV protease inhibitors. 5th Conference on Retroviruses and Opportunistic Infections, Chicago, 1998. Abstract 410.
50. Mann M, Piazza-Hepp T, Koller E, *et al.* Abnormal fat distribution in AIDS patients following protease inhibitors therapy: FDA summary. 5th Conference on Retroviruses and Opportunistic Infections, Chicago, 1998. Abstract 412.
51. Mulligan K, Tai VW, Algren H, *et al.* Evidence of unique metabolic effects of protease inhibitors. 5th conference on Retroviruses and Opportunistic Infections, Chicago, 1998. Abstract 414.
52. Keruly J, Chaisson R, Moore R. Diabetes and hyperglycemia in patients receiving protease inhibitors. 5th Conference on Retroviruses and Opportunistic Infections, Chicago, 1998. Abstract 415.
53. Grob P, Cao Y, Muchmore E, *et al.* Prophylaxis against HIV-1 infection in chimpanzees by nevirapine. 4th Conference on Retroviruses and Opportunistic Infections, Washington, 1997. Abstract 614.
54. Morse G, Shelton M, Hewitt R, *et al.* Ritonavir Pharmacokinetics during combination Therapy with Delavirdine. 5th Conference on Retroviruses and Opportunistic Infections, Chicago, 1998. Abstract 343.
55. Murphy R, Gagnier P, Lamson M, *et al.* Effect of nevirapine on pharmacokinetics of indinavir and ritonavir in HIV-1 patients. 4th Conference on Retroviruses and Opportunistic Infections, Washington, 1997. Abstract 374.
56. Buss N and the Fortovase Study Group. Saquinavir soft gel capsule (Fortovase) pharmacokinetics and drug interactions. 5th Conference on Retroviruses and Opportunistic Infections, Chicago, 1998. Abstract 354.
57. Sahai J, Cameron W, Salgo M, *et al.* Drug interaction study between saquinavir and nevirapine. 4th Conference on Retroviruses and Opportunistic Infections, Washington, 1997. Abstract 614.
58. Skowron G, Leoung G, Dusek A, *et al.* Stavudine, nelfinavir and nevirapine: preliminary safety, activity and pharmacokinetic interactions. 5th Conference on Retroviruses and Opportunistic Infections, Chicago, 1998. Abstract 350.
59. Merry C, Barry M, Mulcahy F, *et al.* The Pharmacokinetics of nelfinavir alone and in combination with nevirapine. 5th Conference on Retroviruses and Opportunistic Infections, Chicago, 1998. Abstract 351.
60. Fiske W, Benedek I, Joseph J, *et al.* Pharmacokinetics of efavirenz and ritonavir after multiple Oral doses in healthy volunteers. 12th World AIDS Conference, Geneva, 1998. Abstract 42269.
61. Fiske W, Benedek L, White S, *et al.* Pharmacokinetic interaction between efavirenz and nelfinavir mesylate in healthy volunteers. 5th Conference on Retroviruses and Opportunistic Infections, Chicago, 1998. Abstract 349.

Exhibit 8: Damm et al., "A Highly Selective Telomerase Inhibitor Limiting Human Cancer Cell Proliferation," *EMBO J.* 20(24):6958–68 (2001).

The EMBO Journal Vol. 20 No. 24 pp. 6958–6968, 2001

A highly selective telomerase inhibitor limiting human cancer cell proliferation

Klaus Damm[1,2], Ulrike Hemmann[3,4], Pilar Garin-Chesa[2], Norbert Hauel[5], Iris Kauffmann[5], Henning Priepke[5], Claudia Niestroj[2], Christine Daiber[2], Barbara Enenkel[2], Bernd Guilliard[2], Ines Lauritsch[2], Elfriede Müller[2], Emanuelle Pascolo[2], Gabriele Sauter[2], Milena Pantic[6,7], Uwe M.Martens[6], Christian Wenz[8], Joachim Lingner[8], Norbert Kraut[3], Wolfgang J.Rettig[9] and Andreas Schnapp[2]

Boehringer Ingelheim Pharma KG, [2]Oncology Research, [3]Genomics, [5]Chemistry, Birkendorfer Strasse 65, D-88397 Biberach, [6]University Medical Center, Department for Hematology/Oncology, Hugstetterstrasse 55, D-79106 Freiburg i. Br., [7]Albert-Ludwigs-University, Department of Biology, D-79106 Freiburg i. Br., Germany, [8]Swiss Institute for Experimental Cancer Research (ISREC), CH-1066 Epalinges, Switzerland and [9]Boehringer Ingelheim Austria GmbH, Dr. Boehringer-Gasse 5–11, A-1120 Vienna, Austria

[4]Present address: Aventis Pharma GmbH, Fraunhofer Strasse 13, D-82152 Martinsried, Germany

[1]Corresponding author
e-mail: klaus.damm@bc.boehringer-ingelheim.com

Telomerase, the ribonucleoprotein enzyme maintaining the telomeres of eukaryotic chromosomes, is active in most human cancers and in germline cells but, with few exceptions, not in normal human somatic tissues. Telomere maintenance is essential to the replicative potential of malignant cells and the inhibition of telomerase can lead to telomere shortening and cessation of unrestrained proliferation. We describe novel chemical compounds which selectively inhibit telomerase *in vitro* and *in vivo*. Treatment of cancer cells with these inhibitors leads to progressive telomere shortening, with no acute cytotoxicity, but a proliferation arrest after a characteristic lag period with hallmarks of senescence, including morphological, mitotic and chromosomal aberrations and altered patterns of gene expression. Telomerase inhibition and telomere shortening also result in a marked reduction of the tumorigenic potential of drug-treated tumour cells in a mouse xenograft model. This model was also used to demonstrate *in vivo* efficacy with no adverse side effects and uncomplicated oral administration of the inhibitor. These findings indicate that potent and selective, non-nucleosidic telomerase inhibitors can be designed as novel cancer treatment modalities.

Keywords: cancer/inhibitor/microarray/senescence/telomerase

Introduction

Telomerase is a cellular RNA-dependent DNA polymerase that serves to maintain the tandem arrays of telomeric TTAGGG repeats at eukaryotic chromosome ends (Morin, 1989; Blackburn and Greider, 1995). In human cells, the enzyme comprises a high molecular weight complex with a template-containing RNA subunit (Feng *et al.*, 1995) and protein components including the catalytic subunit human telomerase reverse transcriptase, hTERT (Harrington *et al.*, 1997; Meyerson *et al.*, 1997; Nakamura *et al.*, 1997). Telomerase activity has been demonstrated in immortalized cell lines and in 80–90% of human cancer specimens representing a range of cancer types (Counter *et al.*, 1994; Kim *et al.*, 1994; Shay and Bacchetti, 1997) and recently, human telomerase has been directly implicated in cellular immortalization and tumorigenesis (Bodnar *et al.*, 1998; Hahn *et al.*, 1999a). In most normal human cells, telomerase activity is low or not detectable, and telomeric DNA is progressively lost at a rate of 30–120 bp with each replication cycle (Harley *et al.*, 1990; Hastie *et al.*, 1990; Counter *et al.*, 1992). Eventually, telomeres shorten to a critical length and lose their ability to protect the ends of chromosomal DNA (Counter *et al.*, 1992; Blasco *et al.*, 1997). Uncapped chromosomes are sensitive to degradation and fusion and can activate DNA damage checkpoints, thus potentially contributing to the replicative senescence and growth arrest observed in aged primary cultured cells (Hayflick and Moorhead, 1961). Indeed, it has been proposed that telomere length specifies the number of cell divisions a cell can undergo prior to senescence (Cooke and Smith, 1986; Harley, 1991). In cancer cells, the reactivation of telomerase is thought to stabilize telomere length, thereby compensating for the cell division-related telomere erosion and providing unlimited proliferative capacity to malignant cells (Counter *et al.*, 1992; Kim *et al.*, 1994). As a corollary to this hypothesis, the inhibition of telomerase in tumour cells should disrupt telomere maintenance and return malignant cells to proliferative crisis followed by senescence or cell death (Harley *et al.*, 1990; Counter *et al.*, 1992). Genetic experiments using a dominant-negative form of human telomerase demonstrated that telomerase inhibition can result in telomere shortening followed by proliferation arrest and cell death by apoptosis (Hahn *et al.*, 1999b; Zhang *et al.*, 1999).

A challenge for the development of pharmaceutically useful telomerase inhibitors is the long lag period required to observe telomere attrition. Cellular growth arrest that depends on telomere shortening will require a series of cell division cycles to become apparent, and treatment may have to be given continuously for weeks to months, potentially in conjunction with other treatment modalities. Therefore, potency of action, selectivity, tolerability and

suitable pharmaceutical formulations are formidable tasks to be met in telomerase drug design. Here we describe a novel structural class of non-peptidic, non-nucleosidic inhibitors of human telomerase that are highly potent and selective *in vitro* and pharmacologically active in the control of human cancer cell proliferation.

Results

Small molecules selectively inhibit telomerase activity in vitro

To characterize small-molecule inhibitors of human telomerase, we used nuclear extracts prepared from HeLa cells to set up an *in vitro* telomerase activity assay (Morin, 1989; Schnapp *et al.*, 1998). Our study focuses on compounds with the general structure shown in Figure 1A, for which systematic structure-activity correlations have been established (N.Hauel *et al.*, manuscript in preparation). Two examples from this class of compounds, designated BIBR1532 {2-[(E)-3-naphtalen-2-yl-but-2-enoylamino]-benzoic acid} and BIBR1591 {5-morpholin-4-yl-2-[(E)-3-naphtalen-2-yl-but-2-enoylamino]-benzoic acid}, inhibit the *in vitro* processivity of telomerase in a dose-dependent manner, with half-maximal inhibitory concentrations (IC_{50}) of 93 and 470 nM, respectively (Figure 1B). The selectivity of BIBR1532 was assessed in a panel of DNA and RNA polymerases, including HIV reverse transcriptase, showing that none of these enzymes was inhibited at concentrations vastly exceeding the IC_{50} for telomerase (Figure 1C). As shown in the direct telomerase assay (Figure 1D), BIBR1532 can also inhibit recombinant, affinity purified telomerase, suggesting that it is indeed the catalytic activity of the telomerase enzyme which is the target for BIBR1532 inhibition.

Telomerase inhibitors induce telomere shortening in cancer cells

The compounds also had no effect on short-term cell viability or proliferation, as determined in a 7 day cytotoxicity assay using concentrations 100-fold above the *in vitro* IC_{50} (i.e. 10 μM for BIBR1532, 50 μM for BIBR1591). To investigate the cellular consequences of long-term treatment with a telomerase inhibitor, we cultivated exponentially growing NCI-H460 lung carcinoma cells in the presence of BIBR1532 (10 μM) or BIBR1591 (50 μM), respectively. As a control, untreated cells or cells treated with the solvent alone were grown using the same culture conditions. Periodically, total DNA samples were prepared from treated and control cells, digested with frequently cutting restriction enzymes and the telomere length examined by Southern blotting. NCI-H460 cells exhibit a heterogeneous size distribution, with an average telomere length of 4 kb and a predominant range of 2 to 6 kb (Figure 2A). As cells are propagated in

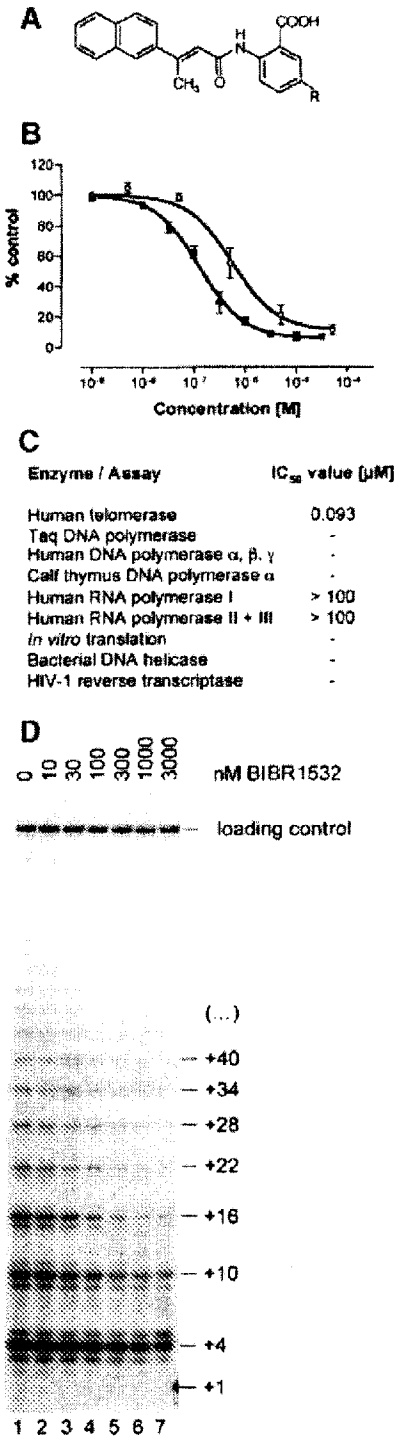

Fig. 1. Specific and selective telomerase inhibitors. (**A**) Chemical structure of the BIBR compound class of inhibitors. BIBR1532, R = H; BIBR1591, R = morpholin-4-yl. (**B**) Dosis-dependent inhibition of telomerase activity by BIBR1532 (solid squares) and BIBR1591 (open circles). Assays were performed and quantified using a PCR-based protocol followed by a TCA precipitation step. The incorporated activity of samples with inhibitor was normalized to the control and plotted against the inhibitor concentration. (**C**) Selectivity profile of BIBR1532. Enzymatic activity was assayed in the presence of 0–50 μM BIBR1532 as described in Materials and methods. –, no effect at 50 μM. (**D**) Direct assay of telomerase activity. Telomerase was reconstituted with insect cell expressed hTERT and *in vitro* transcribed RNA, affinity purified and incubated in the presence of different concentrations of BIBR1532. Telomerase products were separated on a sequencing gel.

the presence of telomerase inhibitor, steady telomere shortening occurred. The average telomere restriction fragment (TRF) size shortened progressively from 4 to 1.5 kb at population doubling (PD) 140 (Figure 2A), corresponding to a telomere loss of 30 bp/PD. We observed a comparable erosion of the telomeres in HT1080 fibrosarcoma, MDA-MB231 breast carcinoma and DU145 prostate carcinoma cells similarly treated with telomerase inhibitor (Figure 2A). In contrast, untreated cells or cells exposed to solvent alone maintained a stable TRF size (Figure 2A).

Telomerase inhibitors limit cancer cell proliferation

The growth kinetics of inhibitor-treated cells initially did not differ from those of untreated or solvent treated control cells, regardless of the cell line used. NCI-H460 cell cultures in the absence or presence of telomerase inhibitor exhibited no or only minor differences in proliferation for more than 120 days of treatment (Figure 2B). However, after PD135 the inhibitor-treated cells slowed their growth and showed an almost complete inhibition of proliferation after additional 4–8 population doublings (Figure 2B). This telomerase inhibitor-induced growth arrest is apparently independent of functional p53 since similar growth curves, with an onset of cellular growth arrest after a significant lag-phase, were obtained for the p53-deficient HT1080, MDA-MB231 and DU145 cell lines (Figure 2B). The reduced proliferation capacity of telomerase-inhibited cells near growth arrest was further substantiated in colony formation assays, with about 50% reduction in colony formation for treated versus mock-treated NCI-H460 and HT1080 cells. As a control for compound specificity we also cultivated telomerase-negative, normal human lung fibroblasts as well as an osteosarcoma cell line (SAOS-2) that exhibits the alternative lengthening of telomere (ALT) phenotype (Bryan *et al.*, 1995). Our results showed that inhibitor treatment had no effect on telomere length, growth kinetics and morphology for the entire time of treatment (8 weeks) in either cell line.

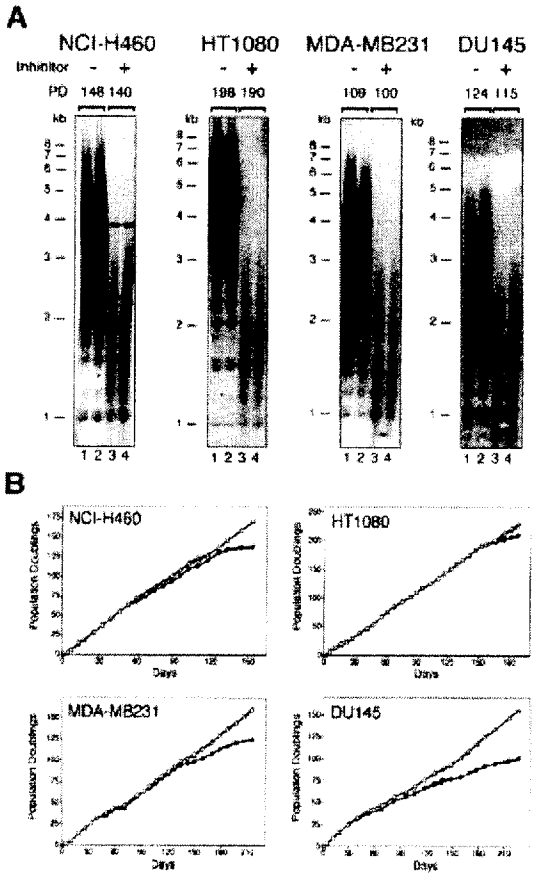

Fig. 2. Telomerase inhibitors induce telomere shortening and limit cell proliferation. (**A**) Total genomic DNA prepared from untreated (lane 1), solvent- (lane 2) or inhibitor-treated (lanes 3 and 4) NCI-H460, HT1080, MDA-MB231 or DU145 cells was assessed for telomere restriction fragment size by Southern blot analysis with a telomeric probe. PD, population doubling; –, absence and +, presence of BIBR1532 or BIBR1591. (**B**) NCI-H460, HT1080, MDA-MB231 and DU145 cells were plated in 24-well plates in duplicate in the presence of 10 μM BIBR1532 or 50 μM BIBR1591 dissolved in 0.1% DMSO (closed symbols). Control cells were untreated (open triangles) or treated with corresponding solvent concentrations (open circles). Cultures were replated every 2–3 days to maintain log-phase growth and to calculate the growth rate.

Reversibility of inhibition

In parallel cultures of the NCI-H460 cells shown in Figure 2B we observed very slowly proliferating cells that were overgrowing the resting, senescent cells in the culture plate, resulting in a flat but measurable growth rate (Figure 3A). Apparently, the treated cells enter senescence not in a parallel but rather in a sequential fashion, which may be due to the heterogeneity of their telomere lengths. We never observed spontaneous telomere lengthening or telomerase-independent growth attributable to the induction of an ALT phenotype. To determine the effect of inhibitor depletion, we transferred the treated cells to normal medium without drug starting at day 220. After a short delay of 3–4 days the cells exhibited a growth rate similar to the control culture (Figure 3A). Examination of

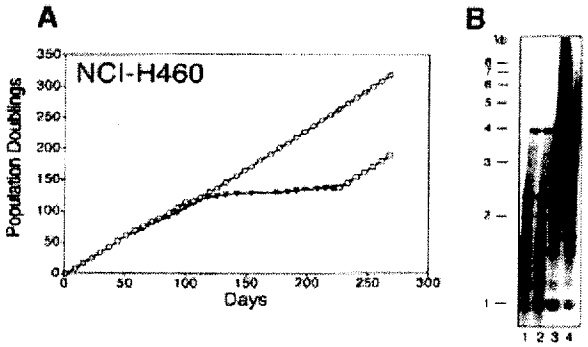

Fig. 3. Reversibility of inhibition. (**A**) NCI-H460 cells were cultivated in 24-well plates in the absence (open circles) or presence of 50 μM BIBR1591 (closed triangles). After 130 days, compound-treated cells were replated only when the culture dishes reached subconfluence. At day 220, these cells were washed, replated in medium without compound and the growth rate monitored for additional 50 days (open squares). (**B**) The median TRF size of inhibitor-treated NCI-H460 cells at day 220 corresponds to only 1.5 kb (lanes 1 and 2). Removal of the inhibitor and cultivation of these cells for 40 PD in absence of inhibitor leads to a significant telomere elongation (lane 3). Untreated control cells at day 260 are also shown for comparison (lane 4).

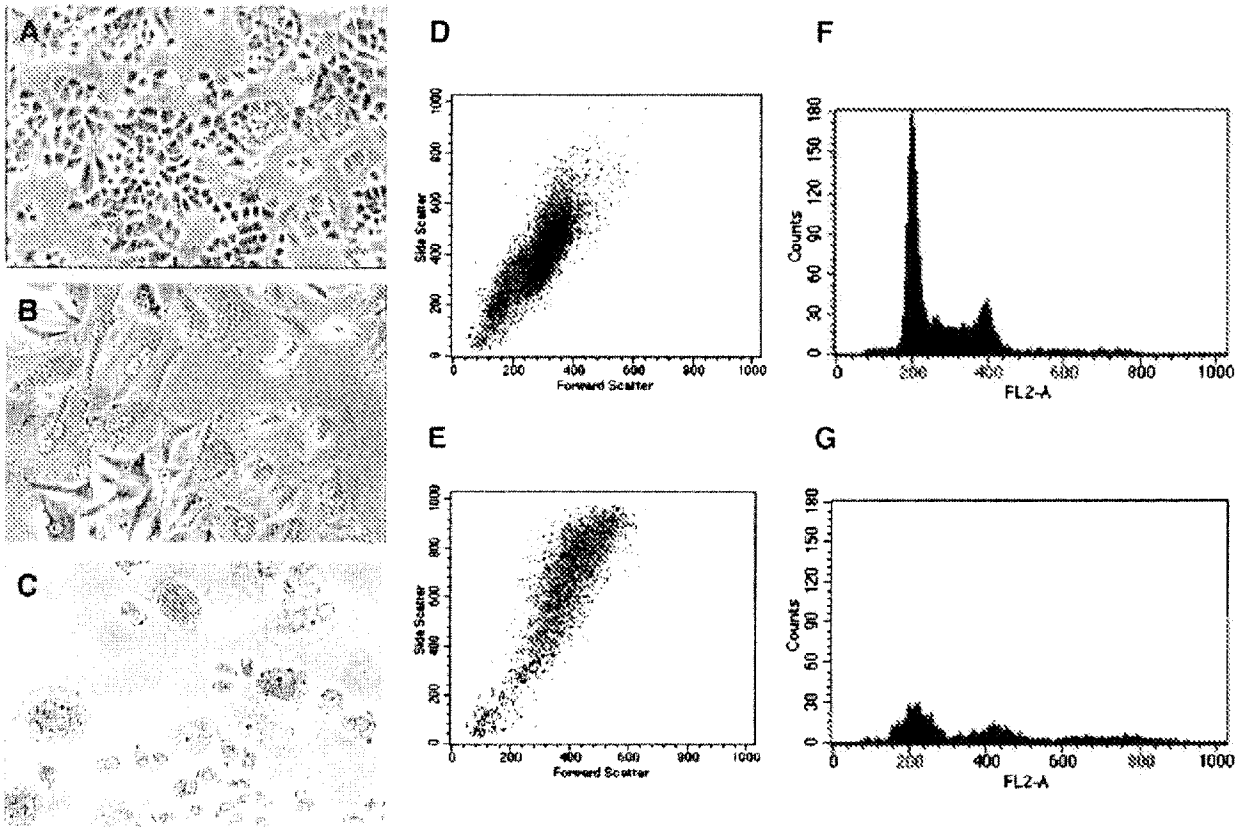

Fig. 4. Induction of a senescence phenotype. Phase contrast micrographs show the cellular morphology of (**A**) untreated and (**B**) inhibitor-treated NCI-H460 cells at PD162 and PD130, respectively. (**C**) Inhibitor-treated NCI-H460 cells from a separate inhibition experiment were stained for β-galactosidase activity at pH 6.0. Phenotypic changes in this experiment were already observed at PD72. (**D–G**) Flow cytometric analysis of NCI-H460 cells shown in (C). Dot density maps of PI-staining (*x*-axis) and 90-degree light scatter (*y*-axis) are shown for control (D), and inhibitor-treated cells (PD72) (E). DNA content analysis of control (F), and inhibitor-treated cells (PD72) (G).

the TRF sizes also revealed a rapid elongation of the telomeres in these cells (Figure 3B), demonstrating that the telomerase inhibition is fully reversible.

Telomerase inhibitors induce a senescent phenotype

The inhibitor-treated, late passage tumour cells showed distinctive morphological features associated with senescence of aged normal human cells. In contrast to untreated cell cultures (Figure 4A), the growth-arrested NCI-H460 cells (Figure 4B) became enlarged, often contained multiple nuclei, had a vacuolated cytoplasm and showed induction of senescence associated β-galactosidase activity (Figure 4C). Similar morphological alterations were observed with late-passage HT1080, MDA-MB231 and DU145 cells (data not shown). FACS analysis of inhibitor-treated NCI-H460 cells revealed an elevated forward and side scatter relative to untreated cells, which may reflect increased cell size and granularity (Figure 4D and E). The inhibitor-treated NCI-H460 cells also showed a heterogeneous cell cycle profile, with broad 2n and 4n peaks and a shift towards higher DNA content (Figure 4F and G). We performed extensive FACS analysis and TUNEL staining in p53 positive (NCI-H460) or p53 negative (HT1080, DU145, MDA-MB231) cell lines at different timepoints, but could not detect an increase in apoptosis comparing treated and control cells.

Inhibitor-treated cells exhibit telomere dysfunction

We next analysed chromosomal metaphase spreads derived from late-passage NCI-H460 cells. Due to the reduced proliferative capacity and the correspondingly low mitotic index only eight metaphases were obtained from the inhibitor-treated cells, and these were compared qualitatively with 20 metaphases from control cultures. The loss of telomeric sequences was readily detected using the Q-FISH technique with a telomere-specific probe (Figure 5A and B) (Martens *et al.*, 1998). Signal intensity, which has been shown previously to correlate directly with the number of TTAGGG repeats, was significantly ($p < 0.0001$) reduced in the inhibitor-treated cells relative to control cells (Figure 5C). The histogram also shows an accumulation of short telomeres and an increased skewness in the distribution of telomere fluorescence

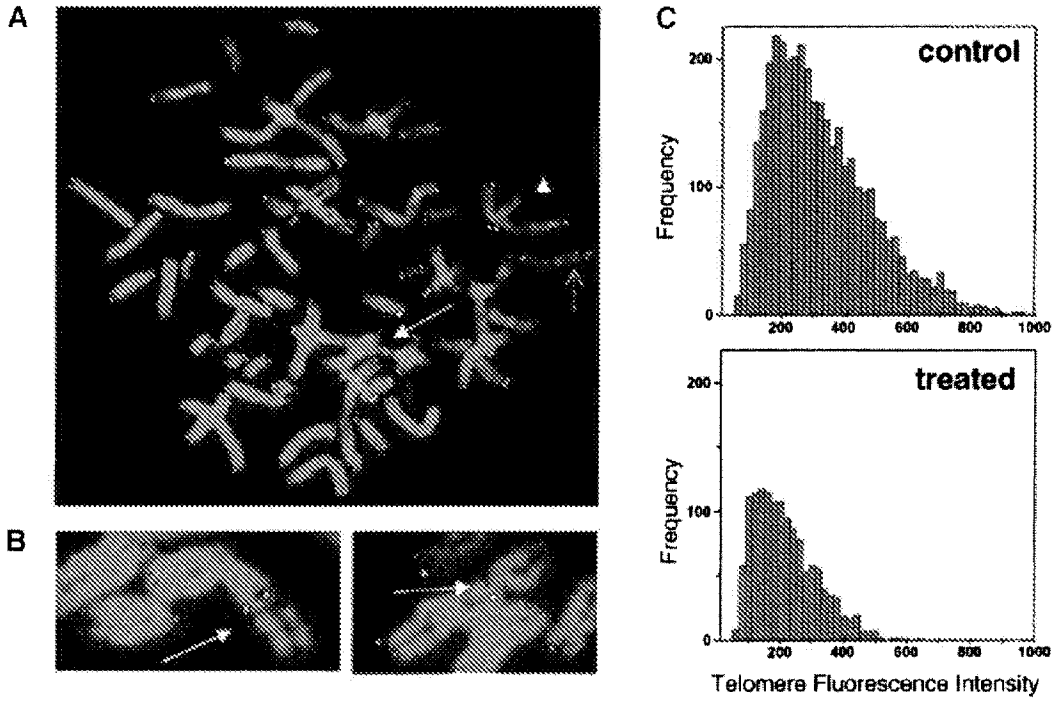

Fig. 5. Telomere analysis of inhibitor-treated NCI-H460 cells. (**A**) Q-FISH analysis of metaphase chromosomes from inhibitor-treated NCI-H460 cells. DAPI-stained chromosomes and Cy-3-labeled telomeres are shown in blue and yellow, respectively. The NCI-H460 cell line is hypotriploid with seven marker chromosomes (modal chromosome number 57) and exhibits a characteristic chromosome with interchromosomal telomere signals. Arrowhead denotes missing telomeres; arrow denotes fused chromosomes; dashed arrow denotes interchromosomal telomere signals. (**B**) Details of end-to-end fusions from another metaphase with telomere signals present at the fusion site. (**C**) Histograms express the fluorescence intensity and frequency of all individual telomere spots from NCI-H460 derived metaphases. Twenty metaphases (n = 3740) were derived from control cultures (PD68) and eight metaphases (n = 1366) were derived from inhibitor treated cells (PD120). n is the number of individual telomere signals. The differences in mean fluorescence intensity (arbitrary fluorescence units ± SD) between the control cells (321 ± 160) and the treated cells (217 ± 101) were highly significant (p <0.0001).

(Figure 5C) which is very similar to the observations in pre-senescent fibroblasts (Martens *et al.*, 2000). Furthermore, we observed an increase in chromosome end fusions (0.88/metaphase in treated versus 0.55/metaphase in control cells) as well as an increased number of chromosomes with no telomere signal at both sister chromatids in treated cells (mean: 3.75/metaphase) compared with control cells (mean: 1.1/metaphase).

Microarray analysis of mRNA expression levels in senescent NCI-H460 cells

To identify genes responsive to pharmacological telomerase inhibition and telomere shortening we determined changes in gene expression levels between inhibitor-treated and untreated NCI-H460 cells using DNA microarrays with the capacity to display transcript levels of 6817 known human genes. Total RNA was prepared from cells exposed to telomerase inhibitor for 7, 28 and 56 days, respectively, or until overt morphological changes characteristic for senescence were apparent. Analysis of the day 7, day 28 and day 56 timepoints revealed only minor variations in RNA transcript patterns without consistent changes. However, in the inhibitor-treated, senescent NCI-H460 cells we identified 302 (4.4%) genes showing at least a 2-fold difference in expression levels in a minimum of three out of four independent comparisons (for complete gene list see Supplementary data available at *The EMBO Journal* Online). The up- or down-regulated genes displaying the largest alterations in expression were assigned to functional categories (Tables I and II).

A large percentage of the 166 down-regulated genes represent proteins involved in cell cycle control, the regulation of DNA synthesis, replication and segregation, and mitosis, as well as transcription and translation processes (Table I). In addition, more than 60 of the 142 up-regulated genes encode lysosomal enzymes, proteins mediating cell-adhesion and growth factors and cytokines with both growth promoting as well as growth inhibitory function (Table II). Only a few of these genes have previously been associated with DNA damage or senescence and most prominent among these is the cyclin-dependent kinase inhibitor $p21^{Waf1}$, which we found to be up-regulated 12.9-fold. In contrast, expression of the breast cancer susceptibility genes BRCA1 and BRCA2 as well as BARD1 (BRCA1-associated Ring domain protein), which are thought to play a key role in the cellular DNA damage response, was found to be repressed. We also observed a 5-fold reduction of hTERT mRNA, encoding the catalytic subunit of telomerase, while the telomere binding protein TRF1 was found among the induced genes. No other genes associated with telomere

Table I. Transcriptional changes induced in NCI-H460 cells by long-term telomerase inhibitor treatment: down-regulation

Accession No.	Fold Δ	Gene name	Identified in context of senescence/ageing
Cell cycle control			
U74612	−11.5	hepatocyte nuclear factor-3/fork head homolog 11A	Ly *et al.* (2000)
X51688	−11.4	cyclin A (*)	Ly *et al.* (2000); Shelton *et al.* (1999)
Z29066	−7.1	NEK2	
X65550	−7.0	mki67a	
X13293	−6.3	B-MYB	Chang *et al.* (2000); Ly *et al.* (2000)
U05340	−4.9	p55CDC	Ly *et al.* (2000)
U33761	−3.9	cyclin A/CDK2-associated p45 (SKP2)	
U77949	−3.5	CDC6-related protein	
M25753	−3.4	cyclin B	Chang *et al.* (2000); Ly *et al.* (2000); Shelton *et al.* (1999)
X54941	−3.3	CKSHS1	Ly *et al.* (2000)
D50914	−3.2	KIAA0124, similar to mouse BOP1	
U65410	−3.1	MAD2	Chang *et al.* (2000)
U01038	−2.9	PLK1	Chang *et al.* (2000); Ly *et al.* (2000)
X05360	−2.5	CDC2	Chang *et al.* (2000); Shelton *et al.* (1999)
U56816	−2.4	MYT1	Ly *et al.* (2000)
X54942	−2.3	CKSHS2	
DNA segregation, mitosis, chromatin assembly			
D38751	−31.0	kinesin-like DNA binding protein (KID)	
U20979	−7.4	chromatin assembly factor-I p150 subunit	
U61145	−7.1	enhancer of Zeste homolog 2 (EZH2)	
D38553	−5.4	XCAP-H condensin homolog	Chang *et al.* (2000)
D63880	−4.2	KIAA0159	
X63692	−3.6	DNA (cytosin-5)-methyltransferase	
U09087	−3.4	thymopoietin β	
U18271	−3.4	thymopoietin	
U37426	−3.3	kinesin-like spindle protein (HKSP)	Ly *et al.* (2000)
X62534	−3.3	HMG2	Chang *et al.* (2000); Ly *et al.* (2000)
D38076	−3.3	RANBP1	Ly *et al.* (2000)
D00591	−3.2	RCC1	
L07515	−3.0	heterochromatin protein homologue (HP1)	
M34458	−2.9	lamin B	Chang *et al.* (2000)
X85137	−2.9	kinesin-related protein	
U14518	−2.7	centromere protein-A (CENP-A)	Chang *et al.* (2000); Ly *et al.* (2000)
M97856	−2.5	histone-binding protein	Ly *et al.* (2000)
X67155	−2.5	mitotic kinesin-like protein-1	Ly *et al.* (2000)
D80000	−2.5	SMC1L1	
D43948	−2.1	TOG	Ly *et al.* (2000)
DNA synthesis, replication			
L16991	−11.1	thymidylate kinase (CDC8)	Ly *et al.* (2000)
M87338	−8.7	replication factor C	
HG2379-HT3996	−8.5	serine hydroxymethyltransferase	
D55716	−5.7	P1CDC47/MCM7	Chang *et al.* (2000)
U40152	−3.5	origin recognition complex 1	Chang *et al.* (2000)
X52142	−3.1	CTP synthetase	
X59618	−2.7	ribonucleotide reductase M2 polypeptide	Chang *et al.* (2000)
M63488	−2.7	replication protein A 70 kDa subunit	
M15205	−2.6	thymidine kinase	Chang *et al.* (2000); Ly *et al.* (2000); Shelton *et al.* (1999)
U00238	−2.5	glutamine PRPP amidotransferase	
J04031	−2.5	MTHFD1	
U81375	−2.5	equilibrative nucleoside transporter 1 (hENT1)	
HG2846-HT2983	−2.3	dihydrofolate reductase	Chang *et al.* (2000)
X06745	−2.3	DNA polymerase α-subunit	Chang *et al.* (2000)
X54199	−2.2	GARS-AIRS-GART	
D84557	−2.2	MCM6	
Transcription, RNA processing, translation initiation			
X89416	−14.8	protein phosphatase 5	
D32002	−8.0	nuclear cap binding protein	
D12686	−7.1	eukaryotic initiation factor 4γ	
M85085	−6.6	cleavage stimulation factor	
U76421	−5.4	dsRNA adenosine deaminase DRADA2b	
X13482	−4.9	U2 snRNP-specific A′ protein	
X75918	−3.1	NOT	
U28042	−2.9	DEAD box RNA helicase-like protein	
M60784	−2.8	U1 snRNP-specific protein A	
U08815	−2.4	splicesomal protein (SAP61)	
L10838	−2.4	pre-mRNA splicing factor (SRP20)	Ly *et al.* (2000)
X67337	−2.2	HPBRII-4	
M86737	−2.2	high mobility group box (SSRP1)	
U90426	−2.1	nuclear RNA helicase	Ly *et al.* (2000)
L03532	−2.1	M4 protein	Ly *et al.* (2000)
Tumour suppressors			
X95152	−3.3	BRCA2	
L78833	−2.9	BRCA1	
U76638	−2.5	BARD1	Ly *et al.* (2000)
Telomerase component			
AF015950	−5.0	hTERT(*)	

The fold decrease shown represents the mean of four pairwise comparisons. A comprehensive list of all regulated genes can be found in the supplementary data. (*) Confirmed by TaqMan RT–PCR.

Table II. Transcriptional changes induced in NCI-H460 cells by long-term telomerase inhibitor treatment: up-regulation

Accession No.	Fold Δ	Gene name	Identified in context of senescence/ageing
Lysosomal proteins			
M16424	14.3	β-hexosaminidase α-chain	Lee *et al.* (1999, 2000)
M59916	10.9	acid sphingomyelinase (ASM)	
X62078	7.2	GM2 activator	
X78687	4.3	sialidase	
L09717	4.1	lysosomal membrane glycoprotein-2 (LAMP2)	
J03060	4.1	glucocerebrosidase (GCB)	
X52151	3.5	arylsulphatase A	
Z12173	3.2	glucosamine-6-sulfatase (GNS)	
X55079	3	GAA gene	Chang *et al.* (2000)
M95767	2.8	di-*N*-acetylchitobiase	
M22960	2.7	protective protein for β-galactosidase	
M29877	2.7	α-l-fucosidase	
D12676	2.6	lysosomal sialoglycoprotein	
U70063	2.5	acid ceramidase	
M63138	2.4	cathepsin D (CAT D)	Lee *et al.* (2000)
M34423	2.2	β-galactosidase (GLB1)	
Mitochondrial proteins			
M68840	10	monoamine oxidase A (MAOA)	
X05409	5.7	aldehyde dehydrogenase I ALDH I	
U54617	5.4	pyruvate dehydrogenase kinase isoform 4	
D87328	5	HCS	
M32879	3	steroid 11-β-hydroxylase (CYP11B1)	
D16481	2.2	3-ketoacyl-CoA thiolase β-subunit	
ECM/ECM signalling/cell adhesion			
L13923	6.5	fibrillin	
X17094	6.5	furin	
U47926	4.4	unknown protein B (homology to mGROS1)	
X03168	4.3	vitronectin	
U13896	3.9	homolog of *Drosophila* discs large protein, isoform 2	
M14648	3.3	vitronectin receptor α subunit	
U64573	3.2	connexin 43	
X52947	2.8	cardiac gap junction protein	
U59289	2.7	H-cadherin	
M61916	2.5	laminin B1 chain	Lee *et al.* (2000)
X68742	2.5	integrin α subunit	
HG2981-HT3125	2.4	Epican, alt. splice 1	
DNA structure			
X57129	10.3	H1.2 gene for histone H1	
X57985	9.5	GL105 gene for histones H2B.1 and H2A	
U90551	3.8	histone 2A-like protein (H2A/l)	
X60487	3.7	H4 histone family, member H	
Z29331	3.6	ubiqutin-conjugating enzyme UBCH2	
U40705	2.3	TRF1 (telomeric repeat binding factor-1)	
Complement, coagulation			
U92971	8.7	protease-activated receptor 3 (PAR3)	
J04080	4.2	complement C1r (multiple probe sets)	Ly *et al.* (2000); Lee *et al.* (2000)
M59499	3.5	lipoprotein-associated coagulation inhibitor (LACI)	
M14113	3.4	coagulation factor VIII:C	
M65292	3	factor H homologue	
Fatty acid oxidation/metabolism			
X14813	4.9	3-oxoacyl-CoA thiolase	
U46689	2.7	microsomal aldehyde dehydrogenase (ALD10)	
L40904	2.3	peroxisome proliferator activated receptor γ	
D16481	2.2	mitochondrial 3-ketoacyl-CoA thiolase β-subunit	
U03688	2.1	dioxin-inducible cytochrome P450 (CYP1B1)	Shelton *et al.* (1999)
Growth factors and cytokine signalling			
HG987-HT987	12.5	MAC25/IGFBP7	
M97936	11.1	STAT1 (multiple probe sets)	
M34057	8.3	transforming growth factor-β1 binding protein	
M62403	8.3	insulin-like growth factor binding protein 4 (*)	
M27288	7.5	oncostatin M	
U23070	6.4	putative transmembrane protein NMA (sim. to BAMBI)	
D37965	6.2	PDGF receptor β-like tumor suppressor (PRLTS)	
L20861	4.6	WNT5a (*)	
X04434	4.4	insulin-like growth factor I receptor	
D87258	3.5	cancellous bone osteoblast serin protease	Ly *et al.* (2000)
AB000584	3.3	TGF-β superfamily protein	Ly *et al.* (2000)
X62320	3.3	acrogranin (epithelin 1 and 2)	
Z29090	2.7	phosphatidylinositol 3-kinase	
X04571	2.3	kidney epidermal growth factor (EGF) precursor	
J04513	2.3	basic fibroblast growth factor (bFGF)	
HG3484-HT3678	2.2	CLK1 dual specificity kinase	
Cell cycle/ DNA damage response			
U09579	12.9	$p21^{MDA6/WAF1}$ (*)	Ly *et al.* (2000); Shelton *et al.* (1999)
U33203	2.3	MDM2-E	

(*) For explanation see footnote to Table I.

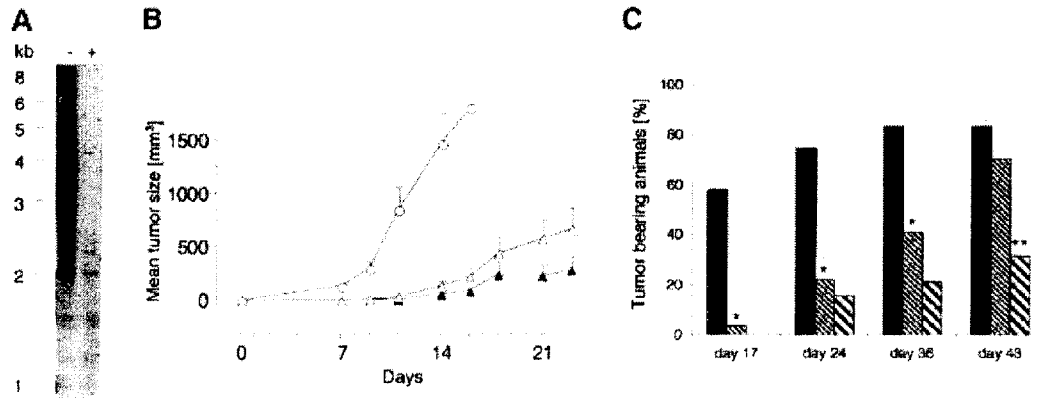

Fig. 6. Tumorigenicity assay. Nude mice were each injected with 1.5×10^6 HT1080 control or pre-senescent, telomere shortened cells. Tumour size was measured in regular intervals. (**A**) Telomere length of untreated control (–) and inhibitor-treated (+) HT1080 cells used to inject nude mice. (**B**) Mean tumour size of animals bearing control ($n = 24$) (open circles) and pre-senescent cells in the absence ($n = 27$) (open triangles) or presence ($n = 19$) (closed triangles) of BIBR1532. (**C**) The number of animals (as a percentage) with a tumour >1000 mm^3 for untreated control (black) and pre-treated cells in the absence (thin stripes) or presence (bold stripes) of BIBR1532 at the indicated days after injection. Statistical analysis was performed using Fisher's exact test, with significant differences ($p < 0.05$) between untreated control and pre-treated cells (*; $p < 0.0002$) as well as between pre-treated cells in the presence or absence of BIBR1532 (**; $p = 0.01034$) at the indicated time points.

biology or DNA damage response were found to be altered in their expression.

Effect of telomerase inhibition on tumorigenic potential

Telomerase is an unusually challenging target for demonstrating *in vivo* efficacy because of the long lag period required until telomeres are sufficiently shortened to produce detrimental effects on cell growth. The treatment of pre-established tumours with a telomerase inhibitor in standard mouse xenograft models will not result in a growth delay during the limited time a mouse can bear a fast-growing tumour xenograft. Thus, we attempted to create a model system expected to be more sensitive to inhibitor treatment by using tumour cells with sufficiently short telomeres. Since established tumour cell lines do not fulfil these criteria, we utilized inhibitor-treated, late-passage HT1080 fibrosarcoma cells with an average TRF size of only 1.6 kb (Figure 6A) but with an *in vitro* growth rate and colony forming ability similar to control cultures. After subcutaneous injection into immunodeficient mice, untreated control cells with telomeres of ~4 kb (Figure 6A) reached a detectable tumour size (≥50 mm^2) in 4.53 ± 0.6 days ($n = 24$) whereas the telomere-shortened cells formed detectable tumours only after a lag period of 16.5 ± 1.8 days ($n = 27$, $p < 0.0001$). The average tumour size (Figure 6B) and incidence (Figure 6C) up to 36 days after injection was significantly lower in animals bearing pre-treated, telomere-shortened cells. This tumour model was also used to study *in vivo* inhibition of human telomerase. We treated mice carrying subcutaneous implants of the telomere-shortened HT1080 cells with BIBR1532 at a dose of 100 mg/kg/day orally beginning on the day of implantation. BIBR1532 is very specific and selective for human telomerase and inhibits mouse telomerase only with an IC_{50} >50 μM. Because of this 500-fold difference in potency, inhibition of host telomerase is not expected. The inhibitor treatment was very well tolerated with no signs of acute and chronic toxicity over the entire treatment period, which lasted 60 days for mice developing no or only small tumours. The lag-period to detectable tumour development was substantially prolonged to 26.2 ± 4.3 days ($n = 19$, $p = 0.0255$). Continued drug exposure inhibited initial tumour growth (Figure 6B) and resulted in a reduced incidence of tumours >1000 mm^3 with only six animals (32%) testing positive at day 43 of treatment compared to 19 animals (70%) not receiving the telomerase inhibitor ($p = 0.01034$, Figure 6C).

Discussion

A number of genetic validation experiments indicate that telomere maintenance by the enzyme telomerase is a key event in the immortalization process and the continuous proliferation of a large proportion of human cancers (Bodnar *et al.*, 1998; Vaziri and Benchimol, 1998; Hahn *et al.*, 1999a). The pharmacological results presented here demonstrate that extended propagation of human tumour cell lines in the presence of compounds from a novel class of selective, non-nucleosidic small molecule telomerase inhibitors results in progressive telomere shortening followed by the induction of a senescence phenotype and profound anti-proliferative effects *in vitro* and *in vivo*.

Several strategies to inhibit telomerase activity have been reported. These include peptide nucleic acids and 2′-O-MeRNA oligonucleotides directed towards the telomerase RNA template (Herbert *et al.*, 1999), compounds that target telomeric DNA such as cationic porphyrins or anthraquinones (Sun *et al.*, 1997) and nucleosidic reverse transcriptase inhibitors (Strahl and Blackburn, 1996). So far, these pharmacological strategies have had only limited success *in vivo* due to moderate efficacy or the inability of test compounds to penetrate cellular membranes under physiological conditions. Another approach described recently made use of dominant-negative alleles of hTERT, expression of which resulted in cell death of telomerase-positive cancer cell lines (Hahn *et al.*, 1999b; Zhang *et al.*, 1999). Although very effective and selective

in vitro, this gene therapy approach may not be readily applicable to the clinical setting.

The non-nucleosidic small molecule telomerase inhibitors described here overcome several of the past obstacles. Telomerase inhibition by BIBR1532 or BIBR1591 results in a continuous erosion of the telomeres in human cancer cell lines derived from fibrosarcoma, lung, breast and prostate carcinoma. No other cellular changes as assessed by morphological or gene expression parameters appear to be triggered by these selective drugs until the telomeres erode to a critically short length and the cells slow their growth. The phenotypic signs of senescence were observed not only in the p53-positive NCI-H460 cells but also in the p53-deficient HT1080, DU145 and MDA-MB231 cell lines, consistent with broad therapeutic utility. In contrast to previous results employing anti-sense oligonucleotides or the expression of dominant-negative hTERT alleles (Hahn *et al.*, 1999b; Herbert *et al.*, 1999; Zhang *et al.*, 1999) we saw no evidence for an increased rate of apoptosis in the inhibitor-treated cells. This could be attributed to the different means employed to inhibit telomerase or to differences in the apoptotic potential of the non-overlapping set of cell lines used in these studies.

Changes that define age-related senescence of normal cells include enlarged and flattened morphology, increased granularity, expression of SA-β-GAL and multiple nuclei (Hayflick and Moorhead, 1961; Smith and Pereira-Smith, 1996). The senescence phenotype may be refined at the molecular level by comparing our list of regulated genes with that of a recent microarray study focusing on gene expression levels in replicative senescence of normal cells and age-related diseases (Chang *et al.*, 2000; Ly *et al.*, 2000). Many of the genes described in the physiological or premature ageing process, such as the down-regulation of mRNAs coding for cell cycle control proteins, proteins required for mitosis, DNA synthesis, replication and repair, are also found in the telomerase-inhibitor-treated, senescent NCI-H460 cancer cells and they may obey a programmed switch for mitotic events in senescent cells. A related feature of the inhibitor-treated NCI-H460 cells may be up-regulation of $p21^{Waf1}$, a cyclin-dependent kinase inhibitor whose induction triggers growth arrest associated with senescence and damage response. The similarities to the gene expression changes observed in recent array studies of p21-induced senescence (Chang *et al.*, 2000) suggest that the senescent phenotype we observed upon telomerase inhibition may result, at least in part, from effects mediated by $p21^{Waf1}$.

The average TRF lengths in all inhibitor treated, senescent cells reach a size of only 1–2 kb at the onset of growth inhibition. A significant portion of these TRFs likely consists of subtelomeric sequences rather than TTAGGG repeats; suggesting that the true length of telomeric TTAGGG repeats has been reduced to only several hundred basepairs. Cytogenetic analysis indicates that some telomeres may even have lost all measurable TTAGGG repeats. Defective telomeres are unable to cap chromosomes effectively and the marked disarray in the genome of the inhibitor-treated cancer cell lines, including telomere loss and chromosomal end-to-end fusions, resembles the karyotypic changes in $mTERC^{-/-}$ mouse cells (Blasco *et al.*, 1997). The role of telomerase in the immortalization of rodent cells may not be identical to human cells in all respects, but this mutant mouse model is extremely valuable for evaluating the biological consequences of telomerase inhibition. The lack of phenotypic effects in the early generation $mTERC^{-/-}$ mice suggests that general telomerase inhibition may be well tolerated with no severe toxic effects (Blasco *et al.*, 1997). The ability of $mTERC^{-/-}$ mice to develop certain cancer types in later generations has been attributed to chromosome end-to-end fusions or the activation of telomerase-independent telomere maintenance mechanisms (Blasco *et al.*, 1997; Greenberg *et al.*, 1999; Rudolph *et al.*, 1999). A similar ALT mechanism has been described for virus-transformed human cells and a small proportion of established human cancer cell lines that lack telomerase activity (Bryan *et al.*, 1995). We have never observed induction of the ALT phenotype in any of the cell lines used in our studies. Induction of ALT has also never been reported in previous publications using other means of telomerase inhibition (Hahn *et al.*, 1999b; Herbert *et al.*, 1999; Zhang *et al.*, 1999). A recent analysis of telomeric recombination mechanisms, which are apparently the mechanistic basis for ALT, suggests that telomere-positive cells may not possess a telomere maintenance mechanism other than telomerase (Dunham *et al.*, 2000).

Recent data suggest that in $mTERC^{-/-}$ mouse cells telomere dysfunction is a prominent trait that impairs DNA repair and enhances sensitivity to ionizing radiation (Wong *et al.*, 2000). This link between telomerase inhibition and radiosensitivity may provide a basis for further studies employing a combination of telomerase inhibitors and radiotherapeutic strategies for cancer treatment. In a clinical setting, the most likely use of telomerase inhibitors would be as an adjuvant treatment in combination with surgery, radiation treatment and conventional chemotherapy. Another potential application would be post-remission therapy in order to eliminate minimal residual disease.

Although an analysis of telomere lengths in primary tumours suggests that tumour telomeres are usually short, predicting that the phenotypic lag may be limited, we nevertheless expect that oral treatment may have to be administered continuously for weeks to months. Therefore, the success of a telomerase inhibitor therapy requires that compounds should be sufficiently well tolerated, have a low toxicity profile and are easy to administer. The compounds described here fulfil many of the required criteria and further studies with continued treatment *in vivo* are needed to determine the best candidates to study for clinical efficacy. At the very least, our discovery of a highly potent and selective class of telomerase inhibitors highlights the potential of targeting this enzyme in a mechanism-based approach to the development of new treatment modalities in cancer.

Materials and methods

Enzyme assays

Telomerase activity assays to determine the IC_{50} curves were performed and quantified using a PCR-based protocol followed by a TCA precipitation step (Schnapp *et al.*, 1998). The total amount of incorporated [^{33}P]dCMP was measured by liquid scintillation counting and normalized to the control. As a source for telomerase, nuclear extracts derived from HeLa cells were used. For the direct telomerase assay, telomerase was reconstituted with insect cell expressed hTERT and *in vitro* transcribed

hTR as described (Wenz *et al.*, 2001). Taq polymerase activity was determined as described by the manufacturer (Promega). The activity of DNA polymerases present in HeLa nuclear extracts (40 μg of total protein) was assayed under the following conditions: 20 mM Tris–HCl pH 7.9, 8 mM $MgCl_2$, 50 mM KCl, 0.5 mg/ml bovine serum albumin, 5 mM dithiothreitol, 2 mM spermidine, 80 μM each of dGTP, dCTP and TTP, 5 μM [α-^{32}P]dATP (3.6 Ci/mmol) and either 4 μg activated calf thymus DNA (Pharmacia) or 2 μg of poly A(dT) (Biotech) as template. Reactions were incubated for 30 min at 37°C and the radioactivity present in trichloroacetic acid precipitates collected on class-fibre filters was determined by liquid scintillation counting. Purified pure calf thymus DNA polymerase was obtained from Professor N.C.Brown (University of Massachusetts Medical School, Worcester) and Cambio (Cambridge, UK) and was assayed in the presence of 4 μg of activated calf thymus DNA as described above. Human RNA polymerase I was purified from HeLa nuclear extracts and assayed as described (MonoQ fraction, Schnapp and Grummt 1996). The activity of human RNA polymerases I, II and III was also assayed in HeLa nuclear extracts in the presence of 200 μg/ml α-amanitin using the same conditions. The activity of RNA polymerase II and III was calculated from the difference of the non-inhibited versus the α-amanitin-inhibited extract. *In vitro* translation assays were performed in the rabbit reticulocyte system as described by the manufacturer (Promega). *Escherichia coli* helicase I (Amersham) and pcTA Helicase from *Bacillus stearothermophilus* (Cambio) were assayed in the helicase ^{3}H SPA enzyme assay system as described by the manufacturer (Amersham). HIV1 reverse transcriptase was tested in the reverse transcriptase SPA enzyme assay (Amersham).

Cell lines

The lung cancer cell line NCI-H460, the fibrosarcoma cell line HT1080, the breast cancer cell line MDA-MB231 and the prostate cancer cell line DU145 were maintained in RPMI supplemented with 5 or 10% fetal calf serum in 5% CO_2 at 37°C. The cells were grown in 24-well tissue culture plates and replated every 2–3 days to ensure log-phase growth. The culture medium contained 10 μM of BIBR1532 or 50 μM of BIBR1591 dissolved in 0.1% DMSO and was replenished at every replating step or every 2–3 days for slower growing cells. The compounds were stable under these conditions. Control cells were untreated or treated with corresponding solvent concentrations. Cell growth and viability in the 7 day cytotoxicity study was determined using the tetrazolium dye assay.

Isolation of cellular DNA and telomere length analysis

Cell samples (2×10^6 cells) were harvested, washed and resuspended in DNazol (Life Technologies). Total cellular DNA was extracted according to the manufacturer's protocol. To measure telomere length, genomic DNA was digested with restriction enzymes *Hin*fI and *Rsa*I, fractionated on 0.6% agarose gel and transferred onto a nylon membrane. Telomere sequences were detected by hybridization with a synthetic oligonucleotide probe $(CCCTAA)_3$ end-labelled with fluorescein-dUTP. Detection relies on an anti-fluorescein-antibody conjugated to alkaline phosphatase (Amersham).

Cellular Assays

SA-β-galactosidase activity was detected as described (Dimri *et al.*, 1995). For cell cycle analysis, cells were fixed with 2% paraformaldehyde for 20 min at room temperature and permeabilized with 0.25% Triton X-100 in phosphate-buffered saline by incubation for 5 min on ice. Cells were pelleted by centrifugation (1000 *g*, 5 min, 4°C), resuspended in propidium iodine staining buffer (0.1% RNase, 10 μg/ml propidium iodine in PBS) and incubated for 20 min at room temperature. The DNA content was analysed using a FACS Calibur (Becton Dickinson, Heidelberg, Germany). TUNEL assay was performed according to the manufacturer's protocol (Pharmingen, Heidelberg, Germany).

Fluorescence in situ hybridization and quantitative image analysis

Individual telomere length was analysed by quantitative fluorescence *in situ* hybridization (Q-FISH) as described previously (Martens *et al.*, 1998, 2000). Digital images of metaphase spreads were recorded with a digital camera (Sensys, Photometrics) on a Zeiss Axioplan II fluorescence microscope using the Vysis workstation QUIPS. Telomere profiles were analysed by the TFL-TELO software (Poon *et al.*, 1999). Telomere fluorescence intensity values were expressed in arbitrary units.

Analysis of gene expression using oligonucleotide arrays

Total RNA was extracted from frozen cell pellets by using Trizol reagent (Life Technologies). RNA was purified on RNeasy Mini columns (Qiagen) for RNA cleanup and DNase treatment (RNase-Free DNase Set Protocol, Qiagen). RNA was converted into double-stranded cDNA by using the Superscript Choice System (Life Technologies). Biotin-labelled cRNA synthesis was carried out using 10 μg of total RNA according to the Affymetrix technical manual (Lockhart *et al.*, 1996; Fambrough *et al.*, 1999). Hybridization, washing, staining, and scanning of Affymetrix Genechip HuGeneFL oligonucleotide arrays (Affymetrix) was carried out according to the Affymetrix technical manual (Lockhart *et al.*, 1996; Fambrough *et al.*, 1999) in an Affymetrix hybridization oven and fluidics station and a Hewlett-Packard GeneArray Scanner. Data analysis was performed using Affymetrix software. Expression levels of untreated or DMSO-treated control cells were compared with expression levels of cells treated with the telomerase inhibitor BIBR1591. Four pairwise comparisons were calculated by comparing two unrelated sets of cells grown with BIBR1591 to either untreated NCI-H460 cells or to cells treated with DMSO as a solvent control. Selected genes were required to show at least a 2-fold regulation in at least three out of four pairwise comparisons.

Quantitative RT–PCR

We used the same RNA preparations for both microarray and quantitative RT–PCR analyses. mRNA quantitation was performed using the TaqMan EZ RT–PCR kit (PE Applied Biosystems) and all samples were analysed in triplicates on the ABI PRISM 7700 Sequence Detection System (PE Applied Biosystems). Gene-specific oligonucleotide probes with 5′-fluorescent and 3′-rhodamine (quench) tags were designed for hTERT, Wnt5a, IGFBP4, p21^{Waf1}, cyclin A, and GAPDH as an internal standard. PCR conditions as well as sequences of RT–PCR primers and probes will be provided on request.

Tumorigenicity assays

The ability of untreated and inhibitor treated HT1080 fibrosarcoma cells to form tumours was determined by injecting 1.5×10^6 cells subcutaneously in immunodeficient nu/nu NMRI mice. BIBR1532 was prepared in a vehicle of 20% cremophore RH40, 80% water with equimolar amounts of NaOH. Treatment was administered by gavage. Growth of the tumours was recorded by calliper measurements determining length and width of the palpatable, subcutaneous tumour mass three times per week.

Supplementary data

Supplementary data for this paper are available at *The EMBO Journal* Online.

Acknowledgements

We thank the members of the Department of Oncology Research for helpful discussions and encouragement, Dr Uwe Bamberger for help with the animal experiments and Josef Eiband, Herbert Fischbach and Michael Koehler for excellent technical assistance. M.P. and U.M.M. were supported by the Deutsche Forschungsgemeinschaft (SFB364). Work in J.L.'s laboratory was supported in part by the Swiss National Science Foundation and the Fifth Framework Program of the European Union (via the Bundesamt fuer Bildung und Wissenschaft, Bern).

References

Blackburn,E. and Greider,C. (eds) (1995) *Telomeres*. Cold Spring Harbor Laboratory Press, Cold Spring Harbor, New York, NY.

Blasco,M.A., Lee,H.W., Hande,M.P., Samper,E., Lansdorp,P.M., DePinho,R.A. and Greider,C.W. (1997) Telomere shortening and tumour formation by mouse cells lacking telomerase RNA. *Cell*, **91**, 25–34.

Bodnar,A.G. *et al.* (1998) Extension of life-span by introduction of telomerase into normal human cells. *Science*, **279**, 349–352.

Bryan,T.M., Englezou,A., Gupta,J., Bacchetti,S. and Reddel,R.R. (1995) Telomere elongation in immortal human cells without detectable telomerase activity. *EMBO J.*, **14**, 4240–4248.

Chang,B.D., Watanabe,K., Broude,E.V., Fang,J., Poole,J.C., Kalinichenko,T.V. and Roninson,I.B. (2000) Effects of p21$^{Waf1/Cip1/Sdi1}$ on cellular gene expression: implications for carcinogenesis, senescence, and age-related diseases. *Proc. Natl Acad. Sci. USA*, **97**, 4291–4296.

Cooke,H.J. and Smith,B.A. (1986) Variability at the telomeres of the

human X/Y pseudoautosomal region. *Cold Spring Harbor Symp. Quant. Biol.*, **51**, 213–219.

Counter,C.M., Avilion,A.A., LeFeuvre,C.E., Stewart,N.G., Greider,C.W., Harley,C.B. and Bacchetti,S. (1992) Telomere shortening associated with chromosome instability is arrested in immortal cells which express telomerase activity. *EMBO J.*, **11**, 1921–1929.

Counter,C.M., Botelho,F.M., Wang,P., Harley,C.B. and Bacchetti,S. (1994) Stabilization of short telomeres and telomerase activity accompany immortalization of Epstein–Barr virus-transformed human B lymphocytes. *J. Virol.*, **68**, 3410–3414.

Dimri,G.P. *et al.* (1995) A biomarker that identifies senescent human cells in culture and in ageing skin *in vivo*. *Proc. Natl Acad. Sci. USA*, **92**, 9363–9367.

Dunham,M.A., Neumann,A.A., Fasching,C.L. and Reddel,R.R. (2000) Telomere maintenance by recombination in human cells. *Nature Genet.*, **26**, 447–450.

Fambrough,D., McClure,K., Kazlauskas,A. and Lander,E.S. (1999) Diverse signaling pathways activated by growth factor receptors induce broadly overlapping, rather than independent, sets of genes. *Cell*, **97**, 727–741.

Feng,J.L. *et al.* (1995) The RNA component of human telomerase. *Science*, **269**, 1236–1241.

Greenberg,R.A., Chin,L., Chin,L., Femino,A., Lee,K.H., Gottlieb,G.J., Singer,R.H., Greider,C.W. and DePinho,R.A. (1999) Short dysfunctional telomeres impair tumorigenesis in the INK4aΔ2/3 cancer-prone mouse. *Cell*, **97**, 515–525.

Hahn,W.C., Counter,C.M., Lundberg,A.S., Beijersbergen,R.L., Brooks, M.W. and Weinberg,R.A. (1999a) Creation of human tumour cells with defined genetic elements. *Nature*, **400**, 464–468.

Hahn,W.C. *et al.* (1999b) Inhibition of telomerase limits the growth of human cancer cells. *Nature Med.*, **5**, 1164–1170.

Harley,C.B. (1991) Telomere loss: mitotic clock or genetic time bomb? *Mutat. Res.*, **256**, 271–282.

Harley,C.B., Futcher,A.B. and Greider,C.W. (1990) Telomeres shorten during ageing of human fibroblasts. *Nature*, **345**, 458–460.

Harrington,L., Zhou,W., McPhail,T., Oulton,R., Yeung,D.S.K., Mar,V., Bass,M.B. and Robinson,M.O. (1997) Human telomerase contains evolutionarily conserved catalytic and structural subunits. *Genes Dev.*, **11**, 3109–3115.

Hastie,N.D., Dempster,M., Dunlop,M.G., Thompson,A.M., Green,D.K. and Allshire,R.C. (1990) Telomere reduction in human colorectal carcinoma and with ageing. *Nature*, **346**, 866–868.

Hayflick,L. and Moorhead,P. (1961) The serial cultivation of human diploid cell strains. *Exp. Cell Res.*, **25**, 585–621.

Herbert,B.S., Pitts,A.E., Baker,S.I., Hamilton,S.E., Wright,W.E., Shay,J.W. and Corey,D.R. (1999) Inhibition of human telomerase in immortal human cells leads to progressive telomere shortening and cell death. *Proc. Natl Acad. Sci. USA*, **96**, 14276–14281.

Kim,N.W. *et al.* (1994) Specific association of human telomerase activity with immortal cells and cancer. *Science*, **266**, 2011–2015.

Lee,C.K., Klopp,R.G., Weindruch,R. and Prolla,T.A. (1999) Gene expression profile of aging and its retardation by caloric restriction. *Science*, **285**, 1390–1393.

Lee,C.K., Weindruch,R. and Prolla,T.A. (2000) Gene-expression profile of the ageing brain in mice. *Nature Genet.*, **25**, 294–297.

Lockhart,D.J. *et al.* (1996) Expression monitoring by hybridization to high-density oligonucleotide arrays. *Nature Biotechnol.*, **14**, 1675–1680.

Ly,D.H., Lockhart,D.J., Lerner,R.A. and Schultz,P.G. (2000) Mitotic misregulation and human ageing. *Science*, **287**, 2486–2492.

Martens,U.M., Zijlmans,J.M., Poon,S.S., Dragowska,W., Yui,J., Chavez,E.A., Chavez,E.A., Ward,R.K. and Lansdorp,P.M. (1998) Short telomeres on human chromosome 17p. *Nature Genet.*, **18**, 76–80.

Martens,U.M., Chavez,E.A., Poon,S.S., Schmoor,C. and Lansdorp,P.M. (2000) Accumulation of short telomeres in human fibroblasts prior to replicative senescence. *Exp. Cell. Res.*, **256**, 291–299.

Meyerson,M. *et al.* (1997) hEST2, the putative human telomerase catalytic subunit gene, is up-regulated in tumour cells and during immortalization. *Cell*, **90**, 785–795.

Morin,G.B. (1989) The human telomere terminal transferase enzyme is a ribonucleoprotein that synthesizes TTAGGG repeats. *Cell*, **59**, 521–529.

Nakamura,T.M., Nakamura,T.M., Morin,G.B., Chapman,K.B., Weinrich, S.L., Andrews,W.H., Lingner,J., Harley,C.B. and Cech,T.R. (1997) Telomerase catalytic subunit homologs from fission yeast and human. *Science*, **277**, 955–959.

Poon,S.S., Martens,U.M., Ward,R.K. and Lansdorp,P.M. (1999) Telomere length measurements using digital fluorescence microscopy. *Cytometry*, **36**, 267–278.

Rudolph,K.L., Rudolph,K.L., Chang,S., Lee,H.W., Blasco,M., Gottlieb,G.J., Greider,C. and DePinho,R.A. (1999) Longevity, stress response, and cancer in aging telomerase-deficient mice. *Cell*, **96**, 701–712.

Schnapp,A. and Grummt,I. (1996) Purification, assay, and properties of RNA polymerase I and class I-specific transcription factors in mouse. *Methods Enzymol.*, **273**, 233–248.

Schnapp,G., Rodi,H.P., Rettig,W.J., Schnapp,A. and Damm,K. (1998) One-step affinity purification protocol for human telomerase. *Nucleic Acids Res.*, **26**, 3311–3313.

Shay,J.W. and Bacchetti,S. (1997) A survey of telomerase activity in human cancer. *Eur. J. Cancer*, **33**, 787–791.

Shelton,D.N., Chang,E., Whittier,P.S., Choi,D. and Funk,W.D. (1999) Microarray analysis of replicative senescence. *Curr. Biol.*, **9**, 939–945.

Smith,J.R. and Pereira-Smith,O.M. (1996) Replicative senescence: implications for *in vivo* ageing and tumour suppression. *Science*, **273**, 63–67.

Strahl,C. and Blackburn,E.H. (1996) Effects of reverse transcriptase inhibitors on telomere length and telomerase activity in two immortalised human cell lines. *Mol. Cell. Biol.*, **16**, 53–65.

Sun,D.Y., Thompson,B., Cathers,B.E., Salazar,M., Kerwin,S.M., Trent,J.O., Jenkins,T.C., Neidle,S. and Hurley,L.H. (1997) Inhibition of human telomerase by a G-quadruplex-interactive compound. *J. Med. Chem.*, **40**, 2113–2116.

Vaziri,H. and Benchimol,S. (1998) Reconstitution of telomerase activity in normal human cells leads to elongation of telomeres and extended replicative life span. *Curr. Biol.*, **8**, 279–282.

Wenz,C., Enenkel,B., Amacker,M., Kelleher,C., Damm,K. and Lingner,J. (2001) Human telomerase contains two cooperating telomerase RNA molecules. *EMBO J.*, **20**, 3526–3534.

Wong,K.K. *et al.* (2000) Telomere dysfunction impairs DNA repair and enhances sensitivity to ionising radiation. *Nature Genet.*, **26**, 85–88.

Zhang,X.L., Mar,V., Zhou,W., Harrington,L. and Robinson,M.O. (1999) Telomere shortening and apoptosis in telomerase-inhibited human tumour cells. *Genes Dev.*, **13**, 2388–2399.

Received September 11, 2001; revised October 23, 2001; accepted October 26, 2001